UNIVERSIDADE FEDERAL DE SANTA CATARINA

CAMPUS FLORIANÓPOLIS

PROGRAMA DE PÓS-GRADUAÇÃO EM OCEANOGRAFIA

Danilo Couto de Souza

REFINAMENTO CLIMÁTICO PARA A REGIÃO COSTEIRA DO SUL DO BRASIL

Florianópolis

2020

Danilo Couto de Souza

REFINAMENTO CLIMÁTICO PARA A REGIÃO COSTEIRA DO SUL DO BRASIL

Florianópolis

2020

Danilo Couto de Souza

REFINAMENTO CLIMÁTICO PARA A REGIÃO SUL DO BRASIL

O presente trabalho em nível de mestrado foi avaliado e aprovado por banca

examinadora composta pelos seguintes membros:

Prof. Pedro Leite da Silvas Dias, Dr.

Instituição Universidade de São Paulo

Prof. Felipe Mendonça Pimenta, Dr.

Instituição Universidade Federal de Santa Catarina

Certificamos que esta é a **versão original e final** do trabalho de conclusão que foi

julgado adequado para obtenção do título de mestre em Oceanografia.

_____

Prof. Paulo Roberto Pagliosa Alves, Dr.

Coordenador do Programa

_____

Prof. Renato Ramos da Silva, Dr.

Orientador

Florianópolis, 2020.

Este trabalho é dedicado aos meus amigos e à minha família.

AGRADECIMENTOS

Primeiramente, um agradecimento especial aos meus pais e irmã. Sem o apoio e carinho deles esse mestrado não teria acontecido.

Um agradecimento especial ao meu orientador, Renato Ramos da Silva, por todos os ensinamentos durante essa jornada, por ter me providenciado sempre toda a estrutura física e intelectual para a realização desse trabalho e por ter nutrido me interesse de aprender sobre os oceanos e atmosfera.

Nada mais justo que agradecer também minha namorada e companheira de vida, Juliana, que "foi obrigada" a entrar nesse mestrado junto comigo, não desistiu de mim em momento algum e sempre me ofereceu todo seu amor e carinho.

Quero agradecer também aos meus amigos, colegas e parceiros de laboratório, república treino, surf, trilhas, jogos e de vida, que me fazem minha vida mais feliz.

Agradeço aos membros do projeto ROAD, por propiciarem o crescimento dessa pesquisa e, especialmente a Paula Gomes pela força na reta final.

Não poderia faltar um agradecimento também ao prof. John Beardall por ter propriamente me introduzido ao mundo acadêmico e ao professor Roberto Fontes (Bob) por ter me aberto as portas ao maravilhoso mundo da oceanografia.

Por último, mas não menos importante, obrigado ao "*lofi hip hop radio - beats to relax/study to*" que possibilitou que eu me concentrasse nos meus estudos, apesar do caos ao meu redor.

"To reach a port we must sail –
Sail, not tie at anchor
Sail, not drift." (Roosevelt, 1938)

RESUMO

No presente trabalho foram aplicadas duas abordagens distintas para realizar um refinamento climático para a região costeira da região sul do Brasil. Primeiramente, foram selecionados eventos extremos para a região de estudo, que ocorreram entre os anos 2000 e 2018. Para a simulação de tais eventos, o modelo numérico *Ocean-Land Atmosphere Model* (OLAM) foi configurado com uma grade global e refinamento regional com alta resolução centradas na região costeira do sul do país. Os resultados do modelo foram avaliados por comparação com observações provenientes de estações meteorológicas e produtos do TRMM, GPM e MERRA-2. O modelo foi capaz de simular bem os campos de temperatura, precipitação, vento e pressão no nível do mar para os eventos selecionados. Os campos de precipitação apresentaram melhores resultados para os eventos mais extremos. A configuração adotada permitiu uma boa representação de fenômenos tanto de escala local quanto de larga escala, capturando a circulação atmosférica relacionada à ocorrência de eventos extremos na região de estudo. Na segunda parte, foi aplicada uma metodologia que considera um refinamento híbrido, o qual inclui uma seleção estatística de padrões atmosféricos e *downscaling* dinâmico. Inicialmente foi aplicada uma metodologia estatística para selecionar 32 *weather types* para a região de estudo. Essa seleção usou como preditor os campos de pressão ao nível do mar na região oceânica adjacente ao sul do Brasil a partir de campos do *Climate Forecast System Reanalysis* (CFSR). Após a seleção desses casos, foi aplicado o modelo OLAM, com a mesma configuração adotada na primeira parte, para fazer o refinamento dinâmico dos mesmos com uma resolução espacial que atingiu 6 km na região de estudo. Os *weather types* selecionados representaram bem os fenômenos meteorológicos predominantes relacionados a circulação da região de estudo, como a propagação dos ciclones

extratropicais e o anticiclone semipermanente do Atlântico Sul. Ao mesmo tempo, o refinamento dinâmico permitiu a obtenção dos campos atmosféricos com alto grau de detalhamento incluindo os campos de mesoescala resultantes das características superficiais da região como relevo e heterogeneidade de tipos de vegetação. A metodologia híbrida proposta mostra que esta ferramenta pode ser usada para avaliar o clima predominante regional em nível de mesoescala, que é de grande interesse para as comunidades locais.

Palavras-chave: Modelagem Numérica. OLAM. Eventos Extremos. *Weather types*.

ABSTRACT

In the present work we applied two distinct approaches aiming a climate downscaling for the coastal region of southern Brazil. Firstly, we selected extreme events that occurred in the study region between the years 2000 and 2018. For the numerical simulations of those events the OLAM model was set up with a global grid and high resolution regional grids centered in the coast of the southern region of Brazil. For model evaluation we compared the results with observations from meteorological stations and TRMM, GPM and MERRA-2 products. The model was capable of providing good results for temperature, precipitation, wind and sea level pressure fields for the selected events. The precipitation fields presented better results for the most extreme cases. The chosen set up allowed a good representation of both local and large scale phenomenon, capturing atmospheric circulation related to the occurrence of extreme events in the study region. In the second part of the current work, we applied a hybrid downscaling methodology, which includes both dynamical and statistical approaches. Initially, we applied a statistical downscaling methodology in order to select 23 weather types for the study area. This selection used daily sea level pressure fields in the oceanic region adjacent to the study area as large scale predictor. After selecting those cases, we used the OLAM model, with the same set up as the previous part of the work, to perform the dynamical downscaling. The selected weather types presented a good representation of the predominant meteorological phenomenon related to the study area atmospheric circulation such as propagation of extratropical cyclones and the quasi-permanent South Atlantic anticyclone. Furthermore, the dynamical downscaling resulted atmospheric fields with a high degree of details and also mesoscale fields resulting from the region surface characteristics such as complex topography and heterogeneous vegetation. The

proposed hybrid methodology showed that this tool can be used in order to evaluate the predominant climate at both regional level and mesoscale, which is of great concern for the local communities.

LISTA DE FIGURAS

LISTA DE TABELAS

LISTA DE ABREVIATURAS E SIGLAS

AC - Anticiclone

CAPES – Coordenação de Aperfeiçoamento do Ensino Superior

CFSR – *Climate Forecast System Reanalysis*

CORDEX - *Coordinated Regional climate Downscaling Experiment*

CPTEC - Centro de Previsão de Tempo e Estudos Climáticos

CS – *Cyclonic System*

DD – *Dynamical Downscaling*

EC – *Extratropical Cyclone*

ENSO – *El-Niño Southern Oscilation/*Oscilação Sul

Flp – Florianópolis

GCM – *General Circulation Model*

GPM – *Global Precipitation Mission*

hPa – hectopascal

HR – *Heavy rain*

HW – *High waves*

INPE – Instituto Nacional de Pesquisas Espaciais

LEAF - *Land Ecosystem-Atmosphere Feedback Model*

m – Metros

MERRA – *Modern-Era Retrospective analysis for Research and Applications*

mm – Milímetros

NCEP – *National Centers for Environmental Protection*

NOAA – *National Oceanic and Atmospheric Administration*

OISST – *Optimum Sea Surface Interpolation*

OLAM – *Ocean Land Atmosphere Model*

PC – *Principal Component*

PCA – *Principal Component Analysis*

Pga – Paranaguá

PR – Paraná

RAMS – *Regional Atmospheric Modeling System*

RCM – Regional Circulation Model

RG – *cyclogenesis region in the South Atlantic*

Rgd – Rio Grande

ROAD-BESM – *Regional oceanic and atmospheric downscaling with the Brazilian Earth System Model*

RS – Rio Grande do Sul

SAAC – *South Atlantic Anticyclone*

SACZ – *South Atlantic Convergence Zone*

SALLJ – *South American Low Level Jet*

SAO – *South Atlantic Ocean*

SBr – *Southern Brazil*

SC – Santa Catarina

SD – *Statistical Downscaling*

SLP – *Sea level pressure*

SS – *storm surge*

SST – *sea surface temperature*

Svp – Santa Vitória do Palmar

SWd – *strong winds*

TRMM – *Tropical Rainfall Mission*

Trs – Torres

UTC - *Coordinated Universal Time*

WT – *weather type*

ZCAS – Zona de Convergência do Atlântico Sul

SUMÁRIO

1 INTRODUÇÃO

Dados climáticos das últimas décadas têm mostrado importantes mudanças climáticas (IPCC, 2014). Dentre as consequências dessas mudanças temos o aumento das temperaturas médias globais, o aumento do nível médio do mar e a maior ocorrência e intensidade de eventos extremos (STOCKER et al., 2013). Nesse contexto, as cidades litorâneas se encontram sob alto risco, visto que são bastante vulneráveis ao aumento do nível do mar, aos aumentos na intensidade e frequência de eventos de precipitação extrema e de ocorrência de ressacas marítimas (MUEHE, 2005). Não obstante, o impacto advindo das mudanças climáticas sob as regiões costeiras pode ser potencializado por fatores como alto grau de urbanização e de uso de atividades humanas em uma determinada área e a consequente degradação ambiental (FIELD et al., 2014).

O último relatório do Painel Intergovernamental sobre Mudanças Climáticas (IPCC) forneceu projeções climáticas de curto a longo prazo baseadas nos resultados do *Coupled Model Inter-comparison Project Phase* 5 (CMIP5) (STOCKER et al., 2013; TAYLOR; STOUFFER; MEEHL, 2012). Atualmente, encontra-se em desenvolvimento o sexto relatório do IPCC, previsto para 2022 (IPCC, 2017), que deverá se basear nos resultados provenientes dos experimentos do CMIP6 (EYRING et al., 2016). O design experimental do CMIP6 foi estruturado visando atender sete objetivos científicos centrais, estabelecidos pelo *World Climate Research Programme*. Dentre estes obstáculos, encontram-se a avaliação de fenômenos climáticos extremos e o entendimento e previsão do aumento do nível do mar em escala regional e suas consequências para a zona costeira.

Entretanto, por utilizarem-se de modelos numéricos de circulação global (*General Circulation Models* - GCMs) com resoluções na ordem de dezenas a centenas de quilômetros, grande parte dos experimentos do CMIP não fornecem informações meteorológicas com detalhamento local. Esse tipo de informação é necessária para a realização de análise de impactos em escalas regionais e consequente elaboração de estratégias de adaptação e mitigação de impactos advindos das mudanças climáticas. A utilização deste nível de resolução também não é capaz de representar propriamente a grande heterogeneidade morfológica e topográfica da América do Sul, podendo resultar em subestimativas de processos climáticos regionais importantes para a mesma. Não obstante, a utilização de GCMs com resoluções baixas não permite que os fenômenos de mesoescala sejam propriamente resolvidos, especialmente em regiões costeiras ou insulares, como por exemplo, o fenômeno de brisa costeira.

Atualmente, grande parte da população mundial reside em regiões costeiras, aonde a densidade populacional média chega a ser até 3 vezes maior do que a média global (SMALL; NICHOLLS, 2003). As zonas costeiras são regiões naturalmente sensíveis às mudanças climáticas, em especial aos fatores associados com mudanças no nível do mar, devido a sua localização (WONG et al., 2015). Nesse contexto, se analisarmos o nível do mar observado como a soma entre a componente astronômica, meteorológica e o nível médio, conforme proposto por Pugh e Vasie (1978), e consideramos as atuais projeções de mudanças climáticas, indicando que o número de pessoas afetadas por ondas de tempestades aumentaria em seis vezes dado um aumento de apenas 0,5m no nível médio do mar (NICHOLLS, 2004), podemos ver que a ocupação humana em regiões adjacentes à costa apresenta um preocupante

problema, visto a existência de um grande potencial para danos sociais e econômicos. De fato, inundações, tanto fluviais quanto costeiras, representam o mais significativo risco advindo de desastres naturais enfrentados atualmente, afetando bilhões de pessoas mundialmente dentre o final do século XX e o começo do século XXI e causando trilhões de dólares em perdas financeiras (JONGMAN; WARD; AERTS, 2012; JONKMAN, 2005; UNISDR, 2009).

Tendo em vista a baixa resolução dos resultados provenientes dos GCMs, a adoção da técnica de refinamento climático (*downscalling*) busca fornecer informação climática regional em alta resolução, propiciando melhores resultados e com detalhamento de variáveis a nível regional e, em alguns casos, local. Essa técnica possui duas vertentes distintas, o refinamento climático dinâmico (*dynamical downscalling* - DD) e o estatístico (*statistical downscalling* - SD).

O DD é baseado na utilização de modelos climáticos regionais (*Regional Circulation Models* - RCMs), com alta resolução, tendo como condições de contorno, resultados provenientes de GCMs ou dados de reanálises. Essa metodologia permite uma melhor representação de padrões de circulação de escala regional influenciados por efeitos orográficos e um maior detalhamento das características da superfície terrestre (ALVES; MARENGO, 2010; CHOU et al., 2012; CHRISTENSEN; CHRISTENSEN, 2007; GIORGI; MARINUCCI, 1996; NOBRE; MOURA; SUN, 2001). Desse modo, há uma melhor representação do campo de ventos (AKHTAR; BRAUCH; AHRENS, 2018) e da precipitação em regiões com terrenos complexos (FOTSO-NGUEMO et al., 2017; NIKIEMA et al., 2017; VARIKODEN et al., 2018). Um exemplo importante de uso do DD é o projeto CORDEX (GIORGI; GUTOWSKI, 2015) cujos resultados têm proporcionado *downscaling* climático para algumas regiões de interesse usando modelos de área limitada com espaçamento de grade

da ordem de 25 km. Embora este método permita melhores dados em escala regional, ainda não é suficiente para representar os fenômenos de mesoescala como as circulações de brisa e tempestades locais (ORLANSKI, 1975). Além do mais, outra desvantagem da utilização desse método se dá pelo fato da alta demanda computacional exigida.

Sendo assim, a metodologia de SD apresenta-se como uma alternativa computacionalmente mais barata para a realização do refinamento climático de projeções feitas pelos GCMs. Essa abordagem baseia-se em relações empíricas entre um preditor de larga escala e um predicante em escala regional/local, como por exemplo dados observados de alta resolução (VON STORCH, 1995, 1999). Desse modo, resultados provenientes de GCMs alimentam modelos estatísticos para que possa inferir-se o estado climático em locais pontuais de maneira relativamente rápida e computacionalmente barata. Entretanto, a maior limitação desse método dá-se pelo fato de que por se basear em relações empíricas relativas ao clima atual, não existem garantias de que estas irão perdurar em um cenário futuro de mudanças climáticas. Além disso, ao contrário do DD, a utilização do SD não permite a investigação dos fenômenos físicos por trás da resposta climática observada.

Entretanto, essas duas abordagens distintas não são necessariamente opostas, podendo ser combinadas a fim de que seja feito proveito de suas respectivas vantagens. A utilização do DD em combinação com o SD é chamada de refinamento híbrido e possui distintas aplicações, conforme os objetivos almejados (ex.: COLETTE; VAUTARD; VRAC, 2012; PRYOR; BARTHELMIE, 2014; SUN; WALTON; HALL, 2015; WALTON et al., 2015). Dentre essas aplicações, uma particularmente útil para estudos climáticos regionais é apresentada por Camus et al. (2014). Nesse caso, a técnica de SD é utilizada para selecionar e

agrupar informação climática em estados representativos, chamados pelos autores de *weather types*, ou, originalmente, padrões de circulação (HUTH, 2000; HUTH et al., 2008), e desse modo realiza-se o DD referente a esses casos.

No Brasil, têm ocorrido muitos processos erosivos ao longo de todo o litoral, que deverão ser intensificados, dado o aumento do nível médio do mar e maior ocorrência de eventos extremos (NEVES; MUEHE, 2008). Paralelamente, temos um cenário onde há um acelerado processo de crescimento populacional das zonas costeiras no país, sendo que a maior parte dessa população se concentra em centros urbanos (BRASIL, 2013). Desse modo, o uso das zonas costeiras no Brasil, onde muitas vezes não são devidamente considerados os processos e ciclos naturais característicos desse meio, acaba por potencializar os riscos advindos das mudanças climáticas (NEVES; MUEHE, 2008). Portanto, é evidente a necessidade por parte das cidades costeiras brasileiras da adoção de medidas de planejamento estratégico no contexto das mudanças climáticas (MARENGO et al., 2016).

Na região costeira do Sul do Brasil há diversos centros urbanos onde a vulnerabilidade às mudanças climáticas é alta ou muito alta (NICOLODI; PETERMANN, 2010). A região apresenta também uma alta exposição a eventos de inundações (DILLEY et al., 2005). Nesse contexto, nota-se historicamente uma grande ocorrência de eventos extremos nessa região, causando muitas perdas econômicas e sociais (HERRMANN, 2006). Casos notáveis incluem as inundações do Vale do Itajaí em 1983 e 2008 (FRAGA, 2009; RIBEIRO et al., 2014), e a ocorrência do Furacão Catarina em 2004 (PEZZA; SIMMONDS, 2005). Não obstante, há também diversas ocorrências de eventos extremos danosos relacionados com a agitação do mar (BITENCOURT; QUADRO; CALBETE, 2002; FUENTES; BITENCOURT; FUENTES, 2013; GUIMARÃES; FARINA; TOLDO, 2014) e eventos meteorológicos

extremos (RODRIGUES; YNOUE, 2016). Sendo assim, apesar da vulnerabilidade local frente às mudanças climáticas ser conhecida, há uma carência de estudos quanto à análise dos impactos associados (MARENGO et al., 2016).

O clima de uma dada região é afetado pela climatologia dos seus padrões meteorológicos característicos (*i.e. weather types*) e também da eventual ocorrência de eventos extremos. Os padrões característicos descrevem o estado atmosférico médio esperado para a maior parte dos dias, enquanto que os eventos extremos denotam ocorrências muito alteradas em relação à média. As variações atmosféricas de alta frequência na América do Sul subtropical podem ser explicadas pela passagem de ondas baroclínicas se propagando a partir do Oceano Pacífico e perturbadas pela presença dos Andes (GARREAUD; ACEITUNO, 2002). A presença do jato subtropical também favorece a formação de complexos convectivos de mesoescala que produzem substancial precipitação e, em alguns casos, com a formação de uma baixa pressão em superfície, levam a ventos fortes que podem atingir a região costeira (LAING; MICHAEL FRITSCH, 1997; ZIPSER et al., 2006).

O estudo das condições meteorológicas características de uma região geralmente é realizado através da classificação de estados atmosféricos em padrões de circulação (HUTH et al., 2008). Esse tipo de metodologia permite uma análise de projeções climáticas através da observação de mudanças nos padrões de circulação futuros em relação aos presentes (HUTH, 2000). Desse modo, é possível identificar mudanças na predominância e ocorrência de certos padrões, e assim inferir mudanças no estado atmosférico característico de uma região de interesse. Mais recentemente, Camus e colaboradores (2014) estabeleceram uma metodologia

que emprega múltiplas técnicas de processamento de dados para realizar a seleção de padrões de circulação de uma determinada área (chamados pelos autores de *weather types)*.

O presente estudo considerou duas abordagens distintas. Primeiramente, foi realizado o refinamento dinâmico, utilizando o *Ocean-Land Atmosphere Model* (OLAM), de eventos extremos ocorridos na região costeira do Sul do Brasil no passado recente. Essa etapa teve como objetivo a avaliação de desempenho desse modelo numérico na simulação destes eventos extremos. Na segunda etapa, foi utilizada a metodologia de refinamento híbrido, com o objetivo de estabelecer uma metodologia para estudos climáticos para a região costeira do Sul do Brasil. Nesse caso, foi empregada uma metodologia de agrupamento de campos atmosféricos para a seleção dos *weather types* representativos da região de estudo e posteriormente refinados dinamicamente através da utilização do modelo numérico OLAM.

1.1   ÁREA DE ESTUDO

A região Sul do Brasil (Figura 1-1) abrange os estados do Paraná, Santa Catarina e Rio Grande do Sul, com populações de 10,444,526, 6,248,436 e 10,693,929 habitantes, respectivamente (BRASIL, 2013). De acordo com o decreto 5.300/2004 (Anexo A), são considerados municípios costeiros aqueles que são defrontantes com o mar, ou que se localizam em regiões metropolitanas litorâneas, ou são conurbados às mesmas. Resultados provenientes do Macrodiagnóstico da Zona Costeira e Marinha do Brasil indicam que 2,5%, 34% e 11% da população de cada estado, respectivamente, se concentram na zona costeira, sendo que a grande maioria se encontra distribuída dentre cidades de pequeno porte, com até 50 mil habitantes (ZAMBONI; NICOLODI, 2008). Segundo o mesmo relatório, a área em

questão apresenta um crescimento demográfico de mais de 3% ao ano, sendo que os principais fatores que desencadearam este crescimento incluem o processo de urbanização do País, principalmente com a reestruturação produtiva tendendo a um modelo urbano-industrial (implementado no final da década de 1950), a exploração turística e imobiliária (com destaque para os loteamentos voltados para segundas residências) e fluxos migratórios intra-regionais e intra-estaduais (MORAES, 2007).

Figura 1-1: Área de Estudo. Zona costeira da região Sul do Brasil. Em destaque encontram-se os municípios costeiros referentes aos estados do Paraná, Santa Catarina e Rio Grande do Sul (ver Apêndice A para lista completa).

Quanto à atividade econômica, as cidades na região Sul de menor concentração demográfica apresentam suas atividades voltadas para o setor primário e o turismo de lazer (ZAMBONI; NICOLODI, 2008), ao passo que dentre as cidades mais populosas destacam-se

a região metropolitana de Florianópolis, importante polo tecnológico no Brasil e crescente polo industrial, e as cidades de Rio Grande e Pelotas, polos econômicos devido às atividades portuárias e industriais. Há na região, no total, a presença de nove portos marítimos, setor estratégico para a economia nacional, com destaque para os portos de Paranaguá, Itajaí e Rio Grande (BRASIL, 2015), que impulsionam a economia local e funcionam como atrativo populacional. Entretanto, os portos brasileiros, incluindo os mencionados, apresentam vulnerabilidade alta perante as mudanças climáticas (BRASIL, 2016), fato este que futuramente poderá acarretar em enormes perdas econômicas a nível regional e nacional.

No âmbito climatológico, a Região Sul se diferencia do restante do Brasil por ser a única a se localizar fora da região intertropical, situando-se entre o trópico de capricórnio e as latitudes médias (com exceção do extremo norte do Paraná), apresentando, assim, clima do tipo subtropical. Há, entretanto, uma heterogeneidade térmica quando comparamos a porção mais ao sul com a mais ao norte da região, com a primeira apresentando uma maior amplitude térmica anual (11°C, comparada com 7°C), devido à maior variação sazonal de radiação solar e ao fato da última receber influência da Corrente do Brasil, responsável por maiores temperaturas da superfície do mar e, consequentemente, maior umidade relativa do ar (GRIMM, 2009). Apesar de apresentar chuvas quase que uniformemente distribuídas ao longo do ano, por estar localizada na transição entre dois regimes climáticos distintos, há diferenças entre a porção norte e sul da região no que diz respeito aos meses que representam o pico de precipitação: ao norte, o pico da estação chuvosa ocorre pelos meses de verão, enquanto que ao sul, o pico ocorre em julho (RAO; CAVALCANTI; HADA, 1996).

A circulação atmosférica na região oceânica próxima ao Sul do Brasil é dominada pela presença da Alta Subtropical do Atlântico Sul. Esse é um sistema de alta pressão

semipermanente, derivado do ramo descendente da circulação de Hadley nos subtrópicos (GARREAUD et al., 2009)**.** Devido a esse sistema, a predominância de ventos na região é da direção nordeste.

O principal fator responsável por variabilidade climática em escalas sinóticas na região é a passagem de massas de ar frias, originadas no extremo sul do continente e causando quedas bruscas nas temperaturas, principalmente no inverno (GARREAUD, 2000). A intrusão de ar frio pode desencadear episódios de friagem, causando impactos na agricultura local (SELUCHI; MARENGO, 2000). Esse tipo de sistema está altamente relacionado com o processo de frontogênese, predominante no clima da região e principal fonte de precipitação durante o inverno (GARREAUD; FALVEY, 2009; REBIOTA; KRUSCHE; PICCOLI, 2006; SATYAMURTY; MATTOS, 1989). Durante o verão, a menor atividade de frentes frias permite a penetração na região de umidade proveniente da Amazônia, transportada por jatos de baixa latitude, contribuindo para a formação de chuva convectiva, predominante durante essa época do ano (SELUCHI; MARENGO, 2000). Há também, durante o verão, a ocorrência da Zona de Convergência do Atlântico Sul (ZCAS), caracterizada por uma banda de nebulosidade que se estende a partir da Bacia Amazônica em direção sudeste. A ZCAS possui persistência de 1 a 10 dias, podendo ocorrer somente sob o continente (continental) ou se estender até o Oceano Atlântico, associada com maior convecção na região Sul do país e maiores níveis de precipitação média e extrema (CARVALHO; JONES; LIEBMANN, 2004; FERNANDES; RODRIGUES, 2018; LIEBMANN et al., 1999; ROBERTSON; MECHOSO, 2000).

Em escalas interanuais, nota-se a influência da Oscilação Sul - *El Niño* (*El Niño Southern Oscillation* - ENSO) no clima da região. Dentre a porção sul da América do Sul, a região Sul do Brasil é a que apresenta o sinal mais forte durante um evento de *El Niño* (*La Niña*), onde nota-se com um fortalecimento (enfraquecimento) do jato subtropical durante a primavera, com advecção de vorticidade ciclônica (anticiclônica) sob a região e aprofundamento (enfraquecimento) da baixa do Chaco, com consequente aumento (diminuição) da advecção de umidade proveniente da bacia amazônica (GRIMM; BARROS; DOYLE, 2000). A fase do ENSO também tem efeitos sob a ZCAS, alterando a proporção entre ocorrência de eventos de ZCAS oceânica e continental e causando aumento na sua intensidade, relacionado com aumento na precipitação sob a bacia do rio Paraná (CARVALHO; JONES; LIEBMANN, 2004). Não obstante, eventos de El Niño também estão relacionados com aumento na ocorrência de complexos convectivos de mesoescala na região, sistemas que comumente desencadeiam chuvas intensas e tempestades de raios (VELASCO; FRITSCH, 1987). Sendo assim, a variabilidade interanual causada por eventos de El Niño (La Niña), está relacionada com maior (menor) precipitação e precipitação extrema na região Sul do Brasil (GARREAUD et al., 2009; GRIMM, 2011; GRIMM; BARROS; DOYLE, 2000).

Outro fator bastante importante para a climatologia da região é a ocorrência de ciclones próximos à costa. Apesar de possuírem estruturas verticais e processos de formação distintos (REBOITA et al., 2017), todos os tipos de ciclones (extratropicais, subtropicais e tropicais) apresentam potenciais impactos para as populações, pois são responsáveis por chuvas intensas e velocidades elevadas de ventos. Nas regiões costeiras, ventos fortes causados por sistemas ciclônicos podem levar a repentinas sobre-elevações do nível do mar (CAMPOS; CAMARGO; HARARI, 2010), ao passo que a perturbação causada pelos ventos

nos oceanos pode resultar na formação de ondas de grandes amplitudes. Esses eventos estão associados com múltiplos impactos para as regiões costeiras, como erosão de praias, inundações costeiras, destruição de infraestrutura e inavegabilidade, pondo em risco atividades econômicas, como atividade a portuária e pesqueira.

A região do Atlântico Sul próxima à costa do Brasil é uma das áreas de mais intensa ciclogênese no Atlântico Sul, onde nota-se a grande frequência de ciclones subtropicais e extratropicais, esse último tipo sendo o mais frequente (REBOITA; ROCHA; AMBRIZZI, 2012; REBOITA et al., 2010). A formação de ciclones subtropicais na região está associada com quebra de ondas de Rossby e ciclogênese orográfica na jusante dos Andes, sobre a Corrente do Brasil (EVANS; BRAUN, 2012). Apesar do baixo fornecimento de umidade para a ciclogênese, o transporte de umidade proveniente da região amazônica e de áreas tropicais do Hemisfério Norte alimenta os processos convectivos pela liberação de calor latente, favorecendo a formação de ciclones extratropicais (GOZZO et al., 2014). Apesar de mais frequentes durante o verão, o aumento na taxa de fluxos turbulentos durante o outono na área, associado com menor cisalhamento vertical, são responsáveis pela ocorrência de ciclones extratropicais mais intensos durante essa época do ano (GOZZO et al., 2014). O Atlântico Sul é a única bacia oceânica onde não há uma ocorrência periódica de Ciclones Tropicais. Esse fato pode ser atribuído ao alto cisalhamento vertical do vento na área, associado com a ocorrência de temperaturas da superfície do mar relativamente baixas (PEZZA; SIMMONDS, 2005; VIANNA et al., 2010). A única exceção registrada foi o Furacão Catarina, que levantou possíveis questões sobre sua relação com as mudanças climáticas.

Analisando projeções futuras para o clima da região, vemos que o cenário das mudanças climáticas apresenta um fator de risco para o Sul do Brasil, apesar da literatura no assunto ainda ser relativamente escassa. Primeiramente, há indícios de que o estado climático do planeta migre para um com um padrão de maior frequência de eventos de El Niño (MEEHL et al., 2000), ao passo que eventos mais intensos e duradouros devem se tornar mais comuns, em resposta ao aumento nas concentrações atmosféricas de gases do efeito estufa (CAI et al., 2014; TRENBERTH; HOAR, 1996). Tais fatores sugerem um futuro com mudanças nos índices de precipitação na região, tal como eventos de precipitação extrema mais frequentes e/ou intensos. Apesar de haver um consenso entre modelos quanto o aumento nas temperaturas médias da região, ao longo do século XXI, o mesmo não ocorre quanto aos índices de precipitação (CHOU et al., 2014; MARENGO et al., 2012; NUÑEZ; SOLMAN; CABRÉ, 2009; RAMOS DA SILVA; HAAS, 2016). Portanto, é evidente a necessidade de projeções regionais de alta resolução do clima na região Sul do Brasil, possibilitando uma análise mais robusta da ocorrência de eventos extremos na região. As projeções atuais ainda não permitem representar os fenômenos de mesoescala que são de extrema importância para as estimativas locais. Este estudo tem como objetivo aplicar uma metodologia nesta escala.

1.2   OBJETIVOS

Nas seções abaixo estão descritos o objetivo geral e os objetivos específicos desta dissertação.

1.2.1 Objetivo Geral

O objetivo geral deste projeto é estabelecer uma metodologia para estudos climáticos para a região costeira do Sul do Brasil.

1.2.2 Objetivos Específicos

1. Identificar eventos meteorológicos extremos que tenham causados danos e prejuízos socioeconômicos no passado recente na área de estudo (2000 e 2018);

2. Realizar simulações numéricas dos eventos selecionados utilizando o *Ocean-Land-Atmosphere Model* (OLAM);

3. Avaliar o desempenho do modelo em simular os casos selecionados;

4. Identificar os *weather types* representativos da região de estudo;

5. Realizar o refinamento dinâmico dos *weather types*;

6. Analisar os campos atmosféricos relacionados aos *weather types*.

1.2.3 Perguntas de Pesquisa

1. O modelo OLAM é capaz de refinar os campos atmosféricos da região costeira Sul do Brasil e representar eventos extremos?

2. O refinamento híbrido (*i.e weather types* e dinâmico) pode ser aplicado para uma região costeira como a esta região de estudo?

3. Quais os principais padrões dos campos atmosféricos simulados para a região costeira sul do Brasil?

1.2.4 Hipóteses

1. A utilização do modelo OLAM com grades regionais de alta resolução permitirá a representação da circulação atmosférica na área de estudo, propiciando a simulação realística de eventos extremos.

2. A utilização de uma metodologia híbrida com o modelo OLAM com grades de alta resolução na região de estudo permitirá melhorar o entendimento dos fenômenos de mesoescala na região costeira do Sul do Brasil.

1.3 ORGANIZAÇÃO DOS RESULTADOS DA DISSERTAÇÃO

Além deste primeiro capítulo introdutório que estabelece o tema e os objetivos do trabalho, os resultados desta dissertação estão divididos em três capítulos subsequentes. No Capítulo 2 são apresentados os resultados das simulações dos eventos extremos com o modelo OLAM. No Capitulo 3 são apresentados os resultados da técnica de *downscaling* hibrido. No Capítulo 4 é realizada a discussão dos resultados e são apresentadas as conclusões desta dissertação.

2 NUMERICAL MODELING OF THE MAJOR EXTREME METEOROLOGICAL EVENTS NEAR THE COASTAL REGION OF SOUTHERN BRAZIL

Nesse capítulo encontra-se o artigo de mesmo nome, submetido à revista *Monthly Weather Review*.

Numerical modeling of the major extreme meteorological events near the coastal region of southern Brazil

D. C. Souza[1] and R. Ramos da Silva[1]

[1]Climate and Meteorology Laboratory, Department of Physics, Federal University of Santa Catarina, Florianópolis, SC, Brazil.

Corresponding author: Danilo Souza (danilo.oceano@gmail.com)

Abstract

Coastal regions are generally densely populated and have become highly vulnerable to the occurrence of extreme events. In recent years, Brazil's southern coastal region has been affected by several different extreme weather events. Those events have caused coastal flooding, with economic losses as well as fatalities. Understanding and improving the predictability of these events has become a major issue for the local population. In this study, a state-of-the-art numerical modeling was applied to this region to assess the model's ability to represent the major extreme events that occurred in recent years. The Ocean Land Atmosphere Model (OLAM) was applied to the region with a high resolution grid refinement technique capable of simultaneously representing global and local atmospheric phenomena. The main events that affected Brazil southern coastal region between 2000 and 2018 were detected and simulated. All selected events occurred associated with cyclonic and/or anticyclonic systems near the coastal region of the study area. Those systems were responsible for bringing heavy rain, strong winds and sea level rise, causing impacts for the coastal region. The results of the numerical simulations were compared with observational data to evaluate the model performance. The model simulated well the air temperature, sea level pressure, wind and precipitation fields. For the latter, the results were better for the most extreme cases. Finally, the results show that the methodology allowed for a detailed representation of sensible and latent heat fluxes for the region allowing a better representation of the local mesoscale features.

2.1 INTRODUCTION

In the near future it is expected a global increase in the frequency and intensity of extreme weather and climate events (STOCKER et al., 2013). This poses a concerning scenario for our society, as extreme events can be a source of risk for populations. For instance, between 1998 and 2017, climate related hazards accounted for more than US\$ 2 trillion of losses worldwide, affecting more than four billion people (UNISDR; CRED, 2017). Societal changes during the previous century such as the rapidly increase of human population in coastal and low-lying areas made the communities more exposed and vulnerable to the impacts of such extreme events (EASTERLING et al., 2000; KARL, T. R., & EASTERLING, 1999; KUNKEL; PIELKE; CHANGNON, 1999; MECHLER; BOUWER, 2015). In developing countries, extreme events are a great source of fatalities and economic losses as the population and governments are less resilient, adapted and prepared (HANDMER et al., 2012).

The southern region of Brazil (SBr), composed by the states of Paraná (PR), Santa Catarina (SC) and Rio Grande do Sul (RS), is a region which suffered very high economic losses due to the meteorological extreme events of recent years (WORLD BANK, 2016). The coastal region of those states is inhabited by about 3.2 million people and develop important economic and technological activities (STROHAECKERI, 2004), as well as 21% of all Brazilian seaports. Impacts of extreme events in this area can be devastating, as urbanized coastal low-lying areas are vulnerable to events such as extreme precipitations and storm surges. Recent examples of such events were the Catarina Hurricane in 2004 and the Itajaí Valley flooding in 2008. Both events directly affected millions of people due to inundations,

landslides and high wind speeds that caused property loss, heavy damage to local infrastructure and fatalities (HERMANN, 2014; NUNES; DA SILVA, 2013; WORLD BANK, 2016).

The extreme weather events at this region are caused by phenomena of large, regional and local scales. For instance, planetary Rossby waves can affect the propagation of mid-latitude cold fronts. Furthermore, remote teleconnections such as the influence of the El-Niño Southern Oscillation conditions of the Pacific ocean shows a high correlation with extreme events over the SBr (GRIMM, 2003). The region has an interface with the Atlantic Ocean and therefore is influenced by the marine Sea Surface Temperature (SST) conditions (RODRIGUES; YNOUE, 2016). Locally, the topography, the sea-ocean interface and the surface heterogeneity can set up mesoscale circulations that may affect the meteorological extreme events (RODRIGUES; YNOUE, 2016).

Climatologically, the southern portion of Brazil is distinct of the other regions of the country as it is located outside of the tropics. Its location, between the Tropic of Capricorn and approximately 35°S, configures a subtropical climate regime, in which monthly precipitation rates and heavy precipitation events are evenly distributed around the year (RAO; HADA, 1990; TEIXEIRA; SATYAMURTY, 2007). Between 20% to 30% of annual precipitation in the region is due to extratropical cyclones (EC) occurring in the vicinity of this area (REBOITA et al., 2018). These systems are important for local weather as they cause cloud formation and thus precipitation and are often associated with strong winds and changes in temperature. Also, the EC are responsible for occurrence of high sea waves (extreme sea waves, in some cases) and storm surges in the Brazilian coast, triggering episodes of coastal

flooding and beach erosion (ALBUQUERQUE et al., 2018; CAMPOS; CAMARGO; HARARI, 2010; GOMES DA SILVA et al., 2016; GUIMARÃES; FARINA; TOLDO, 2014; MACHADO et al., 2010; PARISE; CALLIARI; KRUSCHE, 2009; PARISE; FARINA, 2012).

The western South Atlantic Ocean (SAO) is very cyclogenetic and there are three preferable regions for EC genesis (Figure 2-1 A): south-southeast Brazil (RG1), extreme south Brazil and Uruguay (RG2), and southeast Argentina (RG3) near 45°S (GRAMCIANINOV; HODGES; CAMARGO, 2019; HOSKINS; HODGES, 2005; MENDES et al., 2010; REBOITA; ROCHA; AMBRIZZI, 2012; SINCLAIR, 1995). The geostrophic flow resulting from the interaction between a marine cyclone and the continental anticyclone, moving from the South Pacific to Southern Argentina, is the mechanism for the passage of cold fronts over coastal SBr (COMPAGNUCCI; SALLES, 1997; GARREAUD, 2000). Those frontal systems are the main mechanism of precipitation formation over SBr during the colder months (GARREAUD et al., 2009), while events of explosive cyclogenesis may trigger extreme cold surges in the region (LUPO et al., 2001). The main mechanisms contributing to cyclogenesis in the western SAO are the transient mid-upper level troughs that move from the Pacific to the Atlantic Ocean, the South American Low Level Jet (SALLJ; RG1 and RG2), the latent and sensible heat transfer from the oceans (RG1 and RG3), and the baroclinic instability (GAN; RAO, 1994, 1991; HOSKINS; HODGES, 2005; REBOITA; ROCHA; AMBRIZZI, 2012; VERA; VIGLIAROLO; BERBERY, 2002).

The SALLJ is a low level jet, east of the Andes, that transports moisture from the Amazon basin to southern latitudes of the subtropical South America (MARENGO et al., 2004; SALIO, 2002; SELUCHI et al., 2003; SELUCHI; MARENGO, 2000). The moisture

transport is related with a change in the easterly trade winds direction (from northeast to southwest) as they are blocked by the Andes mountains (MARENGO et al., 2004; SELUCHI; MARENGO, 2000). This phenomena is present all year long, although presents high day to day variability (POVEDA; JARAMILLO; VALLEJO, 2014; SELUCHI; MARENGO, 2000). Episodes of SALLJ explains about 20% to 40% of summertime precipitation in coastal SBr (SALIO 2002, Figure 17) and are important mechanisms for development of mesoscale convective systems in the southeast South America (SALIO; NICOLINI; ZIPSER, 2007).

Important not only for the SALLJ but also for the local water cycle, the South Atlantic Anticyclone (SAAC) dominates the low level circulation over the western SAO (GARREAUD et al., 2009). As a result from this circulation, the predominant wind direction in the coast of SBr is northeasterly with occasional changes to southerly, related mostly to the cyclonic activity in the region.

One of the mechanisms influencing cyclogenesis near the SBr coast is the latent and sensible heat fluxes from the oceans to the atmosphere (REBOITA; ROCHA; AMBRIZZI, 2012). The ocean conditions are influenced by the Brazil-Malvinas confluence near SBr coast which is responsible for high horizontal SST gradients (GORDON, 1989; STRAMMA, 1989). Its exact interface location varies seasonally, being more southward during summer and more northward during winter (GORDON, 1989). As a result, its position affects the local SST gradient at time of cyclogenesis (GRAMCIANINOV; HODGES; CAMARGO, 2019), the moisture transport towards the continent and the local sea-breeze circulations.
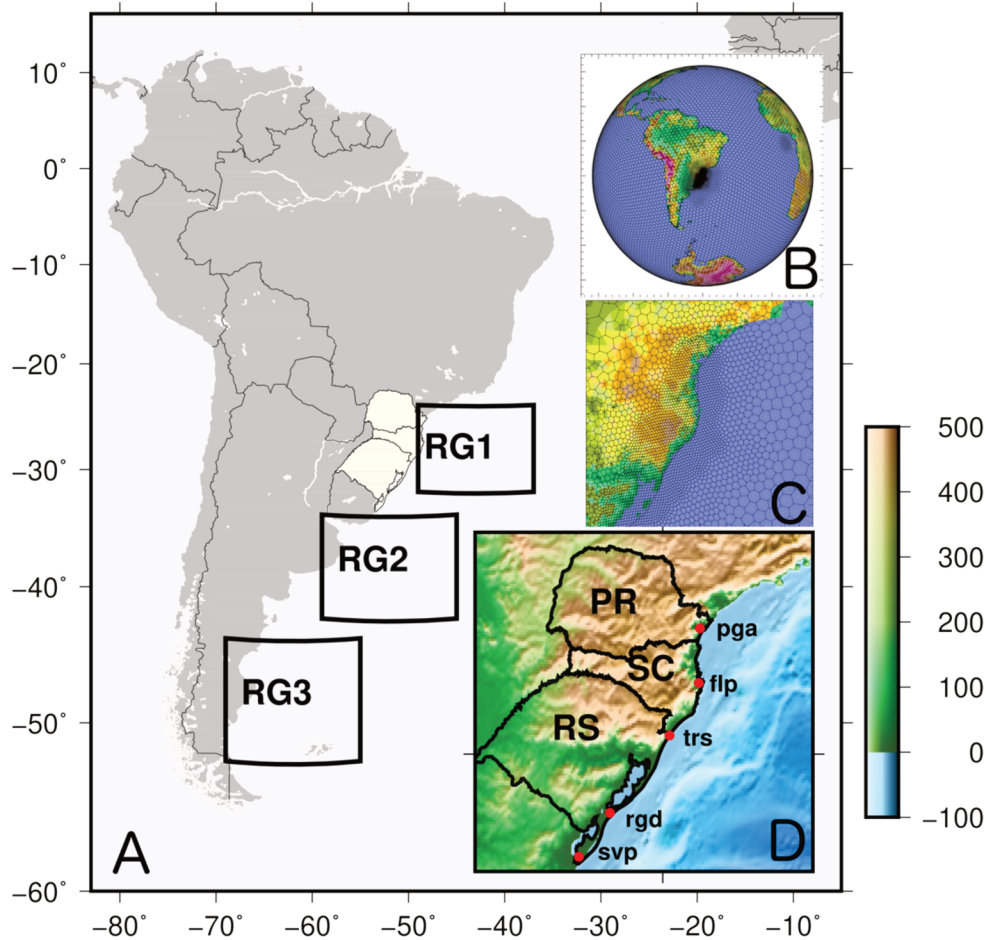
Figure 2-1. South America, the southern Brazil study area (highlighted) and the three cyclogenetic regions in the western South Atlantic (see text for details). B) global computational grid used for the OLAM numerical experiments. C) High resolution regional grid centered on the coastal region of southern Brazil. D) Southern Brazil topography (meters), states boarders and INPE meteorological stations used for model validation (red dots). The abbreviations denote the cities were the stations are located: Paranaguá (pga), Florianópolis (flp), Torres (trs), Rio Grande (rgd) and Santa Vitoria do Palmar (svp).

As in any coastal region, important local-scale phenomena are the land and sea breeze, caused by differential heating of sea-land surfaces. Other local scale features affecting the water cycle are the topography and the heterogeneous surface, marked by the presence of urban areas surrounded by ecosystems such as tropical forests and mangroves, especially in the SC state (Figure 2-1 D). Also, each state coastline presents distinct characteristics: the PR coast is dominated by large estuarine complexes, in SC there are many open beaches, islands, bays, inlets and islands as well as a narrow coastal plain, while the RS coast is more uniform

although it contains the most extensive lagoon system in South America (SHORT; KLEIN, 2016). Those features induce mesoscale circulations that affect the weather.

Furthermore, a synoptic scale phenomenon that influence the precipitation in the region is the South Atlantic Convergence Zone (SACZ), as the SBr coast is located in its climatological position (GARREAUD et al., 2009). The SACZ is the summertime diagonal cloudiness band with NW-SE (Amazon-South Atlantic) orientation (CARVALHO; JONES; LIEBMANN, 2004; KODAMA, 1992). The SACZ formation is attributed to a Rossby wave train originated in the Central Pacific (LIEBMANN et al., 1999; VAN DER WIEL et al., 2015) and/or to the atmospheric response to the localized heat source associated to the precipitation in the Amazon and Central Brazil during the summer monsoon in South America (FIGUEROA; SATYAMURTY; DA SILVA DIAS, 1995). Enhancement (decrease) of SACZ activity is also associated with excessive precipitation (dry conditions) over coastal SBr (FERNANDES; RODRIGUES, 2018; GARREAUD et al., 2009).

Recent studies assessed future regional changes in South American climate. Model ensembles indicate an intensification of the SAAC which may reduce SACZ frequency due to its blocking effect on cold fronts that otherwise would reach lower latitudes (CHOU et al., 2014). It is also expected and increase in the intensity and frequency of the SALLJ (MARENGO et al., 2009). Nevertheless, contrary to what would be expected, mean cyclogenesis in the SAO might become less active, especially for the most intense systems (KRÜGER et al., 2012; REBOITA et al., 2018).

However, those changes are quite heterogeneous for the SAO area. In fact for the two cyclogenetic foci located closest to the Brazilian coast (RG1 and RG2), the climate

projections indicate that a possible increase in the cyclogenesis (REBOITA et al., 2018). Furthermore, the mean reduction in mean SAO cyclogenesis might be related to a poleward shift of the upper polar jet (REBOITA et al., 2018) and the enhancement of winds related to the SAAC (KRÜGER et al., 2012). Overall, the climate model projections suggest an increase in temperature and precipitation for coastal SBr, with wetter summers and dryer winters (CHOU et al., 2014; KRÜGER et al., 2012; RAMOS DA SILVA; HAAS, 2016), and more frequent and intense extreme precipitation events, increasing risk of floods in the region (CHOU et al., 2014; MARENGO et al., 2009; NUÑEZ; SOLMAN; CABRÉ, 2009).

As extreme events in the southern region of Brazil, such as the Catarina Hurricane and the Itajaí Valley flooding in 2008, had caused very high economic and societal costs (HERMANN, 2014; NUNES; DA SILVA, 2013; WORLD BANK, 2016), the responsible authorities need a local assessment of possible future occurrence of similar extreme events. The main tools used in long-term climatic studies are General Circulation Models (GCMs) which have coarser resolutions from 50 km to 450 km, that do not fully resolve the land use, land-sea distribution and the complex topography of South America (TAYLOR; STOUFFER; MEEHL, 2012). Also, this level of resolution are not enough to explicitly simulate mesoscale processes, the smaller extratropical cyclones (REBOITA et al., 2018) and do not simulate well extreme precipitation events (FARNHAM; DOSS-GOLLIN; LALL, 2018). In order to achieve more refined spatial resolutions, two techniques can be used: dynamical downscaling, a process that comprehends nesting a Regional Climate Model (RCM) into a GCM, or the statistical downscaling of GCM output.

The major studies using RCM that have been made in order to estimate future occurrence of extreme events in South America adopted grid space from 40 km to 50 km

(Ambrizzi et al. 2019 and herein references) which do not fully resolve the effects of complex topography of South America and the details of the SBr surface heterogeneity and coastline (Figure 2-1 D). Also, this methodology applies a one-way communication between the GCM and the RCM and thus the local-scale phenomena do not interact with the large-scale circulation. Therefore, novel studies attempting to address future projections of extreme events for the coastal region of southern Brazil would benefit from increased horizontal model resolution and scales interaction.

The novelty of the Ocean-Land Atmosphere Model (OLAM; WALKO; AVISSAR, 2008a, 2008b) is its ability to simulate both local scale weather as well as global scale phenomena simultaneously (Figure 2-1 B). This is achieved by its refining grids method. The model uses a global icosahedric grid as well as high resolution grids and therefore allows a two-way communication between the different large scale and mesoscale processes. The refining grid methodology is useful for saving computational power when large scale needs to be represented while still achieving fine resolutions on regions of interest (MEDVIGY et al., 2013; WALKO; AVISSAR, 2011). Also, Medvigy et al. (2008) demonstrated that a better representation of South American topography by this methodology allowed a more realistic representation of the South America climate under ENSO conditions.

The OLAM model have already been used to estimate the effects of global oceans warming on South American climate (RAMOS DA SILVA; HAAS, 2016) and the effects of the Amazon deforestation on climate extremes in South America (MEDVIGY; WALKO; AVISSAR, 2012) and weather forecasting and regional climate estimates for the Amazon region (RAMOS DA SILVA et al., 2014a, 2014b). Overall, the model provides a good

representation of major coastal convective systems (RAMOS DA SILVA et al., 2014a). Remarkably, a study from Khanna et al. (2017) demonstrated the effects of Amazon deforestation on regional atmospheric circulation, highlighting the utility of the OLAM variable resolution for studies of local scale phenomena.

The goal of the current study is to develop a methodology for meteorological and climate studies for the coastal region of southern Brazil. This is the first study to use a high resolution regional grid to study the major extreme meteorological events in this area. Here, we evaluate the OLAM model capability of downscaling meteorological fields from a coarser resolution model during the occurrence of several extreme meteorological events that affected the study area. The proposed methodology allows the representation of different scale phenomena, from large scale features to local scale circulations. For the analysis, we selected 12 extreme regional events that occurred since the beginning of the current century. We describe the meteorological forcing related to each event and compare the simulated results with observed meteorological and reanalysis data.

2.2 METHODOLOGY

2.2.1 Numerical model description

The OLAM model was developed as an evolution of the Regional Atmospheric Modeling System (RAMS) so its physical parametrizations and computing structure was designed upon on the latter (WALKO; AVISSAR, 2008a, 2008b). The RAMS model enables the achievement of high resolution atmospheric simulations by the use of a nesting grids technique, making it very versatile (PIELKE et al., 1992). However, in the RAMS model the spatial scale of a simulation is limited to regional domains. Capable of performing global

simulations with high resolution regional grids, the OLAM model opens up new possibilities for numerical studies.

The model solves the full non-hydrostatic compressible Navier-Stokes equations using the finite volume method. The grid elements are non-structured hexagons that can be further divided in order to increase horizontal resolution. This makes the OLAM model suited for mesoscale studies, as it can represent the interactions between large-scale phenomena and mesoscale processes simultaneously without adding errors from lateral boundary conditions (WALKO; AVISSAR, 2008a, 2008b).

2.2.2 Extreme events cases selection

Due to the relativeness of the word extreme, the definition of what is an extreme event can often be vague and confuse. Thus, the widespread definition of an event extreme derives from climate statistics. In this case, an extreme event can be identified as some variable exceedance of a certain threshold, for example, an amount of rain above the 90th percentile of historical rainfall ((FRICH et al., 2002). However, sometimes the occurrence of an event, classified as extreme by this definition, might not really represent a damaging or severe event for society. For example, a hydroclimate event of persistent or heavy rain might not cause flooding due to previous river level to be low, thus it might not necessarily cause significant impacts. As our goal was to simulate the main events for the study area based on the impacts felt by society, a distinct approach had to be considered.

We selected cases of extreme events for the coastal region of southern Brazil through the review of online news portals (Table 2-1). This research returned a great amount of damaging events that occurred in the study area and we selected only the major events of 21st

century. We considered as major event the cases that 1) were associated with economic losses for the affected communities, 2) impacted at least a region in the study area (i. e., at least more than one city near the coast) and 3) were reported more than once by local news. Furthermore, we also performed a similar research of extreme events in the scientific literature. This was not our primary source for the chosen case study due to the fact that not all extreme events that occur are indeed studied by the scientific community.

In this study, we defined the start and end days of an event based on the reports. For example, as reported days of consecutive rain or occurrence of high sea waves in one place located in the study region. The approximated peak time of a given event was identified using distinct criteria. Firstly, if the event were already described in the literature, we used the reported peak time. For the remaining cases, we firstly identified what kind of impacts were associated with the event (for example, heavy precipitation) and then analyzed the corresponding meteorological data for the moment of maximum intensity of rain and/or moment of maximum wind speed. We also analyzed the near surface circulation from the National Center for Environmental Protection (NCEP) Reanalysis 2 (SAHA et al., 2014) and the Climatic Analysis Monitoring Bulletin (CLIMANÁLISE) from the Brazilian National Institute for Space Research Center of Weather Forecast and Climate Studies (INPE-CPTEC) so we could check the dynamical atmospheric phenomena leading to the respective extreme event. The CLIMANÁLISE bulletin can be found at: http://climanalise.cptec.inpe.br/~rclimanl/boletim/. This bulletin ranges from 1994 to 2014, so for analysis of events occurred later than 2014 we used the INPE-CPTEC technical bulletin, available at http://tempo.cptec.inpe.br/boletimtecnico/pt.

2.2.3 Numerical experiment design

In order to simulate the selected events, we set the OLAM model with a global grid (Figure 2-1 B) with high resolution in the study area of coastal region of SBr (Figure 2-1 C). There were five levels of refining for the regional grid, apart from the global. This approach allowed the model to represent the major features of this coastal region. The spatial grid size varied from approximately 200 km for the global grid, increasing from 100 km through 50 km, 25 km, 12 km, and finally 6 km. This level of refinement allows representing the mesoscale features in this ocean-land interface. In the vertical, the model was set with 49 atmospheric levels, with resolutions ranging from 60 m in the lower level up to 2000 m in the upper stratospheric levels that reached 35 km high. For the soil, a total of 21 levels were used with high resolution near the surface up to five meters depth. In order to maintain numerical stability, we adopted a 10 second time step, which is applied for the whole domain.

For each event, we set up the simulations to start three days prior to the day of peak time for the model adjustment. Also, the experiments were set to finish six days after the peak. Therefore, the experiments had time length of 10 days in total, except for the events 7 and 12. During event 7 (Itajai-Valley Floodings in 2008), we included an extra day before the event start because there was also large precipitation in the previous day to the peak. For the event 12 (Catarina Hurricane), we considered the peak time as the landfall moment. In this case, we started the simulations 10 days prior to this in order to capture the whole life cycle of this system, from cyclone genesis to landfall. This was important to better represent the atmospheric dynamics associated with this process and the occurring in the study area in the cyclogenesis early stages.

The physical parameterizations adopted included the cumulus convection parameterization (GRELL; FREITAS, 2014), the diffusion coefficient for atmospheric fluxes parameterization (SMAGORINSKY, 1963), the cloud microphysics parameterization (MEYERS et al., 1997; WALKO et al., 1995) and the short and long-wave radiation parameterization (MLAWER et al., 1997). Turbulent fluxes related to soil and vegetation cover were calculated through the use of a sub-model, the Land Ecosystem-Atmosphere Feedback Model (LEAF-3 - WALKO et al., 2000). Global data of topography, vegetation types, and soil texture are used as surface boundary conditions for the respective soil-vegetation sub-models (LEAF-3).

2.2.4 Data

The initial atmospheric conditions used to force the model were the wind fields, geo-potential height, air temperature and relative air humidity, from the NCEP Climate Forecast System Reanalysis (CFSR). Those variables were updated every 6 hours by the model for a light nudging on the coarser grid. The CFSR is a global 6-hourly reanalysis product, ranging from 1979 to present days, with approximately 38 km of global atmospheric resolution. It also provides full coupling between atmosphere and oceans, a sea-ice model and assimilation of satellite radiance data (SAHA et al., 2010, 2014). An assessment of the CFSR performance can be found at Ebisuzaki and Zhang, (2011) and at Wang et al. (2011).

The oceanic boundary condition used was the Optimum Interpolation Sea Surface Temperature (OISST) from the National Oceanic and Atmospheric Administration (NOAA). The NOAA OISST is a weekly 1/4° resolution analysis product ranging from 1981 to the present that combines distinct observation sources such as buoys, ships and satellites and then apply an adjustment in order to remove sensor bias and compensate for differences in

platform measurements (REYNOLDS et al., 2002, 2007). The weekly data is constructed from satellite images that due to clouds obstructions, the weekly superposition is able to get the total global surface (REYNOLDS; SMITH, 1994).

For model performance assessment at local level, we compared the simulated atmospheric variables with observational data from available meteorological stations for the study area (Figure 2-1 D). The data came from the National Institute of Meteorology [*Instituto Nacional de Meteorologia* (INMET)]. The INMET stations used for analysis were located at (city – state) Paranaguá – PR (-25.53 -48.51); Florianópolis – SC (-27.58 -48.56), Torres – RS (-29.35 -49.73), Rio Grande – RS (-32.03 -52.11) and Santa Vitória do Palmar – RS (-35.51 -53.35). These stations were chosen because they presented the most homogenous data available in the region affected by the selected events.

Another model evaluation assessment was performed using atmospheric fields capable of covering both land and oceans. For this evaluation, we compared the model data with precipitation fields from the Tropical Rainfall Measuring Mission (TRMM) and the Global Precipitation Measurement (GPM) missions and with temperature fields from the Modern-Era Retrospective analysis for Research and Applications, Version 2 (MERRA-2). The TRMM precipitation product integrates data from five distinct satellite sensors in order to provide gridded data ranging from 50°N to 50°S in a 0.25° grid, with 3-hourly instantaneous values (HUFFMAN et al., 2007). The TRMM mission ranged from 1997 to 2015, and then it was replaced by the GPM mission. The GPM data uses the IMERG algorithm, which aggregates multi-satellite data to provide 0.1° global half-hourly precipitation fields (HOU et al., 2014). In those cases, we used the 3B42RTv7 and the 3IMERGHHv06 TRMM and GPM

products, respectively. The MERRA-2 reanalysis product includes assimilation of observational data from a wide variety of sources such as gauge stations and satellite data, so the temperature fields are provided 3-hourly in a 0.5° x 0.625° grid (GELARO et al., 2017). A better description of those products can be found at (BUCHARD et al., 2017; DRAPER; REICHLE; KOSTER, 2018; GEBREMICHAEL; KRAJEWSKI, 2004; HUFFMAN et al., 2007; LIU, 2016; RANDLES et al., 2017; WANG et al., 2017).

Statistical analyses were performed to evaluate the model performance. Scatterplot regression curve analysis was obtained between meteorological stations data and model results for the temperature and precipitation. Spatial correlation for the total precipitation and SLP fields were obtained after interpolation of model results into the same grid points of the observed fields.

2.3   RESULTS

This section presents the results of the determination of the main extreme weather events in the study region; a brief description of the atmospheric conditions of occurrence and the results of the OLAM model numerical simulations.

2.3.1   Extreme events selection

The extreme events date of occurrence, associated impacts and atmospheric dynamics are presented in Table 2-1. We selected the major 12 extreme events for the recent past (i.e. 2000-2018). Most of the selected cases were extreme events that damaged urban areas and lead to economic losses for the affected cities. The remaining events were associated with extreme wind speeds, storm surges and high waves that impacted the coastal

infrastructure. Some of the selected events were already mentioned in the literature, such as the occurrence of with high waves (events 4, 6, 9, 10 and 11), strong winds (events 4, 8 and 12) and heavy rainfall (events 7 and 8). Four events (1, 2, 3 and 5) were not already been mentioned by the scientific literature, all of them being related with excessive precipitation. Therefore, our analysis resulted in the selection of events with a combination of hazards.

Event occurrence was uniform all year long, with no clear seasonal pattern. The two most frequent event types, heavy rain (HR) and high wind speeds (HW), occurred preferably during warmer and colder months of the year, respectively. In general, during the austral winter cold fronts pass through the region, while during the summer months strong local convection in association with synoptic scale phenomena (Frontal systems, SALLJ and SACZ) enhances the strength of the local thunderstorms.

All the selected events occurred in association with cyclonic or anti-cyclonic activity near the coastal area of SBr. Half of the events were related to cyclonic activity (one of them being a hurricane), nearly half with both cyclonic and anti-cyclonic transitory activity and a single event was related only to a stationary anticyclone. It was already expected a high number of cyclogenetic events related to impacts such as erosion and coastal flooding. However, the impacts of anticyclonic systems are often not analyzed by the literature, although the orographic rain caused by the easterly flow from the anticyclone together with the mountains close to the coast in this region results in flash floods events (RODRIGUES; YNOUE, 2016).

2.3.2 Event description

In this session, we provide a brief description of each of the twelve events focusing on the predominant atmospheric circulation.

Prior to E01 start (9th Jan 2018) there was anticyclonic conditions near the South and Southeast regions of Brazil. This system acted together with the SALLJ, causing moisture advection to the coastal region of SBr. The extra moisture and also the warm air from the tropics increased instability, further leading to heavy and continuous rain, especially in coastal SC. After the first day (11th Jan), the anticyclone moved away from the coastal zone of Brazil and a low pressure area developed over SBr (12th Jan), which increased the instability in the area. During those days, the rain caused major flooding and landslides in SC central and north coastal region. Close to the event end (14th Jan), there was cyclogenesis in RG2, associated with moisture convergence over SC and PR producing further precipitation. Although precipitation levels were not high, the previous conditions might have contributed for landslides and further damage in the affected cities.

In days that preceded E02 an cyclogenesis event in RG2 region bought precipitation to the SBr coastal region. In the first day of the event (01st Jun 2017) there was cyclogenesis in RG1, associated with instability in the coastal region of SC and RS states and isolated rainfall episodes. As in the previous event, the instability over the region was favored by the SALLJ moisture transport. After the EC moved eastward, there was post-frontal anticyclogenesis (03th Jun) in the coast near the southern and southeastern regions of Brazil. Three days after the event start (04th Jun) there was moisture convergence over many areas of the SBr region, resulting from the combination of northerly/northeasterly flow, related to the marine anticyclone, and with the passage of a cold front due to a cyclogenesis event in RG3.

The precipitation associated with this event displaced thousands of people in the RS state and although most of the damages were reported for the northern part of the state, the coastal area was also affected, with a causality been reported. Furthermore, in the SC capital there were reports of several places with heavy flooding.

Table 2-1. The extreme events (E) selected for the numerical experiments and indicate start, ending and peak (approximated) date (dd/mm/aa). Peak hours are given in UTC. The impacts were: heavy/persistent rainfall (HR), strong winds (SWd), storm surges (SS), high waves (HW) and extreme cold temperatures (EC). The atmospheric dynamic (AD) associated with the events were either or both anticyclonic (AC) or cyclone activity (CS). Scientific literature supporting the classification of an event as an extreme one is indicated, when available.

E	Year	Start	Ending	Peak	Impacts	AD	Ref.
1	2018	10th Jan	16th Jan	11th Jan 18Z	HR	AC, CS	
2	2017	01th Jun	07th Jun	04th Jun 21Z	HR	AC, CS	
3	2011	06th Sep	09th Sep	08th Sep 09Z	HR	CS	
4	2011	25th May	30th May	28th May 06Z	SWd, HW, SS	CS	Candella & Souza (2013)
5	2011	18th Jan	23th Jan	21th Jan 21Z	HR	AC, CS	
6	2010	09th Apr	11th Apr	10th Apr 09Z	HR, SWd, HW	AC, CS	Silva (2013)
7	2008	18th Nov	25th Nov	22th Nov 12Z	HR	AC	Fraga (2009); Minuzzi & Rodrigues (2008); Dos Santos et al. (2014)
8	2008	02th May	04th May	03th May 21Z	HR, SWd, HW	AC, C	Guimarães et al. (2014); Sausen et al. (2009)
9	2007	28th Jul	30th Jul	28th Jul 12Z	HW	CS	Guimarães et al. (2014)
10	2006	01th Sep	06th Sep	03th Sep 18Z	HW, EC	CS	Guimarães et al. (2014); Parise et al. (2009)
11	2005	08th Aug	13th Aug	10th Aug 09Z	SWd, HW	AC, CS	Melo Filho et al. (2006)
12	2004	18th Mar	28th Mar	28th Mar 06Z	HR, SWd, SS	CS	Dias Pinto & Da Rocha, 2011); Pezza & Simmonds (2005)

The E03 was related with heavy rain in the SC state, in contrast with RS and PR states, that were experiencing dry conditions. The position of the anticyclone lead to cold air advection from higher latitudes and favored subsidence over SBr. Then, a cold front moved from the south of RS, associated with a EC in the extreme south of Argentina, became stationary over the southernmost part of PR (06th Sep 2011). This system was favored by an increased intensity of the subtropical jet and lead to high amounts of accumulated precipitation over various localities of SC state.

Although heavy rainfall for some localities was reported during E04, the main impacts were high oceanic waves, strong winds and storm surge. The event started with a cyclogenesis over RG2 (25th may 2011), favored by the position of subtropical jet over Uruguay and Argentina, which increased instability over SBr. The EC initially moved southeastward, as most cyclones in the SAO (HOSKINS; HODGES, 2005), but later on (27th May) it began to move northwestward and presented hybrid features, being classified as subtropical (CANDELLA; SOUZA, 2013). The cyclone would retake its normal eastward and poleward track only two days later (29th May). It was reported strong winds and restless sea for all states in southern and southeastern Brazil. The maximum wave height reached 10m in some localities, the highest values registered for the buoys located in the region, while wind speeds over the ocean reached values as high as 100 km/h (CANDELLA; SOUZA, 2013).

The E05 resulted from the combination of various phenomena. Firstly, the CPTEC-INPE reported a SACZ condition (18th Jan 2011), with enhanced convection due to the presence of the SALLJ and middle-level cyclonic circulation over SBr, converging moisture to the area. Pinheiro (2011) highlighted the contribution of moisture advection from easterly winds in the coast of SC, which were further trapped due to the local topography. The easterly winds were related to an anticyclone located near southeastern Uruguay coastal region. The cumulative effect of those phenomena resulted in heavy precipitation for the southern and southeastern regions of Brazil. Furthermore, there was cyclogenesis over RG1 (20th Jan), associated with more episodes of heavy rainfall over the PR and SC states. After the poleward displacement of the EC there was one more event of anticyclogenesis close to the coast of southeastern Uruguay (21th Jan). Again, the easterly flow over the coast of SC triggered precipitation over the area.

The E06 was related with strong cyclogenesis north of RG1, prior to the event start, and a post-frontal anticyclone located southeast of Argentina (7th June 2010). The EC was slow moving, staying over the latitude of the SC state for more than one day (8th-9th June). This resulted in an extensive fetch over the coastal region between SC and the northeast Brazilian coast, which generated extreme high waves that propagated to this part of the Brazilian coast (SILVA, 2013) and caused storm surges in some localities.

Considered to be the most extreme weather event for the SC up to this date, during the E07 record amounts of precipitation were registered for the northern and central regions of coastal SC. November 2008 was the wettest month ever recorded for the coastal northern region of SC while the 22nd/23rd presented the highest amounts of accumulated precipitation for a single day (MINUZZI; RODRIGUES, 2008). The event was caused by a persistent blocking condition over the western SAO and therefore easterly winds, associated with moisture transport from the ocean. There were already high values of accumulated precipitation for the three months prior to the event therefore there were already high levels of ground water. In the 21st a cold core high-level cyclonic vortex was positioned above SC and established dynamical and thermo-dynamical conditions that increased precipitation rates (Silva-Dias, 2008). Due to the excessive and continuous rain, flooding and landslides had occurred over large areas, affecting over 1.5 million people in 63 cities and causing over 100 fatalities (FRAGA, 2009).

The E08 was associated with a EC with an abnormal track, considered one of the stronger systems recorded for the study area (GUIMARÃES; FARINA; TOLDO, 2014). The cyclogenesis occurred in RG2 (2nd May 2008) but due to the presence of a blocking pattern,

the cyclone remained very close to the coast for two days. There were reported high southerly wind speeds and severe storms in the RS and SC coastal regions (SAUSEN et al., 2009) and numerical models indicated high waves, up to approximately 8m in the oceanic region near the RS northern coast (GUIMARÃES; FARINA; TOLDO, 2014).

The E09 was also one of the strongest EC recorded for the study area (Guimarães et al., 2014). However, in this case cyclogenesis occurred in the south at RG03 prior to the event date (26th July 2007). After genesis, the system had a slightly northward track, approaching the SBr coastal zone (until the 28th July). Although the system produced light precipitation, numerical models estimated that the swell generated waves of more than 8m high in the oceanic region near the RS southern coast (Guimarães et al., 2014) and the sea level rise contributed to major erosion episodes along the RS and SC coast.

The E10 presented similar characteristics to both E08 and E09, also being one of the extreme events reported by Guimarães et al. (2014). It was related to strong cyclogenesis in RG2 (2nd September 2006) that followed a southeastward trajectory and caused major erosion over the RS coast (PARISE; CALLIARI; KRUSCHE, 2009) and high southerly wind speeds over all coastal SBr. This EC is estimated to have generated waves of approximately 8m high in the oceanic region near the RS coast (GUIMARÃES; FARINA; TOLDO, 2014). There was also cold air incursions over most central-southern parts of Brazil, causing snowfall in some southern cities, a uncommon event in Brazil.

Prior to E11 there was cyclogenesis in RG2 with the EC having a southeasterly trajectory (5th August 2005). After this, there was anticyclogenesis over southern Argentina (7th August), and further cyclogenesis in RG2 (10th August). This combination of both EC and anticyclone resulted in an extensive south-southeast fetch in the western SAO. The resulting

swell had the highest wave heights recorded for the for the buoy in the oceanic area close to the SC coast (7.2m), for the period ranging from years 2002 to 2005 (MELO FILHO; HAMMES; FRANCO, 2006). The high windspeed caused by this system and the sea level rise caused coastal flooding and landslides in some cities.

The E12 is the Catarina Hurricane, the first hurricane ever reported in the SAO (MCTAGGART-COWAN et al., 2006), which caused losses of half billion US dollars for the Brazilian government and 11 deaths. The damage was caused by high wind speeds, of 150 km h^{-1} at the landfall location, high precipitation rates and storm surge. As a result, many cities were flooded and urban infrastructure was compromised displacing thousands of people. The hurricane began as an subtropical cyclone with genesis north of RG2 (20th March 2004) and an eastward trajectory. It undergone tropical transition three days later (23th March) and developed a westward track, making landfall in the 28th March (PEZZA; SIMMONDS, 2005). Normally, the oceanic and atmospheric conditions over SAO would suppress the development of tropical cyclones, however, the Catarina encountered an environment of low wind-shear and strong blocking conditions that were unprecedent in this region (PEZZA; SIMMONDS, 2005). As the hurricane moved westward, air-sea fluxes counterbalanced the relatively cool SST conditions and further favored the system intensification (PEREIRA FILHO et al., 2010).

2.3.3 Model results evaluation

Figure 2-2 shows the total accumulated precipitation comparison between the model results and the observations (TRMM and GPM) for each case study. The results show that for all events but E07, E08 and E12 the OLAM model underestimated the maximum values of accumulated precipitation. However, the spatial distribution was well represented, including

the regions where the maximum precipitation occurred, although in the estimated fields it was relatively more spread across the domain.

Statistical spatial correlation between the observed and simulated accumulated total precipitation presented heterogeneous results (Figure 2-2). The lowest spatial correlations were found for E02, E01, E09 and E08, respectively. For E01 and especially for E02 the low spatial correlation was due to the model not representing the rain over the ocean, as the precipitation over the coast of SC and PR states closely matched the GPM data. In both E06 and E10 there was no significant precipitation in the study area as much of the rain fell over the ocean or land areas further away from the coast. For the two most extreme events E07 and E12, and for E08, the comparison of precipitation spatial distribution in Figure 2-2 indicated that the OLAM model simulated higher values of accumulated precipitation than those estimated by the TRMM.

In order to evaluate the overall domain accumulated precipitation, we performed a comparison between the model and the TRMM/GPM spatial distributions (Figure 2-3). This comparison indicates that the model simulated well the precipitation behavior for most events as both modeled and estimated precipitation distributions presented similar slopes, except for E02 and E06 as the GPM/TRMM presented higher frequency for higher precipitation points. Both cases represent events in which the higher amounts of precipitation were located over the ocean. Nevertheless, the analysis confirms that the model underestimates the precipitation for most of the selected events, except for E07, E08 and E12, as previously discussed. For E07, one of the most extreme events, the OLAM simulated more precipitation than the TRMM estimates. However, for this case the TRMM may have underestimated the

precipitation. Overall, the results indicate that the setup chosen for the experiments is suited

for simulations of extreme precipitation events in the study area.
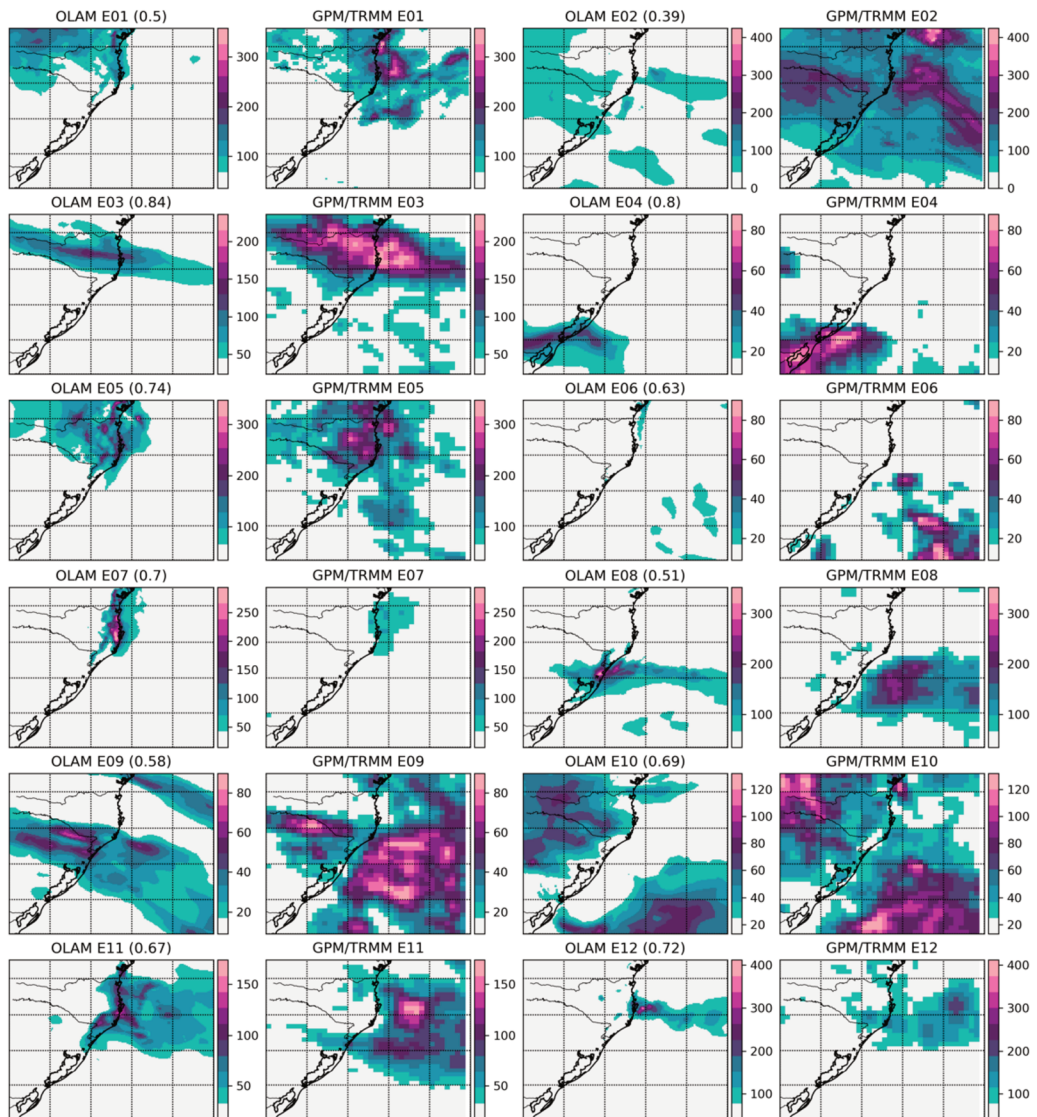
Figure 2-2. OLAM and TRMM/GPM accumulated precipitation for each selected extreme event. Due to availability of data, GPM fields was used for events 1 and 2 and the TRMM for the remaining events. The color intervals are specified in milliliters (mm) units. The values placed in parenthesis next to the titles are the statistical spatial correlation indices between the OLAM results and the TRMM/GPM estimates (0.65 mean, 0.13 standard deviation).
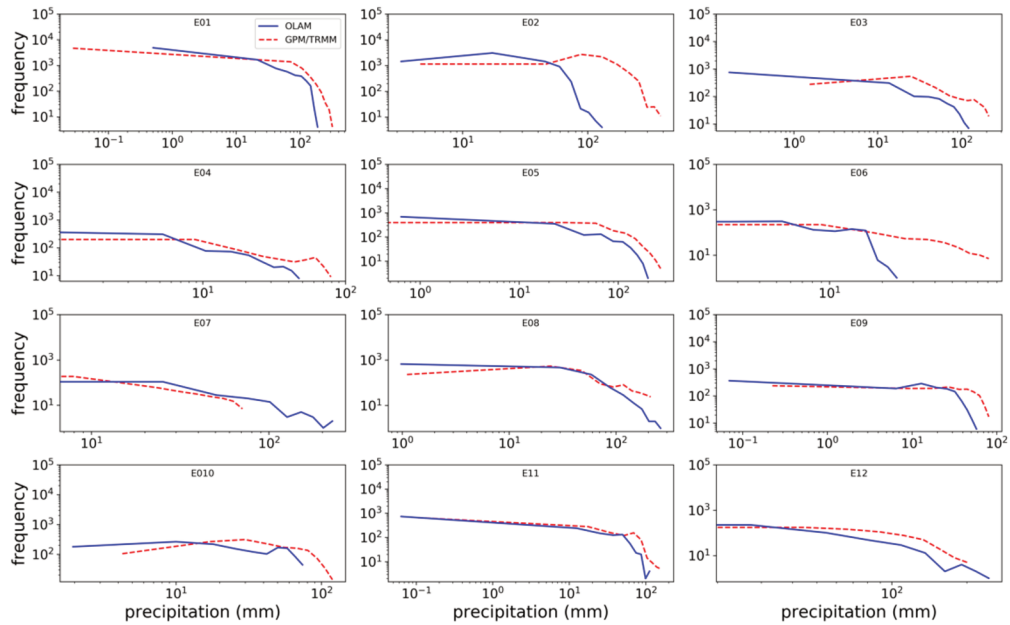
Figure 2-3. Precipitation distribution integrated for the whole domain for the twelve selected extreme events. The x-axes represent the amount of precipitation while the y-axes are the frequency of each class. The model results and TRMM/GPM data were interpolated to the same resolution of 0.25° of latitude-longitude. The data corresponded for the accumulated precipitation during all simulation time which was 10 days except for events E07 (11 days) and E (18 days)

In Figure 2-4, we compared the simulated wind field and sea level pressure (SLP), during each event peak time, with the estimates from the MERRA-2. Although the OLAM model had slightly underestimated the intensity of low pressure zones, overall there was a good agreement between simulations and observations for both wind and SLP data. This bias was evident especially for E02 and E11. Nevertheless, for E04, the OLAM SLP and wind results were consistent with the ECMWF model data studied by Candella and Souza (2013). Also, the simulated cyclone position for E08 and E12 matched the synoptic charts analyzed by Suasen (2009) and the tracking calculated by Pezza and Simmonds (2005), respectively. Nevertheless, the model presented consistent results for the high pressure zones, for both intensity and location. Overall there was a much higher spatial correlation as compared to the precipitation fields.
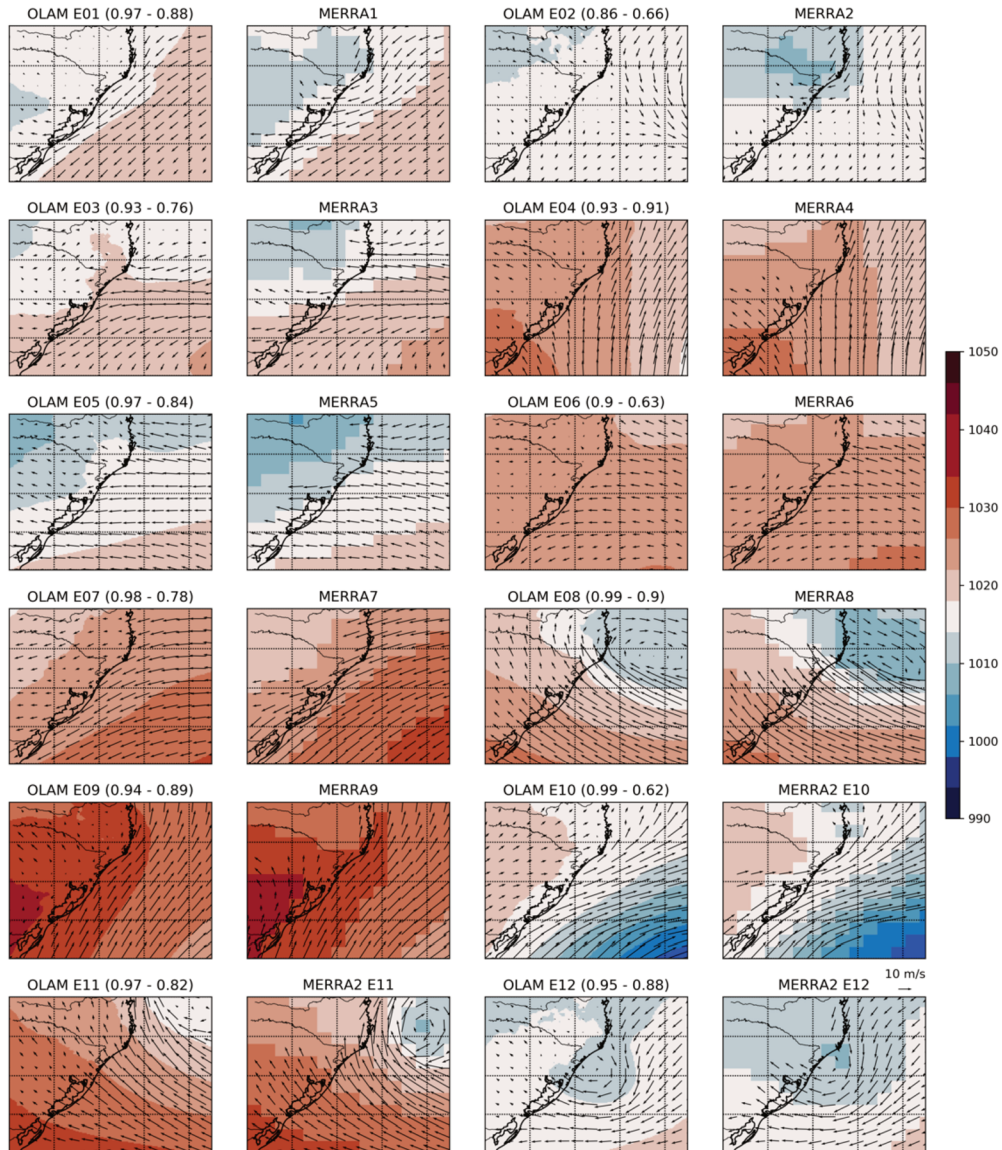
Figure 2-4. OLAM and MERRA-2 sea level pressure (shaded, units in hPa) and winds (vectors) for peak time of the selected events. For OLAM data we skiped every ten grid points for clarity. The values placed in parenthesis near the titles are the statistical spatial correlation indices between the OLAM results and the MERRA2 (SLP and wind speed, respectively) estimates for that snapshot.

The model performance for the wind field was directly correlated with its ability to represent the high and low pressure systems. Thus, when the low pressure systems were offset there was also a mismatch between the estimated and simulated wind intensity and direction

near the system center. Nevertheless, the wind direction and intensity across the analysis domain closely matched those estimated by the MERRA-2. To illustrate the model ability to represent the wind field related to the extreme events presented here, we compared the OLAM results with the Aqua satellite image for the Catarina Hurricane event on the day before its landfall on the southern coast of the SC state (Figure 2-6). There is a good correspondence between the modeled and the actual eye of the hurricane despite the time lag between the observation and model output.
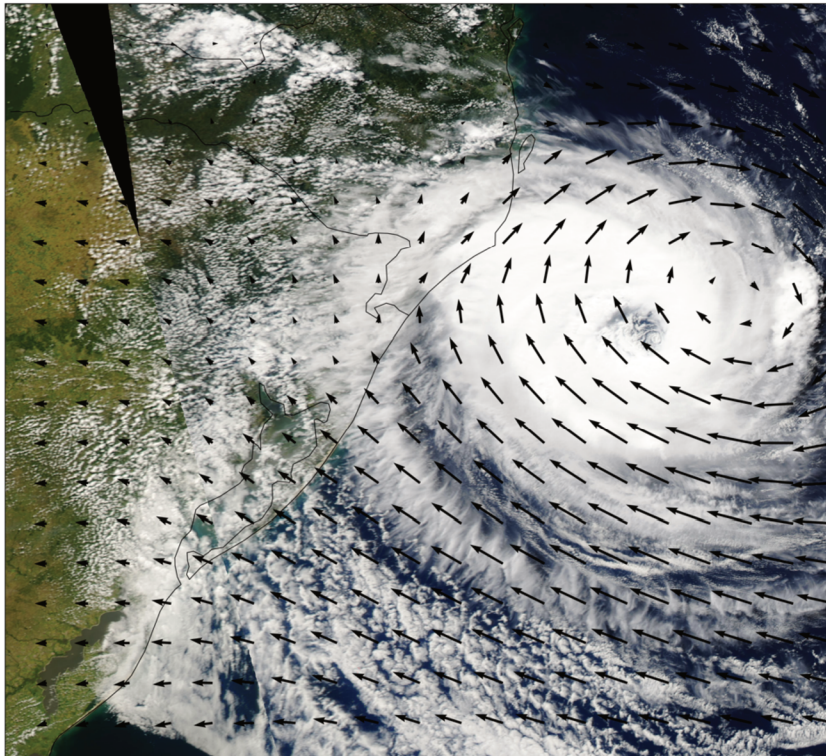
Figure 2-5: Aqua/MODIS satellite image showing the Catarina Hurricane (E12) one the day before its landfall, at 1630 UTC 2004 Mar 27.. Superimposed are the OLAM surface wind vectors for 1500 UTC of the same day.

In order to access the model performance at local level, we compared model results with precipitation and temperature data from all the INMET meteorological stations (Figure 2-6). This analysis included only the event time period indicated in Table 2-1, which does not represent the entire simulations time. The temperature data were available for 00Z, 12Z and

18Z while the precipitation corresponded to daily accumulated values. This analysis showed a good correspondence for temperature, which shows a good capacity of the model to simulate the local daily cycle. However, the analysis indicated a slightly negative bias by modeled precipitation data but with better results for higher precipitation. The bias was not related to individual stations, instead, model accuracy changed accordingly to each event. The same could be observed when comparing the accumulated precipitation spatial distribution between model results and GPM/TRMM data (Figure 2-2).
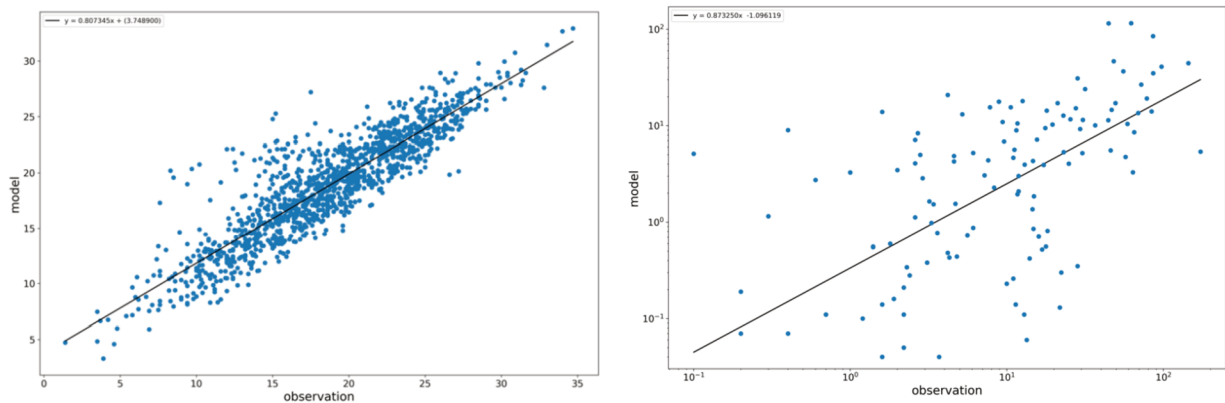
Figure 2-6. Comparison between simulated and observed temperature (left) and accumulated precipitation (right, logarithm scale) for all 12 events and INMET weather station described in section 2.d. Temperature and accumulated precipitation data are shown in Celsius degrees and millimeters, respectively. The temperature data corresponds to instantaneous values (at 00Z, 12Z and 18Z) and precipitation correspond to daily accumulated values.

2.4   CONCLUSIONS AND DISCUSSION

The mid-latitude region of the Southern Hemisphere is strongly influenced by Rossby planetary waves that travel around the region at approximately 4-6 days. On the other hand, the surface-atmosphere-ocean interface produces strong temperature gradients that affect surface fluxes like sensible and latent heat fluxes. Representing both the propagation of

planetary waves and simultaneously the heterogeneity of the surface and its effects on local circulation is of fundamental importance for a good representation of mesoscale processes. In this study, the presented methodology allowed to represent these phenomena of global and local scale simultaneously in the interface of the coastal region of southern Brazil using a state-of-the-art modelling approach. Figures 2-7 and 2-8 present a snapshot of sensible and latent heat flux emission for each of the twelve cases studied. These fluxes represent the surface interaction with the atmosphere. The sensible heat flux responds to the surface temperature, radiation and vertical air velocity near the boundary layer (Figure 2-7). Also, the latent heat flux shows the evaporation of surface water in addition to the transpiration of local vegetation (

 Figure 2-8). Soil moisture, radiation and temperature conditions are critical in controlling evaporation and transpiration of vegetation that is controlled by stomatal resistance (WALKO et al., 2000). The generation of these surface fluxes produces local breeze circulation such as sea breeze and mountain breeze that are of great importance for the establishment of the moisture flow and the local water cycle.

Phenomena such as heavy rainfall and rising sea levels can occur simultaneously and have impacts on densely populated coastal regions. Identifying the strengths and bias in modeling and improving the predictability of these extreme events has therefore become of great importance, as climate projections suggest an increase in frequency and intensity of these events (STOCKER et al., 2013).

The atmospheric results of the present study will be applied as forcing fields for ocean models that allow simulating the variability of ocean currents and the dynamics of local waves. In this way, a more complete system might allow a better capacity to represent the

atmosphere and the ocean conditions and therefore better predict the cases in which we have the simultaneous conditions of heavy rainfall and sea level rise. The methodology presented for this coastal region can be adapted to any other regions. To do this, one may simply adapt the OLAM grid system to the center of the region of interest.
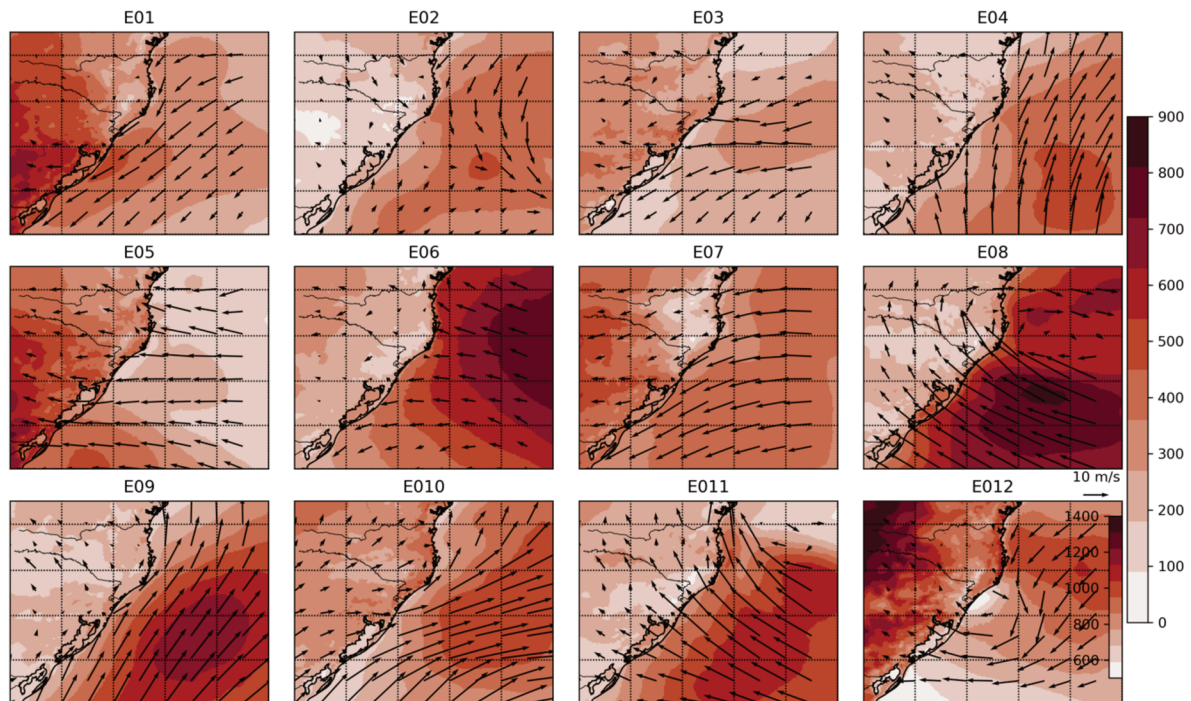
Figure 2-7. Upward latent heat flux (W m^{-2}) and near surface wind vectors simulated by the OLAM model for each event. For each case, we selected the time frame corresponding to the same day as the peak time but the chosen hour was 15:00 UTC.

After evaluating the occurrence of extreme events in the southern coastal region of Brazil, we detected a total of twelve cases. The simulation of these cases by the OLAM model allowed a good representation of temperature, surface pressure and rainfall distribution evolution. Although the results showed a bias for the rainfall, the best results occurred for the most extreme cases showing the simulation capacity for these events. The method applied to this coastal region of southern Brazil allowed a detailed representation of the sensible and latent heat fluxes that are fundamental in the establishment of local mesoscale

circulations. Therefore, these results show that this methodology is an important tool for coastal studies of any region of interest.
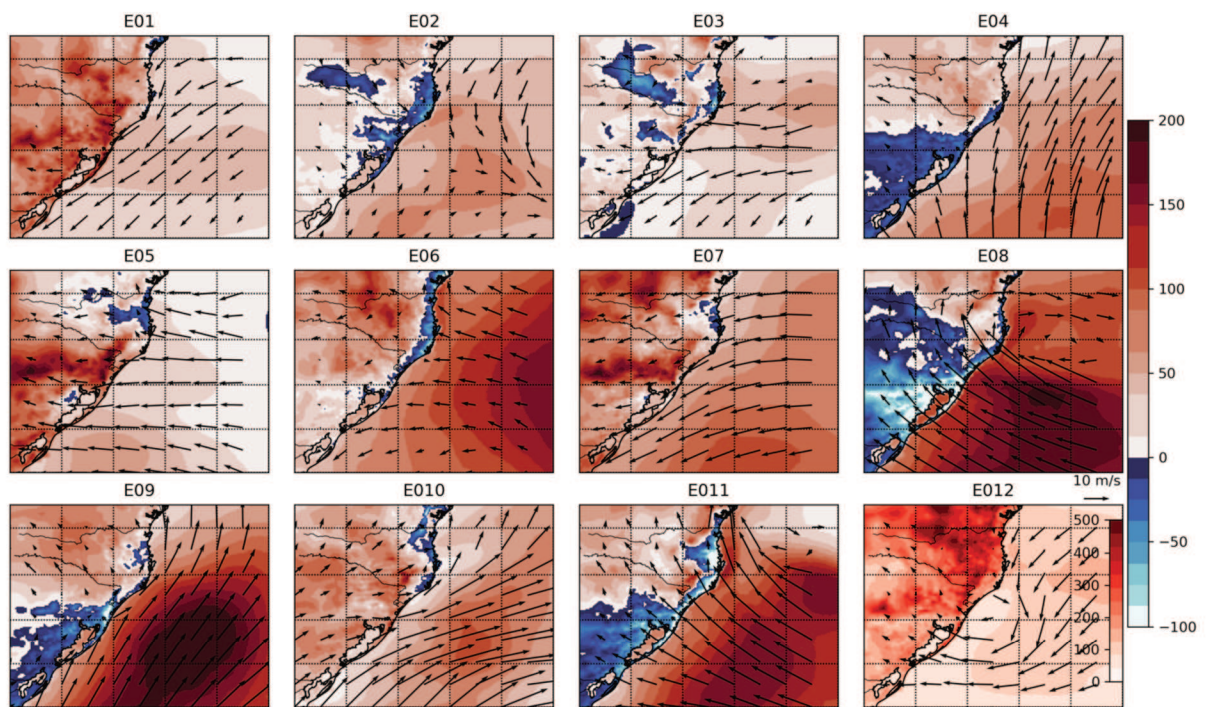
Figure 2-8. Same as Figure 6 but for sensible heat flux (W m^{-2}).

3 A CLIMATE DOWNSCALING FOR THE SOUTHERN BRAZIL COASTAL REGION WEATHER TYPES

Nesse capítulo encontra-se o artigo de mesmo nome, que será submetido à revista *Journal of Climate*.

Climate downscaling for the southern Brazil coastal region weather types

D. C. Souza[1], R. Ramos da Silva[1] and David Werth[2]

[1]Climate and Meteorology Laboratory, Department of Physics, Federal University of Santa Catarina, Florianópolis, SC, Brazil.

[2] Savannah River National Laboratory, Building 773-A, Aiken, SC 29808, USA

Corresponding author: Danilo Souza (danilo.oceano@gmail.com)

66

Abstract

A hybrid downscaling method is proposed to produce a high-resolution regional downscaling for a coastal region of southern Brazil. The method initially applied a cluster analysis method to estimate the major weather types for the region based on daily fields of the sea level pressure (SLP) data from the NCEP-CFSR reanalysis. After the empirical estimates using this approach, we ended with dates representing the most predominant weather patterns for the study region. A total of 32 weather types were estimated accounting for 90% of the explained variance. The estimated weather types were able to represent the major atmospheric systems that affect the local climate including cyclones and anticyclones that are usually present in this region. Then, we applied the numerical Ocean-Land-Atmosphere model (OLAM) to produce a dynamical downscaling of these predominant weather types with 6 km grid space resolution. The model was set with a global grid and used a refining approach to set the high resolution grid for a coastal region of south Brazil. This approach allowed representing simultaneously the planetary waves and the local mesoscale systems, and their mutual interactions. The results provided new high resolution fields for the coastal region of study capable of resolving the major local mesoscale features. This methodology can be applied for any other coastal region and therefore provide a detailed local climate that is potentially important to give support to decision-makers.

3.1 INTRODUCTION

Assessment analysis required for climate change planning policies need projection estimates on regional and mesoscale scales. However, most studies of climate projections use General Circulation Models (GCMs) which have coarse resolution grids (TAYLOR; STOUFFER; MEEHL, 2012) and therefore do not provide the needed information for climate change impact assessments. They do not fully represent regional features such as the effects of complex coastlines, heterogeneous topography and land use mosaics over urban and rural areas. Thus, local circulation patterns that affect regional climate might not be properly represented by those models.

In order to properly simulate regional climate and provide outputs at finer scales, modelers use the downscaling methodology, which consists of two distinct approaches: dynamical downscaling (DD) and statistical downscaling (SD). Dynamical downscaling consists of using high resolution Regional Climate Models (RCMs) forced by a GCM output (GIORGI & GUTOWSKI 2015; MEARNS et al. 2004). For instance, the Coordinated Regional Climate Downscaling (CORDEX) project applies limited area RCMs to particular regions to produce regional projections using spatial grid cells reaching 25 km (GIORGI & GUTOWSKI, 2015). However, this resolution is still not enough to represent the local mesoscale features. The SD method assumes empirical relationship between local climate variables and large scale GCM predictors (BENESTAD, 2004; WILBY et al., 2004). A major conclusion from the application of the RCMs were that the simulations should be able to represent the major weather patterns of the studied region (TAKLE et al., 1999).

The obvious advantage of using the statistical approach over the dynamic one is the reduced demand for computational power, as long-term, high resolution RCM runs often

require large amounts of computer power not available for most research groups. Given the nonstationary nature of the earth climate system, there is some concern whether SD can provide accurately projections of future climate (WILBY; WIGLEY, 1997). Also, the use of numerical models for DD allows the investigation of the underlying physics of a given climate response such as interaction between distinct variables which adds credibility to the results.

In order to provide robust climate representation with low computational burden, the hybrid downscaling approach combine both DD and SD techniques. Applications of this method include: further downscaling of RCM output using SD models (PRYOR; BARTHELMIE, 2014), statistical models that "mimic" the DD (SUN; WALTON; HALL, 2015; WALTON et al., 2015), statistical bias correction of GCM output to be downscaled by RCM (COLETTE; VAUTARD; VRAC, 2012) and use of statistical analyses to select representative cases (also called as Weather Types) of a region climate and then DD them (CAMUS; MENDEZ; MEDINA, 2011). The latter is an adaptation of the circulation pattern methodology for studying regional climate where atmospheric information is disaggregated into representative states (HUTH, 2001; HUTH et al., 2008). This methodology has been widely used for distinct finalities (e.g.: HAY et al., 1991; SHERIDAN, 2002; TRIGO et al., 2016) and is especially useful for climate change studies through the analysis of changes in the patterns of a given region over time (HUTH, 2000).

In the present study, we applied the approach of Camus et al. (2011) mentioned above. Initially, we used large scale reanalysis data to select the major weather types for the southern Brazil coastal region. Then, dynamically downscaling the atmospheric components

for the selected cases using high resolution numerical integration for the study area using the Ocean Land Atmosphere Model (OLAM - WALKO; AVISSAR, 2008b).

The OLAM model was chosen because it has the capability to represent simultaneously the global and local atmospheric features though a refining grid approach. This model has been tested in several recent studies on mesoscale and regional climate modeling (MEDVIGY et al., 2013; MEDVIGY; WALKO; AVISSAR, 2008; RAMOS DA SILVA et al., 2014a; RAMOS DA SILVA; HAAS, 2016). More recently it demonstrated promising results for simulations of extreme events in the coastal region of Brazil (Souza & Ramos da Silva – manuscript submitted).

The aim of the current study is to propose a hybrid methodology for studies concerning the coastal region of southern Brazil. We combined the statistical and dynamical downscaling methodologies to select and simulate 32 weather types for the study region with high resolution regional grids in the OLAM global atmospheric model. The proposed methodology selected the major weather patterns for the study region while the high resolution grids allowed the representation of phenomena ranging from large scale to local scale circulation. We analyze the low level atmospheric circulation related to the weather types and discuss applicability of the proposed methodology.

3.2   METHODOLOGY

3.2.1   Study area

The southern region of Brazil (SBr), composed by Paraná (PR), Santa Catarina (SC) and Rio Grande do Sul (RS) states (Figure 3-1). The climate of the coastal SBr is strongly influenced by the presence of the South Atlantic Anticyclone (SAAC), a high pressure system resulting

from the subsidence side of the Hadley Cell (GARREAUD et al., 2009). Therefore, in general, the prevailing wind direction for the SBr coast is northeasterly. Low pressure transient systems associated with the planetary Rossby wave propagation has also important effects on the local climate. Those cyclonic systems are responsible for abrupt southerly wind changes and the passage of cold fronts, the main cause for precipitation in this area during winter (GARREAUD et al., 2009). The mechanism for the passage of cold fronts in the region is the geostrophic flow resulting from a marine cyclone and an anticyclone over the continent (COMPAGNUCCI; SALLES, 1997; GARREAUD, 2000).
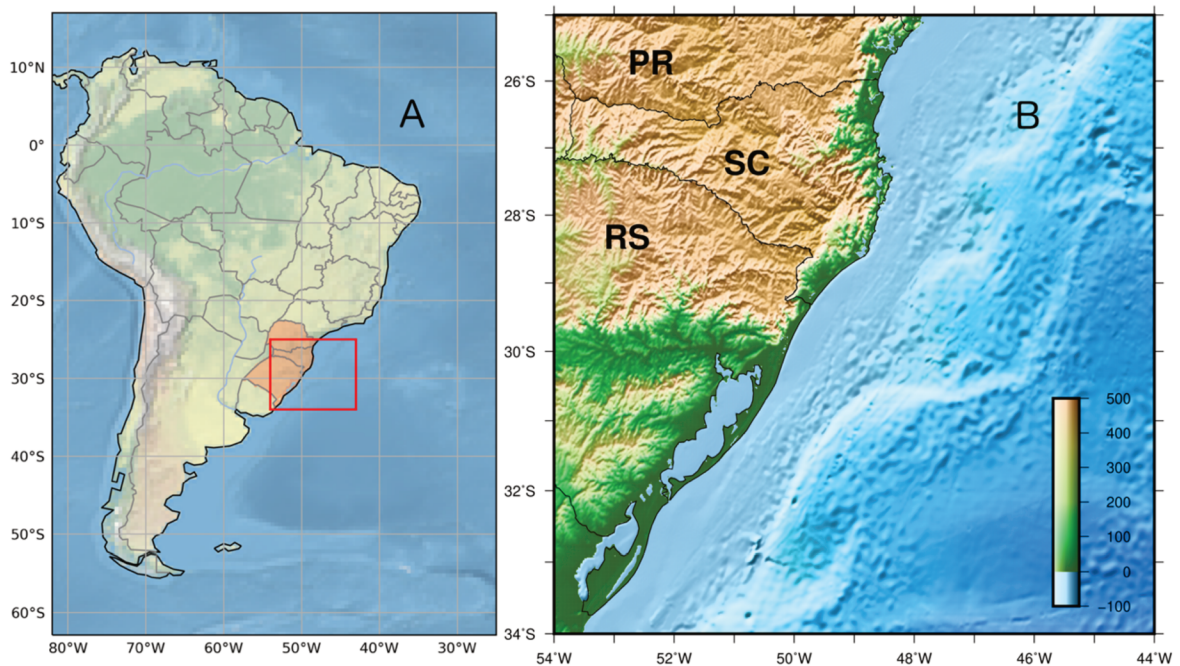
Figure 3-1. A) South America and B) the Southern Brazil states and topography.

Almost one third of the region annual precipitation is related to extratropical cyclones in the western South Atlantic (SAO) (REBOITA et al., 2018). Nevertheless, the cloudiness and strong winds associated often with those systems also influence local weather.

They also affect local communities by producing high sea waves and causing sea level rise, which triggers beach erosion episodes in SBr (ALBUQUERQUE et al., 2018; GOMES DA SILVA et al., 2016; GUIMARÃES; FARINA; TOLDO, 2014; MACHADO et al., 2010; PARISE; CALLIARI; KRUSCHE, 2009; PARISE; FARINA, 2012)**.**

Another important feature for the region climate is the South American Low Level Jet (SALLJ) which transports moisture from the Amazon basin (MARENGO et al., 2004; SALIO, 2002; SELUCHI et al., 2003; SELUCHI; MARENGO, 2000). Episodes of SALLJ are related to development of mesoscale convective systems over the region (SALIO; NICOLINI; ZIPSER, 2007) and 20% to 40% of summer precipitation (SALIO 2002).

This coastal region has a complex land cover. It presents a variable topography, a very heterogenic vegetation surface and a complex coastal interface with the Atlantic Ocean (Fig. 1B). This complex surface has an important influence on the mesoscale atmospheric circulation such as the local breeze circulations. For instance, Orlanski (1975) defines the mesoscale gamma, beta and alfa as phenomena with 2-20 km, 20-200 km, and 200-2000 km, respectivelly. Thus, the model is able to represent the major mesoscale features.

3.2.2   Weather type classification from the statistical downscaling

The processes used for determining the weather types (WT) for the coastal region of southern Brazil followed the framework described by Camus et al. (2014). In this case, the procedure classified the distinct weather states based on daily mean sea level pressure (SLP) fields from the National Centers for Environmental Protection (NCEP) Climate Forecast System Reanalysis (CFSR) Version 2 (SAHA et al., 2014) with 1° horizontal resolution. The time period used for this analysis was from 1981 to 2010.

The bounding box used to limit the SLP fields for this analysis was 62°S to 25°S and 70°W to the 0° longitude. For the analysis of the synoptic conditions, we considered this domain as specified at

Figure 3-2. Then, we categorized the presence of high or low pressure systems accordingly to its position in the subdomains. The idea was to have a representative picture of the low and high pressure systems that act in the Southern Atlantic Ocean basin while limiting the area to reduce noise from atmospheric systems that did not directly affect study area weather.
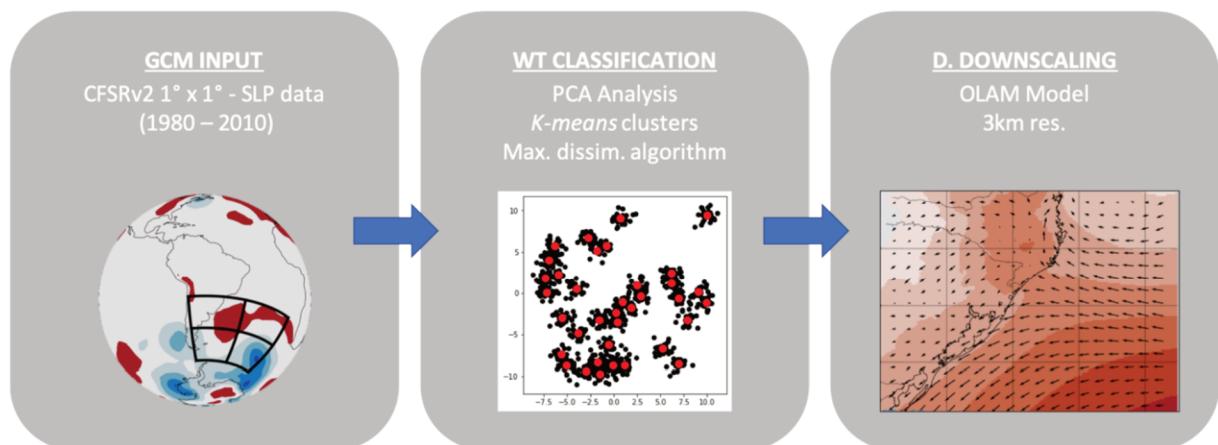
Figure 3-2. Methodological flow chart. Left: low resolution GCM input and domain selected for the SLP analysis. The domain was further divided in subdomains for the surface conditions analysis (Table 1). Middle: statistical downscaling approach, each black dot representing a distinct event and the red dots representing the centroid of each cluster determined by the k-mean algorithm The centroids of each cluster are virtual events that might not have occurred. Therefore, for defining the WT we choose the event (black dots) closest to each centroid. Right: high resolution domain centered in the coastal area of SBr (Figure 1).

The methodology is summarized in

Figure 3-2. In order to make the WT classification and selection a principal component analysis (PCA) is initially applied to the selected data. The computed empirical functions (eigenvalues of the covariance matrix) are ranked by the amount of sample data explained variance. We only used the principal components (PCs) that in total explained 95%

of the variance, in this case, 87 PCs. This allowed reducing the dimensional space while still maintaining a high variance. Then, a *k-mean* clustering technique is applied to aggregate the data into distinct clusters. The number (N) of clusters is predetermined by the user. At last, the maximum dissimilarity algorithm is applied for best classifying the data among the N clusters.

The final results provided maps representing synoptic atmospheric circulation patterns, each map corresponding to a specific time frame of the original SLP dataset. In the original study by Camus et al. (2014) dealing with wave modeling, the authors adopted an N of 100 WT. However, for our study region this resulted in an excessive amount of redundant WT. Thus, we set up the *k*-mean algorithm for a N of 36 WT. Four, out of those 36 WT (WTs 12, 19, 24 and 35), corresponded to time periods too old with unsatisfactory data homogeneity for the southern hemisphere, so we excluded them from our analysis (STERL, 2004). Therefore, our final dataset contained 32 WT, that explain approximately 90% of the data variance.

3.2.3 Numerical model description and dynamical downscaling experimental design

The OLAM model computing structure and parameterizations were built upon the Regional Atmospheric Modeling System (RAMS) (WALKO; AVISSAR, 2008a, 2008b). The major novelty is that the OLAM has a global computational grid with a refining resolution approach for regions of interest. The use of a global domain with high resolution regional grids with a two way communication between them makes the OLAM model very versatile with many possibilities for numerical studies.

The model resolves the Navier-Stokers equations through a finite-volume method (WALKO; AVISSAR, 2008a, 2008b). The mass and moment fields coupling of grid elements are made though an Arakawa-C scheme (WENNEKER; SEGAL; WESSELING, 2002) and

the adjustment to the topography follows the shaved grid scheme (ADCROFT; HILL; MARSHALL, 1997). The grid elements are non-structured hexagons that can be further divided in order to increase horizontal resolution.

For the current study we adopted a model grid set up with the global domain having about 200 km of horizontal resolution, which increased up to approximately 6 km in the coastal southern Brazil study area (Figure 3-3). This level of refinement allows representing the regional scale features in this ocean-land interface that affect local weather. We adopted 49 atmospheric levels with varying resolution in the vertical component, reaching 35 km high. The vertical resolutions ranged from 60 m in the levels closer to the surface to 2000 m in the upper stratosphere.
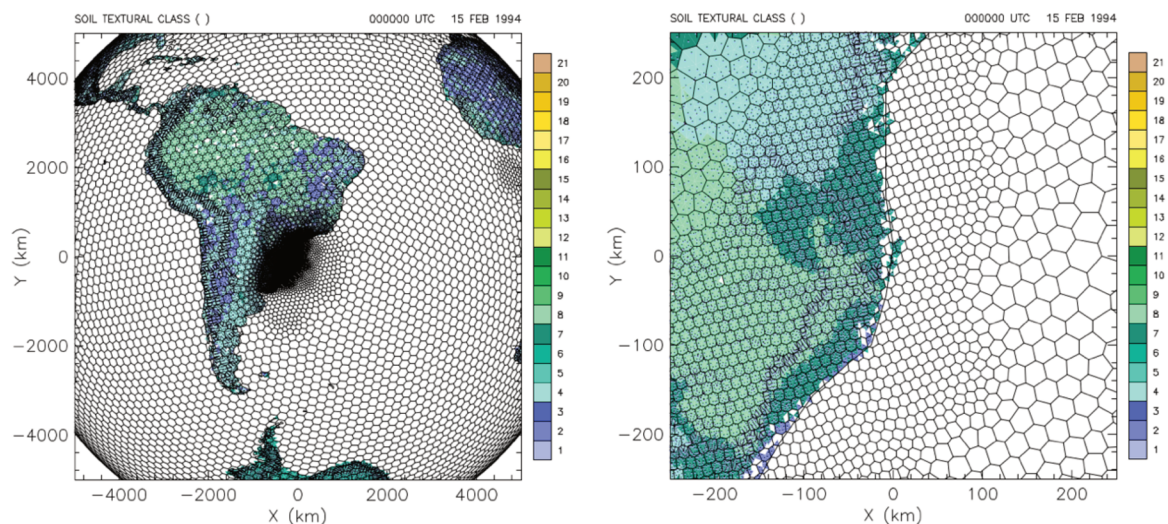
Figure 3-3. Model global grid used for the dynamical downscaling and the regional grids centered in the coastal region of southern Brazil.

The numerical simulations started 3 days prior to the date chosen in the clustering method (Table 3-1) for model spin up and lasted for 10 days in total. This time range was chosen to represent the complete evolution of the major weather patterns and its further effects on near coast oceanic conditions. These results will be useful for future studies

accessing hydrological and oceanographic conditions associated with those weather types. In order to maintain numerical stability, we adopted a 10 second time step for the simulations.

The initial atmospheric conditions were obtained from the CFSR fields (SAHA et al., 2010, 2014). The variables used were the wind fields (u and v components), geopotential height, air temperature and relative air humidity which were updated every 6 hours by the model for a light nudging on the coarser grid. For the oceanic conditions, we used the Optimum Interpolation Sea Surface Temperature (OISST) from the National Oceanic and Atmospheric Administration (NOAA), updated weekly (REYNOLDS et al., 2002, 2007).

The physical parameterizations adopted for the current study included the cumulus convection parameterization (GRELL; FREITAS, 2014), the diffusion coefficient for atmospheric fluxes parameterization (SMAGORINSKY, 1963), the cloud microphysics parameterization (MEYERS et al., 1997; WALKO et al., 1995) and the short and long-wave radiation parameterization (MLAWER et al., 1997). Turbulent fluxes related to soil and vegetation cover were calculated through the use of a sub-model, the Land Ecosystem-Atmosphere Feedback Model (LEAF-3) (WALKO et al., 2000).

3.3 RESULTS

The dates of the 32 selected WTs and the corresponding surface synoptic conditions is presented at Table 3-1, and Figure 3-4 shows the WTs resulting from the statistical downscaling of SLP. All the WTs could be explained by the presence of transient high and low pressure systems in the study area or the adjacent oceanic region. The synoptic conditions presented at Table 3-1 do not match the conditions seen in Figure 3-4 as the latter contains

daily means while the former was estimated by evaluating the six hourly pressure and wind fields from CFSR data.

Table 3-1. Synoptic conditions related to each Weather Type (WT) and wind direction in the coastal SBr. More than one direction indicates that it varies along the PR, SC and RS coastlines. Surface conditions acronyms are designed accordingly to the position of the prevailing cyclonic (CS)/anticyclonic (AC) features in the subdomain of SLP analysis (Figure 3-2). *anticyclonic pattern across most of the domain

No.	Dates	Surface conditions	Wind	No.	Dates	Surface conditions	Wind
1	2000-05-21	NW-AC/NE-CS	E/NE/N	17	1987-07-01	NE-AC/SE-CS	NW/SE
2	2004-04-05	NW-AC/SE-CS	S/E/NE	18	1994-02-06	NW-AC/NE-AC/SE-CS	SE
3	2000-10-01	AC*/SE-CS	N/NE	19	2002-03-04	NE-AC/SW-CS	NE/N
4	2009-01-28	NW-AC/NE-AC	NE/E	20	1989-09-30	NW-AC/NE-AC/SE-CS	S/NW
5	1997-05-22	NW-C/NE-AC	W	21	1999-02-15	NW-CS/NE-CS	E/NE
6	2005-05-07	NW-AC/NE-AC	S/SW	22	2004-03-08	NE-AC/SE-CS	NE
7	2006-10-20	NWSW-AC/SE-CS	SE/E	23	1998-02-13	NW-AC/NE-AC	E
8	2004-01-07	NW-AC/SW-AC	NE	24	1990-11-30	NW-C/NE-AC/SE-AC	E/NE
9	1982-10-01	NWSW-AC	NE	25	2005-11-29	NE-AC/SW-CS	NE/E
10	1998-10-04	SW-CS/NE-AC	N/NE	26	2003-11-30	NE-AC/SE-CS	E/NE
11	1986-05-03	SW-CS	SE	27	1983-09-18	NW-AC/NE-CS/SW-CS	E/NE/SW
12	2004-02-06	NW-AC/SE-CS	S/SE	28	2010-05-04	NE-AC/SW-CS/SE-CS	N/W/S
13	2005-02-24	NW-AC/NE-AC	E/NE	29	1999-09-27	NW-AC/SE-CS	SW/SE
14	1986-12-02	NE-AC/SE-CS	SW/NE/NW	30	1998-08-15	NE-AC/SW-CS/SE-CS	N/S
15	1998-12-28	NE-AC/SE-CS	NE	31	1986-03-15	NE-AC/SW-CS	S/E
16	1983-03-08	NE-AC	W/NE	32	1994-01-14	SW-CS/SE-CS	NE

In most of the WTs there was an anticyclone (AC) located in central SAO (South Atlantic Ocean - NE of the domain). This pattern occurs in 22 of all WT (04 to 06, 10, 13 to 28, 30 and 31), corresponding to the presence of the South Atlantic anticyclone (SAAC). The second most prevailing condition was a cyclonic system (CS) in southern SAO (SE of the domain), occurring in 15 of the WT (02, 03, 07, 12, 14, 15, 17, 18, 20, 22, 26 , 28 to 30 and 32). Other frequent feature was the AC positioned closer to the continent (NW of the domain),

mostly like associated with a post frontal anticyclone and the positioning of a CS in the central part of the SAO (SW of the domain - related to cyclogenesis close to the SBr region prior to the WT date). Least common were the occurrence of a CS close to the Brazilian coast (SW of the domain) and in the central SAO (SW of the domain). Less than one sixth of the events together presented more than 20% of the total probability (WTs 10, 14, 27, 02 and 16, from highest to lowest probability). All of those WT were associated with an anticyclonic system in the NE of the domain and four of them with a cyclonic system in the SE (WT14 and WT22) or SW (WT10 and WT27) of the domain.

The most frequent surface circulation pattern was an AC in the NE/NW of the domain in association with a CS in the SE/SW of the domain. Those patterns correspond to the position of the SAAC and a CS moving from the southern part of South America towards the Southern Ocean. Other frequent pattern was a CS in the NW of the domain in association with a CS in the NE parts of the domain. This pattern illustrates a transient AC before merging with the SAAC. The other patterns were heterogenous among the WTs.
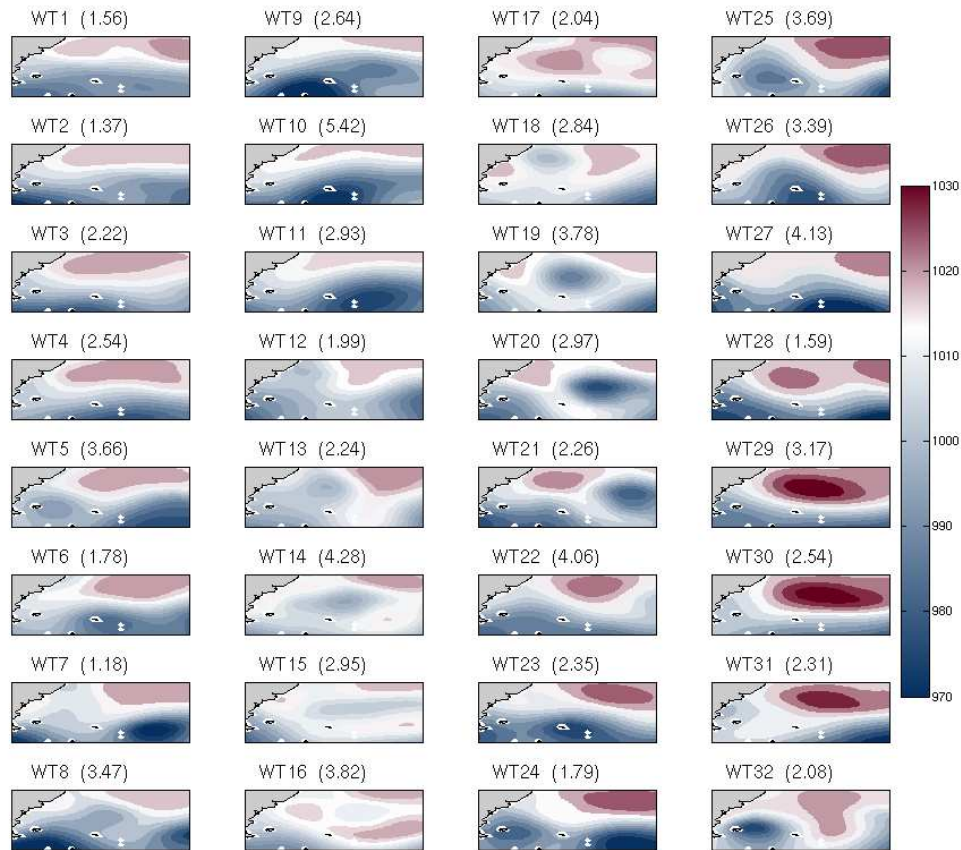
Figure 3-4. The 32 weather types selected from the statistical downscaling. The contours indicates isobars from SLP (hPa) daily mean, relative to the dates in Table 1. The numbers in brackets indicate the occurrence probability (in percentage) of each event (mean = 2.77%, std = 0.97). The probabilities sum up to 90% of the explained variance.

Figure 3-5. OLAM model results snapshot for the selected weather types (WT) SLP (hPa) and wind field vectors at 12:00LT. From the first to the last WT, they are grouped from top to down and from left to the right. The color contours represent the position of low/high pressure systems in blue/red respectively, while the vectors indicate the wind direction.

shows the dynamically downscaled results from OLAM model for the SLP along with the wind field across the high resolution domain. The most frequent wind direction in all parts of coastal SBr was northeasterly, while the second most frequent was easterly. Both are

related to the SAAC positioned in the middle of the SAO (northern part of the domain). In general, the position of the SAAC further away from the SBr coast resulted in more northeasterly then easterly winds. This configuration favoring NE winds occurred preferably during austral summer. Southerly winds occurred mostly associated to the position of an anticyclone close to the continent (NW of the domain – likely a post-frontal anticyclone). Wind direction related to cyclonic systems changed accordingly with the position of the system and also along the coast. For example: in WT05, the position of the cyclone south of the RS state coast was associated with northwesterly winds in the northernmost part of SBr coast, westerly winds in the central parts and southwesterly winds along the RS coast. Meanwhile, in WT16 the position of the cyclone in the oceanic area close to the RS coastline was associated with mostly easterly winds along the RS coast and southerly winds for the SC coast. The highest wind velocities (Figure 3-6) are presented by WT27, WT05 and WT09. Wind speed was often higher for the RS state and southern SC state coasts. In contrast, the PR state coastal area mostly presented calmer conditions, with lower wind velocities.

Figure 3-7 shows the OLAM results for the 10 day precipitation accumulation for each WT. The results shows that WT27, WT30 and WT21 had the highest amounts of precipitation for the study area (and also for the more continental parts of SBr), each WT representing an episode of high precipitation for each state, SC, RS and PR, respectively. In both WT27 and WT30 the precipitation occurred most likely related to a cold front passing over SBr, related to the CS in the SW of the domain. WT21 was most likely an event of orographic rain associated with moisture advection from the SAO. Among the 10 events related with precipitation in the SBr coast (WTs 02, 04, 06, 08, 12, 18, 21, 23, 27 and 30), nine of them were associated with the presence of an AC in the NW part of the domain. Most

likely for those cases this AC was a post frontal cyclone. However in order to infer if the precipitation was related with a frontal system or other meteorological phenomena one would need to analyze the temporal evolution of each event, which is beyond the scope of the present study.
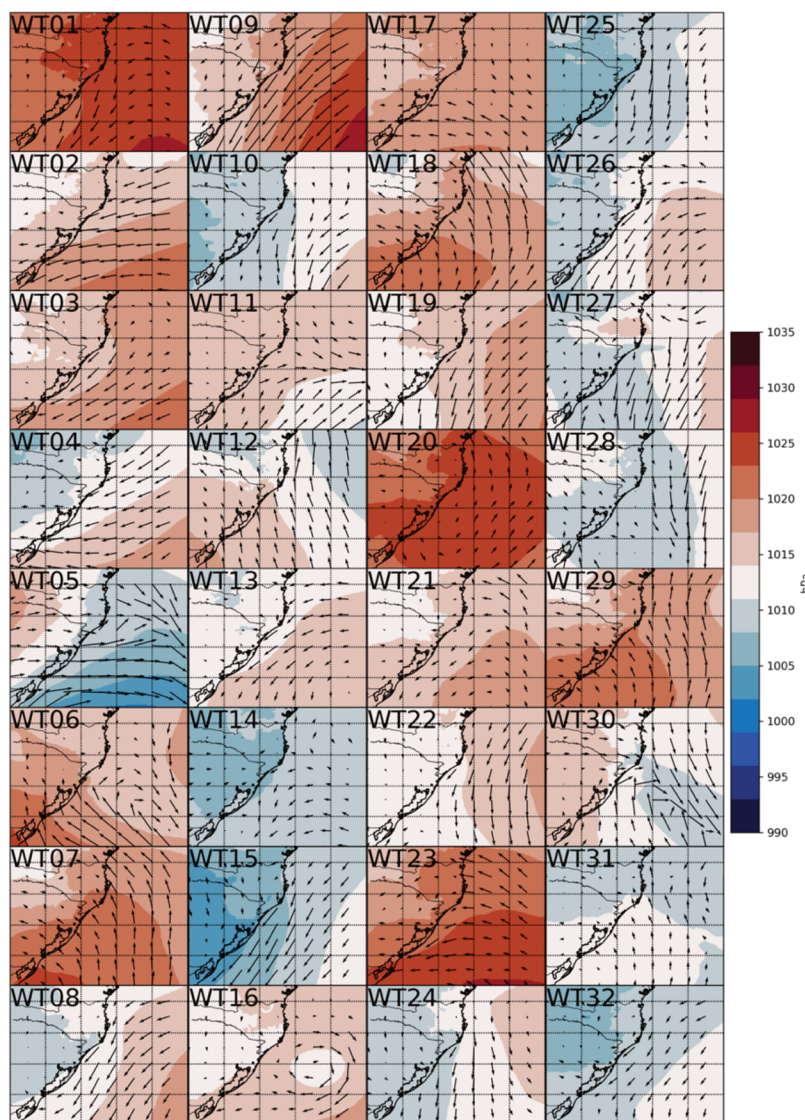
Figure 3-5. OLAM model results snapshot for the selected weather types (WT) SLP (hPa) and wind field vectors at 12:00LT. From the first to the last WT, they are grouped from top to down and from left to the right. The color contours represent the position of low/high pressure systems in blue/red respectively, while the vectors indicate the wind direction.
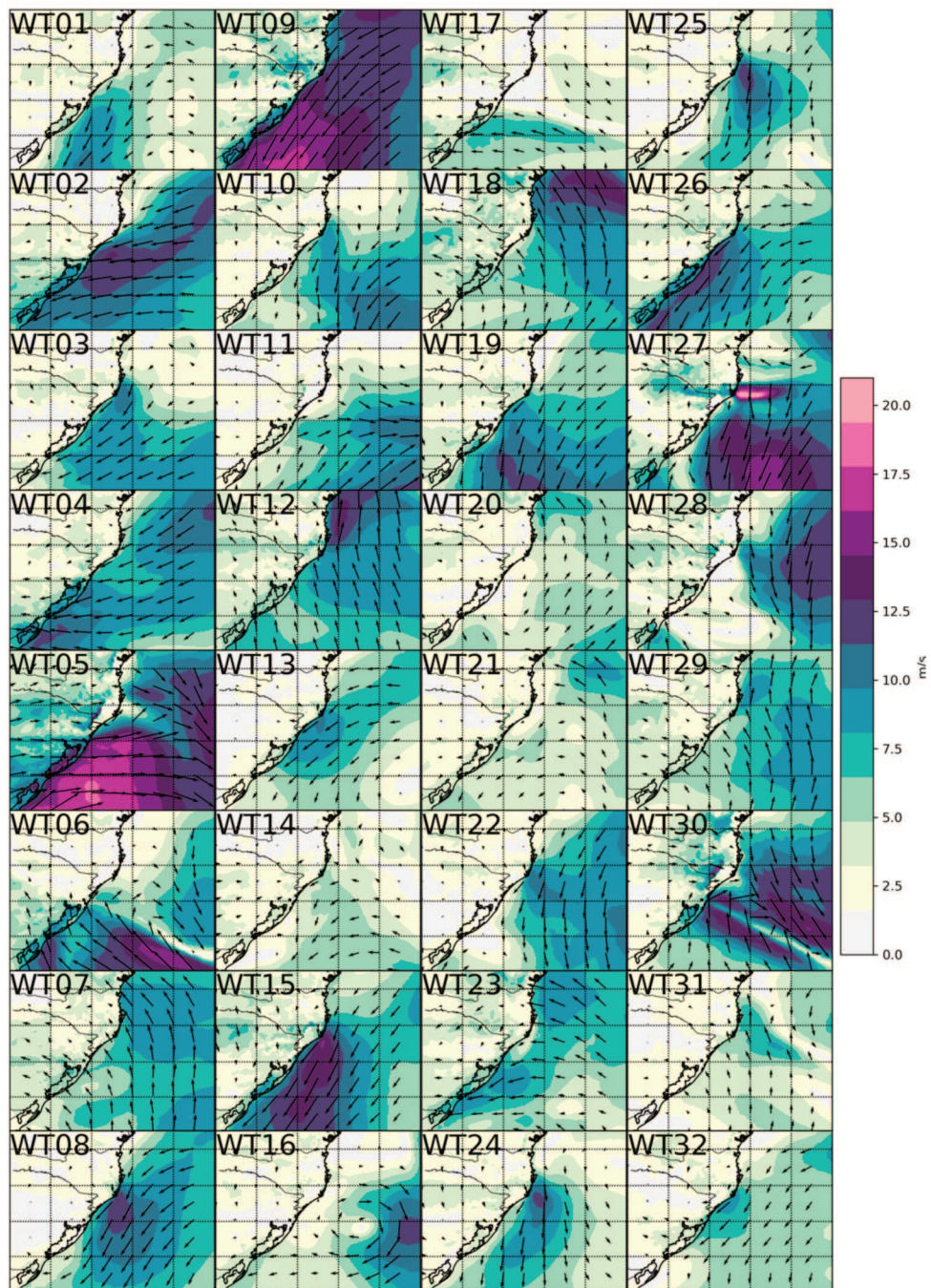
Figure 3-6. Same as Figure 3-5, but for wind speed (m/s).
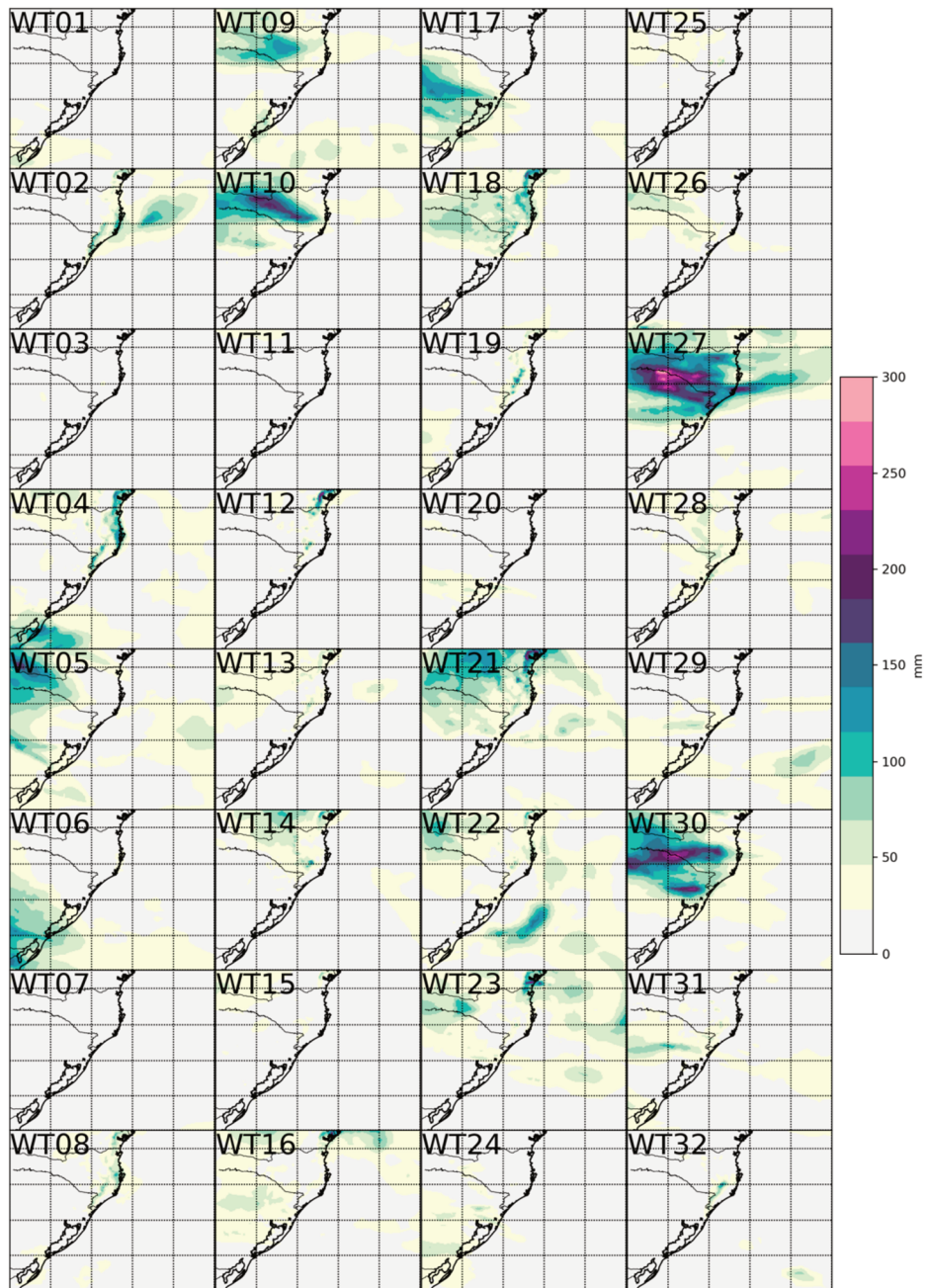
Figure 3-7. Same as Figure 3-5. but for the total accumulated precipitation (mm) during all 10 days of simulation.

Figures 3-8 and 3-9 show the OLAM downscaling results for sensible and latent heat surface fluxes. The results show that the model is able to represent the major surface

heterogeneity effects on the near surface atmospheric fluxes. These results show that this approach is able to represent the major local mesoscale features and therefore the high detailed weather types of the local interest. For example, it is able to represent well the major sea-land interface that is responsible for the breeze circulations. Over land, the model captures the effects of topography and vegetation heterogeneity and therefore can represent better their effects on the local weather types.

3.4 CONCLUSIONS AND DISCUSSION

The weather types presented here provide a comprehensive representation of the region climate and the final downscaled high resolution estimates can provide mesoscale climate variables that are important for the local population. The proposed methodology allowed the high resolution atmospheric simulations for the study area that represented meteorological patterns without much computational cost. For this study each simulation (10 days) was carried out in about one day (24 hours) using 16 processors. In contrast, a complete 30-year (1980-2010) climatology for the region using the same model setup would require approximately three years of computing time. Moreover, as a climatology derivate from climate statistics it foreshadows details of day to day atmospheric circulation. The proposed weather types captured well the major regional weather patterns while the dynamical downscaling methodology provided high resolution atmospheric fields that captured well phenomena ranging from local scale to mesoscale.
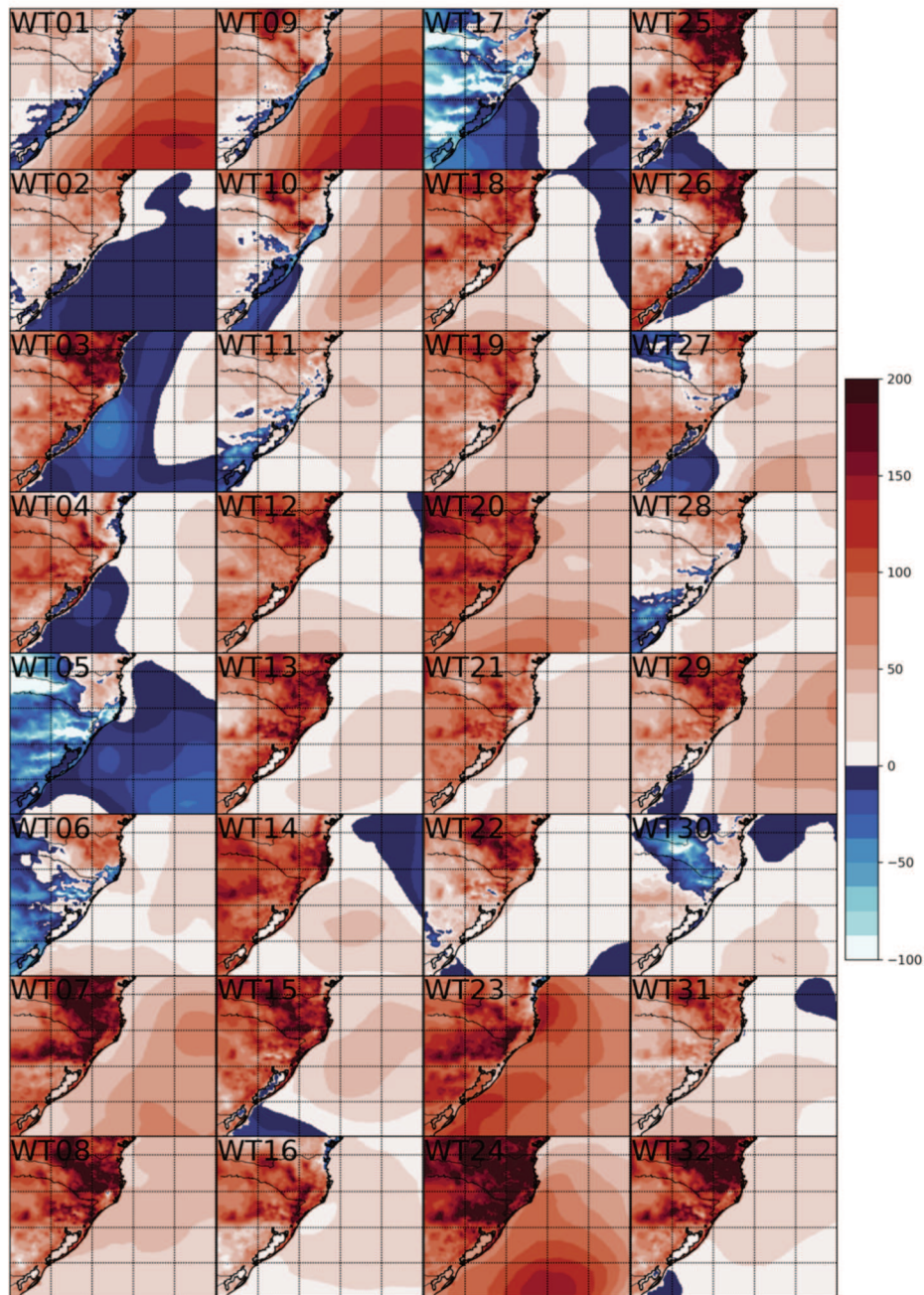
Figure 3-8. Same as Figure 3-5, but for sensible heat flux (W/m^2).
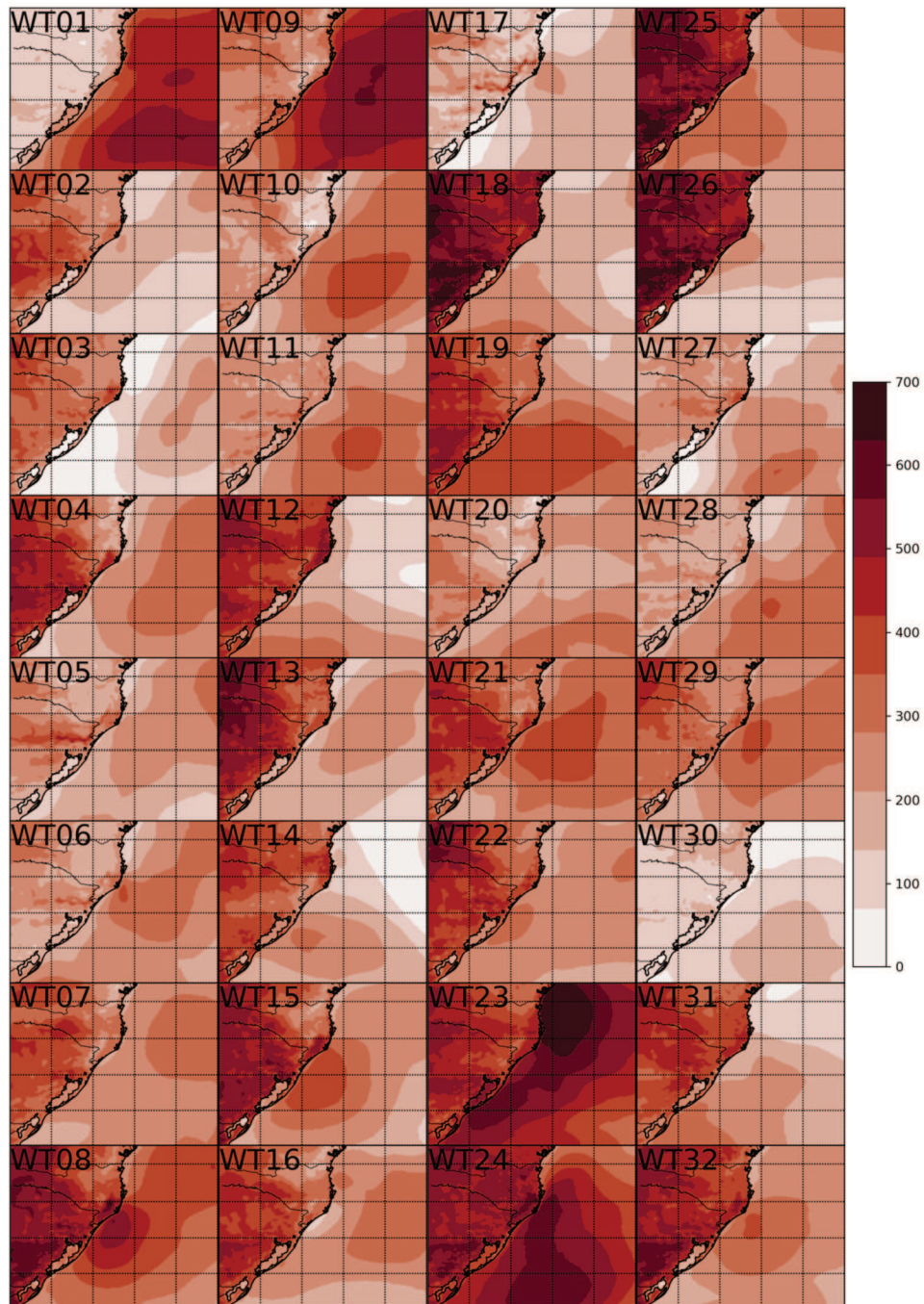
Figure 3-9. Same as Figure 3-5, but for latent heat flux (W/m²).

One of the key characteristics of the low level circulation related to the WTs is a prevailing NE wind direction near coastal SB. The NE winds occurred mostly during austral summer WTs, which is consistent to the works of Zhou and Lau (1998) and Garreaud et al. (2009). Another important feature is the passage of transient high/low pressure systems through the region. The CS cold fronts moving northward over subtropical South America (and hence, linked to southerly winds) often cause temperature drops and instability (SELUCHI et al., 2003). These cold air incursions are the leading mode of synoptic variability for the region (GARREAUD, 2000; GARREAUD et al., 2009).

The WT occurrence probability allows identification of prevailing conditions for the study area and the associated potential meteorological risks. For instance, WT10 which presented the highest occurrence probability was linked to high precipitation for SBr. Also, WT27 presented one of the highest occurrence probabilities and the highest accumulated precipitation among all of the simulated events. Therefore, if a model aims to correctly represent the precipitation regimen for SBr it needs to provide an accurate representation of the atmospheric phenomena related to those events.

We acknowledge that we only accessed the position of the AC and CS relative to the proposed subdomains. Variations in the position of those systems inside of a given subdomain probably have influence on the resulting atmospheric conditions of the study area, but our objective here was simply identifying patterns associated to the WT and their effects to the coastal SBr. Also, the SLP domain choosen for the analysis this study is not suited to fully identify occurrence South Atlantic Convergence Zone and SALLJ events, important phenomenon for the region during summer (CARVALHO; JONES; LIEBMANN, 2004;

FERNANDES; RODRIGUES, 2018; GARREAUD et al., 2009; KODAMA, 1992; MARENGO et al., 2004; SALIO, 2002). However, using SLP as a predictor for local weather we still were able to represent the most important atmospheric systems occurring in the region study, such as cold fronts, orographic rain, post frontal anticyclones and the SAAC.

In the present study we used a statistical downscaling approach to select 32 weather types for the coastal region of southern Brazil. The dynamical downscaling by the OLAM model provided high resolution atmospheric fields for the coastal southern Brazil area. The horizontal resolutions achieved here are of approximately 6 km, which is at least 4 times higher than the CORDEX initiative (GIORGI; GUTOWSKI, 2015) and 20 times higher than most GCM output. This allowed better representation of the SBr complex coastline and heterogenous topography and thus, the model was able to capture well distinct scale phenomena such as land-sea breeze and planetary Rossby waves. The proposed methodology can also be applied to any other region by selecting WT and adapting the OLAM grid system for the interest region. In the future, this methodology will be used to access climate change scenarios for the study region and to access the impact on surface gravity waves, storm surges and coastal flooding. Changes in frequency and atmospheric patterns related to the WT may project the expected impacts and thus provide important data for the local decision-makers.

4 CONCLUSÃO

Na primeira parte do presente trabalho foram identificados 12 eventos meteorológicos extremos que ocorreram na região costeira do sul do Brasil no passado recente. Esses eventos foram simulados numericamente utilizando o modelo OLAM e posteriormente avaliados através de comparações com dados provenientes de observações. Já na segunda parte, utilizamos a metodologia de refinamento híbrido para selecionar, simular e analisar 32 casos referentes a padrões de circulação típicos para a área de estudo, chamados de *weather types*. Dessa forma, foram atingidos os seis objetivos específicos deste trabalho.

Quando comparamos variáveis simuladas como precipitação, temperatura pressão ao nível do mar e componentes horizontais do vento com as observações, vemos que as configurações adotadas permitiram uma boa representação das circulações de larga escala e local da região de estudo. No caso, o modelo é capaz de representar a posição média dos centros de baixa e alta pressão relacionados aos eventos (índice de correlação espacial média de 0.94 para o momento de intensidade máxima de cada evento), tal como seus máximos e mínimos de pressão. A correlação espacial da velocidade do vento para o período de pico de cada evento também apresentou bons resultados (correlação média de 0.79). Também é reportada uma correspondência satisfatória para os dados de precipitação, principalmente os eventos mais extremos, sendo que o modelo captura a precipitação acumulada relacionada a esses eventos quase que em sua totalidade e apresenta uma distribuição espacial da precipitação próxima da observada pelas e estimativas por satélite (índice médio de correlação espacial de 0.64). Dessa forma, temos que a resposta para a pergunta de pesquisa 1 é de que o modelo OLAM tem uma boa capacidade de realizar simulações dos eventos extremos

ocorridos na região costeira do Sul do Brasil dentre os anos 2000 e 2018. Mesmo assim, o uso de grades com resolução horizontal mais refinadas (ex.: menores que 3 km) poderia propiciar uma melhora nas simulações dos eventos. Sendo essa uma sugestão para trabalhos futuros.

A metodologia de refinamento híbrido foi capaz de selecionar casos que representam bem os padrões de circulação atmosférica típicos da região, como a propagação de ciclones extratropicais e a predominância do anticiclone semipermanente do Atlântico Sul. Não obstante, o refinamento dinâmico propiciou campos atmosféricos de alta resolução com um grande detalhamento para a região costeira. Esses resultados permitem uma análise a nível local da circulação da área de estudo e podem servir como entrada para modelos oceânicos e hidrológicos a fins de realizar estudos regionais e análises de impacto. Temos assim, que a resposta para pergunta de pesquisa 2 é de que o método de refinamento hibrido pode ser aplicado satisfatoriamente para a região de estudo. Entretanto, a quantidade de *weather types* selecionados pode ter levantado uma quantidade de eventos que talvez sejam redundantes. Sendo assim, uma sugestão para trabalhos futuros seria a avaliação de diferentes quantidades *de weather types* para a região, a fim de indicar qual número seria o mais apropriado. No mais, o domínio espacial utilizado para as análises de SLP não propicia a representação do fenômeno da ZCAS, importante para a precipitação de verão na área de estudo. Um estudo futuro poderia utilizar algum método que busque integrar a ocorrência desse fenômeno. Entretanto, é necessária cautela para não adicionar ruído às análises, visto que aumentar o domínio pode adicionar variância aos dados, que não necessariamente está ligada diretamente com o clima da região.

Quanto a última pergunta de pesquisa, temos que os principais padrões atmosféricos para a região costeira sul do Brasil estão relacionados com a passagem periódica de sistemas

de baixa pressão nas três regiões de ciclogênese localizadas no Atlântico Sul. Esses sistemas estão relacionados com impactos como instabilidade atmosférica e geração de ondas, que propagam-se para as regiões costeiras. A trajetória dos ciclones extratropicais possui sentido à Antártida, porém alguns possuem trajetória anômalas, relacionadas com a ocorrência de eventos extremos na região. Durante o verão, esses sistemas estão relacionados com o estabelecimento da zona de convergência do Atlântico Sul, que pode desencadear em episódios de precipitação extrema para a região. A propagação dos ciclones extratropicais é geralmente seguida por um anticiclone pós-frontal, desencadeando mudanças na direção do vento na região costeira sul do país, levando a advecção de massas de ar frio em sentido aos trópicos. Não obstante, o anticiclone posicionado nas porções centrais do Atlântico Sul está relacionado com advecção quente e úmida para a região em questão, podendo desencadear episódios de precipitação orográfica.

Tendo esse cenário em vista, tem-se que as hipóteses do trabalho foram confirmadas. Primeiramente, o uso do modelo OLAM com as configurações adotadas aqui permitiu que os resultados dos campos atmosféricos provenientes de simulações de eventos extremos na região de estudo se aproximassem dos dados reais, com valores de correlação espacial médios entre os campos modelados e observados/reanálises de 0.94, 0.79 e 0.64 para os dados de SLP, velocidade do vento e precipitação acumulada, respectivamente. Para os dados de precipitação, os valores de correlação foram melhores quando analisados os campos relacionados aos eventos mais extremos, demonstrando que o modelo possui a capacidade de representar os fenômenos associados a ocorrência desses eventos. Quanto à segunda hipótese, temos que a utilização de uma metodologia híbrida com o modelo OLAM com grades de alta

resolução na região de estudo propiciou um melhor entendimento dos fenômenos de mesoescala na região costeira do Sul do Brasil. Sendo assim, o presente estudo foi capaz de atingir o objetivo final de estabelecer uma metodologia para estudos climáticos regionais para a região costeira da região sul do Brasil com sucesso.

Os resultados obtidos aqui serão aplicados futuramente em estudos regionais com o intuito de representar com alta resolução fenômenos oceanográficos e hidrológicos relacionados com a região de estudo. Além disso, tendo em vista a boa representação dos principais padrões atmosféricos da região de estudo, a metodologia proposta será utilizada para analisar projeções futuras de cenários de mudanças climáticas.

REFERÊNCIAS

ADCROFT, Alistair; HILL, Chris; MARSHALL, John. Representation of Topography by Shaved Cells in a Height Coordinate Ocean Model. **Monthly Weather Review**, [s. l.], v. 125, n. 9, p. 2293–2315, 1997. Disponível em: <http://journals.ametsoc.org/doi/abs/10.1175/1520-0493%281997%29125%3C2293%3AROTBSC%3E2.0.CO%3B2>

AKHTAR, Naveed; BRAUCH, Jennifer; AHRENS, Bodo. Climate modeling over the Mediterranean Sea: impact of resolution and ocean coupling. **Climate Dynamics**, [s. l.], 2018.

ALBUQUERQUE, Miguel da G. et al. Determining Shoreline Response to Meteo-oceanographic Events Using Remote Sensing and Unmanned Aerial Vehicle (UAV): Case Study in Southern Brazil. **Journal of Coastal Research**, [s. l.], v. 85, n. May 2018, p. 766–770, 2018.

ALVES, Lincoln M.; MARENGO, José. Assessment of regional seasonal predictability using the PRECIS regional climate modeling system over South America. **Theoretical and Applied Climatology**, [s. l.], v. 100, n. 3, p. 337–350, 2010.

AMBRIZZI, Tércio et al. The state of the art and fundamental aspects of regional climate modeling in South America. **Annals of the New York Academy of Sciences**, [s. l.], v. 1436, n. 1, p. 98–120, 2019.

BENESTAD, R. E. Empirical-statistical downscaling in climate modeling. **Eos**, [s.

l.], v. 85, n. 42, p. 3–5, 2004.

BITENCOURT, Daniel Pires; QUADRO, Mário F. Leal De; CALBETE, Nuri O. De. Análise de dois casos de ressaca no litoral da região Sul no verão de 2002. **XII Congresso Brasileiro de Meteorologia**, [s. l.], p. 469–479, 2002.

BRASIL. **Censo Demográfico 2010**. 2013. Disponível em: <https://www.ibge.gov.br>. Acesso em: 5 jul. 2018.

BRASIL. **PLANO NACIONAL DE LOGÍSTICA PORTUÁRIA**. [s.l: s.n.]. Disponível em: <https://infraestrutura.gov.br/images/SNP/planejamento_portuario/arquivos_pnlp/Diagnostico PNLP.pdf>.

BRASIL. **RELATÓRIO ANUAL DE AVALIAÇÃO: SUMÁRIO EXECUTIVO**. [s.l: s.n.].

BUCHARD, V. et al. The MERRA-2 Aerosol Reanalysis, 1980 Onward. Part II: Evaluation and Case Studies. **Journal of Climate**, [s. l.], v. 30, n. 17, p. 6851–6872, 2017. Disponível em: <http://journals.ametsoc.org/doi/10.1175/JCLI-D-16-0613.1>

CAI, Wenju et al. Increasing frequency of extreme El Niño events due to greenhouse warming. **Nature Climate Change**, [s. l.], v. 4, n. 2, p. 111–116, 2014. Disponível em: <http://dx.doi.org/10.1038/nclimate2100>

CAMPOS, Ricardo Martins; CAMARGO, Ricardo De; HARARI, Joseph. Caracterização de eventos extremos do nível do mar em Santos e sua correspondência com as reanálises do modelo do NCEP no sudoeste do Atlântico Sul. **Revista Brasileira de Meteorologia**, [s. l.], 2010.

CAMUS, Paula et al. A weather-type statistical downscaling framework for ocean

wave climate. **Journal of Geophysical Research: Oceans**, [s. l.], v. 119, n. 11, p. 7389–7405, 2014. Disponível em: <http://doi.wiley.com/10.1002/2013JC009563>

CAMUS, Paula; MENDEZ, Fernando J.; MEDINA, Raul. A hybrid efficient method to downscale wave climate to coastal areas. **Coastal Engineering**, [s. l.], 2011.

CANDELLA, Rogério Neder; SOUZA, Shirley Marques Lima. Ondas oceânicas extremas na costa sul-sudeste Brasileira geradas por ciclone com trajetória anormal em maio de 2011. **Revista Brasileira de Meteorologia**, [s. l.], v. 28, n. 4, p. 441–456, 2013.

CARVALHO, Leila M. V.; JONES, Charles; LIEBMANN, Brant. The South Atlantic Convergence Zone: Intensity, Form, Persistence, and Relationships with Intraseasonal to Interannual Activity and Extreme Rainfall. **Journal of Climate**, [s. l.], v. 17, n. 1, p. 88–108, 2004. Disponível em: <http://journals.ametsoc.org/doi/abs/10.1175/1520-0442%282004%29017%3C0088%3ATSACZI%3E2.0.CO%3B2>

CHOU, Sin Chan et al. Downscaling of South America present climate driven by 4-member HadCM3 runs. **Climate Dynamics**, [s. l.], v. 38, n. 3–4, p. 635–653, 2012.

CHOU, Sin Chan et al. Assessment of Climate Change over South America under RCP 4.5 and 8.5 Downscaling Scenarios. **American Journal of Climate Change**, [s. l.], v. 03, n. 05, p. 512–527, 2014. Disponível em: <http://www.scirp.org/journal/doi.aspx?DOI=10.4236/ajcc.2014.35043>

CHRISTENSEN, Jens Hesselbjerg; CHRISTENSEN, Ole Bøssing. A summary of the PRUDENCE model projections of changes in European climate by the end of this century. **Climatic Change**, [s. l.], v. 81, n. S1, p. 7–30, 2007. Disponível em: <http://link.springer.com/10.1007/s10584-006-9210-7>

COLETTE, A.; VAUTARD, R.; VRAC, M. Regional climate downscaling with prior statistical correction of the global climate forcing. **Geophysical Research Letters**, [s. l.], 2012.

COMPAGNUCCI, Rosa Hilda; SALLES, Maria Alejandra. Surface Pressure Patterns During The Year Over Southern South America. **International Journal of Climatology**, [s. l.], v. 17, n. 6, p. 635–653, 1997. Disponível em: <http://doi.wiley.com/10.1002/%28SICI%291097-0088%28199705%2917%3A6%3C635%3A%3AAID-JOC81%3E3.3.CO%3B2-2>

DIAS PINTO, João Rafael; DA ROCHA, Rosmeri Porfírio. The energy cycle and structural evolution of cyclones over southeastern South America in three case studies. **Journal of Geophysical Research Atmospheres**, [s. l.], v. 116, n. 14, p. 1–17, 2011.

DILLEY, Maxx et al. **Natural disaster hotspots: A global risk analysis**. [s.l: s.n.].

DOS SANTOS, Caio Floriano; TORNQUIST, Carmen Susana; MARIMON, Maria Paula Casagrande. Indústria das enchentes? Impasses e desafios dos desastres socioambientais no vale do Itajaí. **Geosul**, [s. l.], v. 29, n. 57, p. 197, 2014.

DRAPER, Clara S.; REICHLE, Rolf H.; KOSTER, Randal D. Assessment of MERRA-2 Land Surface Energy Flux Estimates. **Journal of Climate**, [s. l.], v. 31, n. 2, p. 671–691, 2018. Disponível em: <http://journals.ametsoc.org/doi/10.1175/JCLI-D-17-0121.1>

EASTERLING, D. R. et al. Climate extremes: Observations, modeling, and impacts. **Science**, [s. l.], v. 289, n. 5487, p. 2068–2074, 2000.

EBISUZAKI, Wesley; ZHANG, Li. Assessing the performance of the CFSR by an ensemble of analyses. **Climate Dynamics**, [s. l.], v. 37, n. 11–12, p. 2541–2550, 2011. Disponível em: <http://link.springer.com/10.1007/s00382-011-1074-5>

EVANS, Jenni L.; BRAUN, Aviva. A climatology of subtropical cyclones in the South Atlantic. **Journal of Climate**, [s. l.], 2012.

EYRING, Veronika et al. Overview of the Coupled Model Intercomparison Project Phase 6 (CMIP6) experimental design and organization. **Geoscientific Model Development**, [s. l.], v. 9, n. 5, p. 1937–1958, 2016. Disponível em: <https://www.geosci-model-dev.net/9/1937/2016/>

FARNHAM, David J.; DOSS-GOLLIN, James; LALL, Upmanu. Regional Extreme Precipitation Events: Robust Inference From Credibly Simulated GCM Variables. **Water Resources Research**, [s. l.], v. 54, n. 6, p. 3809–3824, 2018. Disponível em: <http://doi.wiley.com/10.1002/2017WR021318>

FERNANDES, Laís G.; RODRIGUES, Regina R. Changes in the patterns of extreme rainfall events in Southern Brazil. **International Journal of Climatology**, [s. l.], 2018.

FIELD, C. B. et al. Foreword. In: FIELD, Christopher B. et al. (Eds.). **Climate Change 2014 Impacts, Adaptation, and Vulnerability**. Cambridge: Cambridge University Press, 2014. p. vii–viii.

FIGUEROA, S. N.; SATYAMURTY, P.; DA SILVA DIAS, P. L. Simulations of the summer circulation over the South American region with an eta coordinate model. **Journal of the Atmospheric Sciences**, [s. l.], 1995.

FOTSO-NGUEMO, Thierry C. et al. On the added value of the regional climate model REMO in the assessment of climate change signal over Central Africa. **Climate Dynamics**, [s. l.], 2017.

FRAGA, Nilson Cesar. Enchentes urbanas no Vale do Itajaí, Brasil. 25 anos da

enchente catástrofe de 1983-reflexos socioambientais e culturais no século XXI. **Encuentro de Geógrafos da América Latina: Caminando a una América Latina en Trasnformación**, [s. l.], v. 12, 2009.

FRICH, P. et al. Observed coherent changes in climatic extremes during the second half of the twentieth century. **Climate Research**, [s. l.], v. 19, n. 3, p. 193–212, 2002.

FUENTES, Eduardo Vetromilla; BITENCOURT, Daniel Pires; FUENTES, Márcia Vetromilla. Análise da velocidade do vento e altura de onda em incidentes de naufrágio na costa brasileira entre os estados do Sergipe e do Rio Grande do Sul. **Revista Brasileira de Meteorologia**, [s. l.], v. 28, n. 3, p. 257–266, 2013. Disponível em: <http://www.scielo.br/scielo.php?script=sci_arttext&pid=S0102-77862013000300003&lng=pt&tlng=pt>

GAN, Manoel Alonso; RAO, V. B. **The influence of the Andes Cordillera on transient disturbancesMonthly Weather Review**, 1994.

GAN, Manoel Alonso; RAO, Vadlamudi Brahmananda. Surface Cyclogenesis over South America. **Monthly Weather Review**, [s. l.], v. 119, n. 5, p. 1293–1302, 1991. Disponível em: <http://journals.ametsoc.org/doi/abs/10.1175/1520-0493%281991%29119%3C1293%3ASCOSA%3E2.0.CO%3B2>

GARREAUD, R. D.; ACEITUNO, P. Atmospheric circulation over South America: mean features and variability. In: VEBLEN, T.; ORME, A.; YOUNG, K. (Eds.). **The Physical Geography of South America**. Oxford: Oxford Univ. Press, 2002.

GARREAUD, René D. D. Cold air incursions over subtropical South America: Mean structure and dynamics. **Monthly Weather Review**, [s. l.], v. 128, n. 7 II, p. 2544–2559, 2000. Disponível em: <http://journals.ametsoc.org/doi/abs/10.1175/1520-

0493%282000%29128%3C2544%3ACAIOSS%3E2.0.CO%3B2>

GARREAUD, René D. D. et al. Present-day South American climate. **Palaeogeography, Palaeoclimatology, Palaeoecology**, [s. l.], v. 281, n. 3–4, p. 180–195, 2009. Disponível em: <https://linkinghub.elsevier.com/retrieve/pii/S0031018208005002>

GARREAUD, René D.; FALVEY, Mark. The coastal winds off western subtropical South America in future climate scenarios. **International Journal of Climatology**, [s. l.], v. 29, n. 4, p. 543–554, 2009. Disponível em: <http://cdiac.esd.ornl.gov/oceans/GLODAP/glodap_pdfs/Thermohaline.web.pdf>

GEBREMICHAEL, Mekonnen; KRAJEWSKI, Witold F. Assessment of the Statistical Characterization of Small-Scale Rainfall Variability from Radar: Analysis of TRMM Ground Validation Datasets. **Journal of Applied Meteorology**, [s. l.], v. 43, n. 8, p. 1180–1199, 2004. Disponível em: <http://journals.ametsoc.org/doi/abs/10.1175/1520-0450%282004%29043%3C1180%3AAOTSCO%3E2.0.CO%3B2>

GELARO, Ronald et al. The Modern-Era Retrospective Analysis for Research and Applications, Version 2 (MERRA-2). **Journal of Climate**, [s. l.], v. 30, n. 14, p. 5419–5454, 2017. Disponível em: <http://journals.ametsoc.org/doi/10.1175/JCLI-D-16-0758.1>

GIORGI, Filippo; GUTOWSKI, William J. Regional Dynamical Downscaling and the CORDEX Initiative. **Annual Review of Environment and Resources**, [s. l.], v. 40, n. 1, p. 467–490, 2015. Disponível em: <http://www.annualreviews.org/doi/10.1146/annurev-environ-102014-021217>

GIORGI, Filippo; MARINUCCI, Maria Rosaria. A Investigation of the Sensitivity of Simulated Precipitation to Model Resolution and Its Implications for Climate Studies.

Monthly Weather Review, [s. l.], v. 124, n. 1, p. 148–166, 1996. Disponível em: <http://journals.ametsoc.org/doi/abs/10.1175/1520-0493%281996%29124%3C0148%3AAIOTSO%3E2.0.CO%3B2>

GOMES DA SILVA, Paula et al. Estimating Flooding Level Through the Brazilian Coast Using Reanalysis Data. **Journal of Coastal Research**, [s. l.], v. 75, n. sp1, p. 1092–1096, 2016. Disponível em: <http://www.bioone.org/doi/10.2112/SI75-219.1>

GORDON, Arnold L. Brazil-Malvinas Confluence–1984. **Deep Sea Research Part A. Oceanographic Research Papers**, [s. l.], v. 36, n. 3, p. 359–384, 1989. Disponível em: <https://linkinghub.elsevier.com/retrieve/pii/0198014989900423>

GOZZO, Luiz Felippe et al. Subtropical Cyclones over the Southwestern South Atlantic: Climatological Aspects and Case Study. **Journal of Climate**, [s. l.], v. 27, n. 22, p. 8543–8562, 2014. Disponível em: <http://journals.ametsoc.org/doi/abs/10.1175/JCLI-D-14-00149.1>

GRAMCIANINOV, C. B.; HODGES, K. I.; CAMARGO, R. The properties and genesis environments of South Atlantic cyclones. **Climate Dynamics**, [s. l.], v. 53, n. 7–8, p. 4115–4140, 2019. Disponível em: <https://doi.org/10.1007/s00382-019-04778-1>

GRELL, G. A.; FREITAS, S. R. A scale and aerosol aware stochastic convective parameterization for weather and air quality modeling. **Atmospheric Chemistry and Physics**, [s. l.], v. 14, n. 10, p. 5233–5250, 2014. Disponível em: <https://www.atmos-chem-phys.net/14/5233/2014/>

GRIMM, Alice M. The El Niño Impact on the Summer Monsoon in Brazil: Regional Processes versus Remote Influences. **Journal of Climate**, [s. l.], v. 16, n. 2, p. 263–280, 2003. Disponível em: <http://journals.ametsoc.org/doi/abs/10.1175/1520-

0442%282003%29016%3C0263%3ATENIOT%3E2.0.CO%3B2>

GRIMM, Alice M. Interannual climate variability in South America: impacts on seasonal precipitation, extreme events, and possible effects of climate change. **Stochastic Environmental Research and Risk Assessment**, [s. l.], v. 25, n. 4, p. 537–554, 2011. Disponível em: <http://link.springer.com/10.1007/s00477-010-0420-1>

GRIMM, Alice M.; BARROS, Vicente R.; DOYLE, Moira E. Climate Variability in Southern South America Associated with El Niño and La Niña Events. **Journal of Climate**, [s. l.], 2000.

GRIMM, Alice Marlene. Clima da região Sul do Brasil. In: **Tempo e clima no Brasil**. 2. ed. [s.l: s.n.]. p. 259–275.

GUIMARÃES, P. V.; FARINA, L.; TOLDO, E. E. Analysis of extreme wave events on the southern coast of Brazil. **Natural Hazards and Earth System Sciences**, [s. l.], v. 14, n. 12, p. 3195–3205, 2014.

HANDMER, John et al. Changes in impacts of climate extremes: Human systems and ecosystems. In: **Managing the Risks of Extreme Events and Disasters to Advance Climate Change Adaptation: Special Report of the Intergovernmental Panel on Climate Change**. [s.l: s.n.].

HAY, Lauren E. et al. Simulation of precipitation by weather type analysis. **Water Resources Research**, [s. l.], v. 27, n. 4, p. 493–501, 1991.

HERMANN, Maria Lucia de Paula. **Atlas de Desastres Naturais do Estado de Santa Catarina: perìodo de 1980 a 2010**. Florianopolis: IHGSC, 2014. v. 2

HERRMANN, Maria Lúcia de Paula. **Atlas de Desastres Naturais do Estado de**

Santa Catarina. Florianópolis. Disponível em: <http://www.ceped.ufsc.br/wp-content/uploads/2006/01/Atlas_Ceped.pdf>.

HOSKINS, B. J.; HODGES, Kevin I. A new perspective on Southern Hemisphere storm tracks. **Journal of Climate**, [s. l.], v. 18, n. 20, p. 4108–4129, 2005.

HOU, Arthur Y. et al. The Global Precipitation Measurement Mission. **Bulletin of the American Meteorological Society**, [s. l.], v. 95, n. 5, p. 701–722, 2014. Disponível em: <http://journals.ametsoc.org/doi/abs/10.1175/BAMS-D-13-00164.1>

HUFFMAN, George J. et al. The TRMM Multisatellite Precipitation Analysis (TMPA): Quasi-Global, Multiyear, Combined-Sensor Precipitation Estimates at Fine Scales. **Journal of Hydrometeorology**, [s. l.], v. 8, n. 1, p. 38–55, 2007. Disponível em: <http://journals.ametsoc.org/doi/10.1175/JHM560.1>

HUTH, Radan. A circulation classification scheme applicable in GCM studies. **Theoretical and Applied Climatology**, [s. l.], v. 67, n. 1–2, p. 1–18, 2000. Disponível em: <http://link.springer.com/10.1007/s007040070012>

HUTH, Radan. Disaggregating climatic trends by classification of circulation patterns. **International Journal of Climatology**, [s. l.], v. 21, n. 2, p. 135–153, 2001. Disponível em: <http://doi.wiley.com/10.1002/joc.605>

HUTH, Radan et al. Classifications of atmospheric circulation patterns: Recent advances and applications. **Annals of the New York Academy of Sciences**, [s. l.], v. 1146, p. 105–152, 2008.

IPCC. **Climate Change 2014**. [s.l: s.n.].

IPCC. **The IPCC and the Sixth Assessment cycle**. Geneva. Disponível em: <https://www.ipcc.ch/site/assets/uploads/2018/11/AR6_brochure_en.pdf>.

JONGMAN, Brenden; WARD, Philip J.; AERTS, Jeroen C. J. H. Global exposure to river and coastal flooding: Long term trends and changes. **Global Environmental Change**, [s. l.], 2012.

JONKMAN, S. N. Global perspectives on loss of human life caused by floods. **Natural Hazards**, [s. l.], 2005.

KARL, T. R., & EASTERLING, D. R. Climate extremes selected review and future research directions. **Weather and Climate Extremes**, [s. l.], v. 42, n. 1, p. 309–325, 1999.

KHANNA, Jaya et al. Regional dry-season climate changes due to three decades of Amazonian deforestation. **Nature Climate Change**, [s. l.], v. 7, n. 3, p. 200–204, 2017. Disponível em: <http://www.nature.com/articles/nclimate3226>

KODAMA, Yasumasa. Large-Scale Common Features of Subtropical Precipitation Zones (the Baiu Frontal Zone, the SPCZ, and the SACZ) Part I: Characteristics of Subtropical Frontal Zones. **Journal of the Meteorological Society of Japan. Ser. II**, [s. l.], v. 70, n. 4, p. 813–836, 1992. Disponível em: <https://www.jstage.jst.go.jp/article/jmsj1965/70/4/70_4_813/_article>

KRÜGER, Luiz Fernando et al. RegCM3 nested in HadAM3 scenarios A2 and B2: Projected changes in extratropical cyclogenesis, temperature and precipitation over the South Atlantic Ocean. **Climatic Change**, [s. l.], v. 113, n. 3–4, p. 599–621, 2012.

KUNKEL, Kenneth E.; PIELKE, Roger A.; CHANGNON, Stanley A. Temporal Fluctuations in Weather and Climate Extremes That Cause Economic and Human Health Impacts: A Review. **Bulletin of the American Meteorological Society**, [s. l.], v. 80, n. 6, p. 1077–1098, 1999. Disponível em: <https://journals.ametsoc.org/doi/pdf/10.1175/1520-

0477%281999%29080%3C1077%3ATFIWAC%3E2.0.CO%3B2>

LAING, Arlene G.; MICHAEL FRITSCH, J. The global population of mesoscale convective complexes. **Quarterly Journal of the Royal Meteorological Society**, [s. l.], 1997.

LIEBMANN, Brant et al. Submonthly Convective Variability over South America and the South Atlantic Convergence Zone. **Journal of Climate**, [s. l.], v. 12, n. 7, p. 1877–1891, 1999. Disponível em: <http://journals.ametsoc.org/doi/abs/10.1175/1520-0442%281999%29012%3C1877%3ASCVOSA%3E2.0.CO%3B2>

LIU, Zhong. Comparison of Integrated Multisatellite Retrievals for GPM (IMERG) and TRMM Multisatellite Precipitation Analysis (TMPA) Monthly Precipitation Products: Initial Results. **Journal of Hydrometeorology**, [s. l.], v. 17, n. 3, p. 777–790, 2016. Disponível em: <http://journals.ametsoc.org/doi/10.1175/JHM-D-15-0068.1>

LUPO, Anthony R. et al. South American Cold Surges: Types, Composites, and Case Studies. **Monthly Weather Review**, [s. l.], v. 129, n. 5, p. 1021–1041, 2001. Disponível em: <http://journals.ametsoc.org/doi/abs/10.1175/1520-0493%282001%29129%3C1021%3ASACSTC%3E2.0.CO%3B2>

MACHADO, Arthur A. et al. Historical assessment of extreme coastal sea state conditions in southern Brazil and their relation to erosion episodes. **Pan-American Journal of Aquatic Sciences**, [s. l.], v. 5, n. 2, p. 277–286, 2010.

MARENGO, Jose et al. **Impacto, vulnerabilidade e adaptação das cidades costeiras brasileiras às mudanças climáticas: Relatório Especial do Painel Brasileiro de Mudanças Climáticas**. [s.l: s.n.]. Disponível em: <https://www.google.com/url?sa=t&rct=j&q=&esrc=s&source=web&cd=1&ved=2ahUKEwi

I7Yz2ku3mAhV9EbkGHa6PAYoQFjAAegQIBRAC&url=http%3A%2F%2Fppgoceano.pagi
nas.ufsc.br%2Ffiles%2F2017%2F06%2FRelatorio_DOIS_v1_04.06.17.pdf&usg=AOvVaw0
oyzCrmarx8ybE0U7KwudO>.

MARENGO, Jose A. et al. Climatology of the Low-Level Jet East of the Andes as Derived from the NCEP–NCAR Reanalyses: Characteristics and Temporal Variability. **Journal of Climate**, [s. l.], v. 17, n. 12, p. 2261–2280, 2004. Disponível em: <http://journals.ametsoc.org/doi/abs/10.1175/1520-
0442%282004%29017%3C2261%3ACOTLJE%3E2.0.CO%3B2>

MARENGO, Jose A. et al. Future change of temperature and precipitation extremes in South America as derived from the PRECIS regional climate modeling system. **International Journal of Climatology**, [s. l.], v. 29, n. 15, p. 2241–2255, 2009. Disponível em: <http://cdiac.esd.ornl.gov/oceans/GLODAP/glodap_pdfs/Thermohaline.web.pdf>

MARENGO, Jose A. et al. Development of regional future climate change scenarios in South America using the Eta CPTEC/HadCM3 climate change projections: climatology and regional analyses for the Amazon, São Francisco and the Paraná River basins. **Climate Dynamics**, [s. l.], v. 38, n. 9–10, p. 1829–1848, 2012. Disponível em: <http://link.springer.com/10.1007/s00382-011-1155-5>

MCTAGGART-COWAN, Ron et al. Analysis of Hurricane Catarina (2004). **Monthly Weather Review**, [s. l.], v. 134, n. 11, p. 3029–3053, 2006. Disponível em: <http://journals.ametsoc.org/doi/abs/10.1175/MWR3330.1>

MEARNS, L. O. et al. **Guidelines for Use of Climate Scenarios Developed from Regional Climate Model ExperimentsData Distribution Centre of the Intergovernmental**

Panel on Climate Change. [s.l: s.n.].

MECHLER, Reinhard; BOUWER, Laurens M. Understanding trends and projections of disaster losses and climate change: is vulnerability the missing link? **Climatic Change**, [s. l.], v. 133, n. 1, p. 23–35, 2015. Disponível em: <http://link.springer.com/10.1007/s10584-014-1141-0>

MEDVIGY, David et al. Simulated Changes in Northwest U.S. Climate in Response to Amazon Deforestation*. **Journal of Climate**, [s. l.], v. 26, n. 22, p. 9115–9136, 2013. Disponível em: <http://journals.ametsoc.org/doi/abs/10.1175/JCLI-D-12-00775.1>

MEDVIGY, David; WALKO, Robert L.; AVISSAR, R. Modeling interannual variability of the Amazon hydroclimate. **Geophysical Research Letters**, [s. l.], v. 35, n. 15, p. 2–6, 2008.

MEDVIGY, David; WALKO, Robert L.; AVISSAR, Roni. Simulated Links between Deforestation and Extreme Cold Events in South America. **Journal of Climate**, [s. l.], v. 25, n. 11, p. 3851–3866, 2012. Disponível em: <http://journals.ametsoc.org/doi/abs/10.1175/JCLI-D-11-00259.1>

MEEHL, Gerald A. et al. Response of the NCAR Climate System Model to Increased CO 2 and the Role of Physical Processes. **Journal of Climate**, [s. l.], v. 13, n. 11, p. 1879–1898, 2000. Disponível em: <http://journals.ametsoc.org/doi/abs/10.1175/1520-0442%282000%29013%3C1879%3AROTNCS%3E2.0.CO%3B2>

MELO FILHO, Eloi; HAMMES, Guilherme R.; FRANCO, Davide. Estudo de Caso: A Ressaca de Agosto de 2005 em Santa Catarina. In: 2º SEMINARIO E WORKSHOP EM ENGENHARIA OCEÂNICA 2006, **Anais**... [s.l: s.n.]

MENDES, David et al. Climatology of extratropical cyclones over the South

American–southern oceans sector. **Theoretical and Applied Climatology**, [s. l.], v. 100, n. 3–4, p. 239–250, 2010. Disponível em: <http://link.springer.com/10.1007/s00704-009-0161-6>

MEYERS, Michael P. et al. New RAMS cloud microphysics parameterization. Part II: The two-moment scheme. **Atmospheric Research**, [s. l.], v. 45, n. 1, p. 3–39, 1997. Disponível em: <https://linkinghub.elsevier.com/retrieve/pii/S0169809597000185>

MINUZZI, Rosandro; RODRIGUES, Laura. **Novembro com recordes de chuva em SC: 1000 mm em Blumenau**. [s.l: s.n.].

MLAWER, Eli J. et al. Radiative transfer for inhomogeneous atmospheres: RRTM, a validated correlated-k model for the longwave. **Journal of Geophysical Research: Atmospheres**, [s. l.], v. 102, n. D14, p. 16663–16682, 1997. Disponível em: <http://doi.wiley.com/10.1029/97JD00237>

MORAES, Antonio Carlos Robert. **Contribuições para a gestão da zona costeira do Brasil: elementos para uma geografia do litoral brasileiro**. 1. ed. São Paulo, Brasil.

MUEHE, Dieter. Aspectos gerais da erosão costeira no brasil. **Mercator**, [s. l.], 2005.

NEVES, Claudio Freitas; MUEHE, Dieter. Vulnerabilidade, impactos e adaptação a mudanças do clima: a zona costeira. **Parcerias Estratégicas**, [s. l.], v. 13, n. 27, p. 217–296, 2008. Disponível em: <http://seer.cgee.org.br/index.php/parcerias_estrategicas/article/view/325>

NICHOLLS, Robert J. Coastal flooding and wetland loss in the 21st century: Changes under the SRES climate and socio-economic scenarios. **Global Environmental**

Change, [s. l.], 2004.

NICOLODI, João Luiz; PETERMANN, Rafael Mueller. Potential vulnerability of the Brazilian coastal zone in its environmental, social, and technological aspects. **Pan-American Journal of Aquatic Sciences**, [s. l.], v. 5, n. 2, p. 184–204, 2010. Disponível em: <http://www.panamjas.org/pdf_artigos/PANAMJAS_5(2)_12-32.pdf>

NIKIEMA, Pinghouinde Michel et al. Multi-model CMIP5 and CORDEX simulations of historical summer temperature and precipitation variabilities over West Africa. **International Journal of Climatology**, [s. l.], 2017.

NOBRE, Paulo; MOURA, Antonio D.; SUN, Liqiang. Dynamical downscaling of seasonal climate prediction over Nordeste Brazil with ECHAM3 and NCEP's regional spectral models at IRI. **Bulletin of the American Meteorological Society**, [s. l.], v. 82, n. 12, p. 2787–2796, 2001.

NUNES, André Becker; DA SILVA, Gilson Carlos. CLIMATOLOGY OF EXTREME RAINFALL EVENTS IN EASTERN AND NORTHERN SANTA CATARINA STATE, BRAZIL: PRESENT AND FUTURE CLIMATE. **Revista Brasileira de Geofísica**, [s. l.], v. 31, n. 3, p. 413, 2013. Disponível em: <http://sbgf.org.br/revista/index.php/rbgf/article/view/314>

NUÑEZ, Mario N.; SOLMAN, Silvina A.; CABRÉ, Maria Fernanda. Regional climate change experiments over southern South America. II: Climate change scenarios in the late twenty-first century. **Climate Dynamics**, [s. l.], v. 32, n. 7–8, p. 1081–1095, 2009. Disponível em: <http://link.springer.com/10.1007/s00382-008-0449-8>

ORLANSKI, I. A rational subdivision of scales for atmospheric processes. **Bull. Amer. Meteor. Soc.**, [s. l.], 1975.

108

PARISE, Cláudia Klose; CALLIARI, Lauro Júlio; KRUSCHE, Nisia. Extreme storm surges in the south of Brazil: Atmospheric conditions and shore erosion. **Brazilian Journal of Oceanography**, [s. l.], v. 57, n. 3, p. 175–188, 2009.

PARISE, Cláudia Klose; FARINA, Leandro. Ocean wave modes in the South Atlantic by a short-scale simulation. **Tellus A: Dynamic Meteorology and Oceanography**, [s. l.], v. 64, n. 1, p. 17362, 2012.

PEREIRA FILHO, Augusto José et al. New perspectives on the synoptic and mesoscale structure of Hurricane Catarina. **Atmospheric Research**, [s. l.], v. 95, n. 2–3, p. 157–171, 2010. Disponível em: <http://dx.doi.org/10.1016/j.atmosres.2009.09.009>

PEZZA, Alexandre Bernardes; SIMMONDS, Ian. The first South Atlantic hurricane: Unprecedented blocking, low shear and climate change. **Geophysical Research Letters**, [s. l.], v. 32, n. 15, 2005.

PIELKE, R. A. et al. A comprehensive meteorological modeling system-RAMS. **Meteorology and Atmospheric Physics**, [s. l.], v. 49, n. 1–4, p. 69–91, 1992. Disponível em: <http://link.springer.com/10.1007/BF01025401>

PINHEIRO, Henri. **CHUVAS INTENSAS PROVOCAM ALAGAMENTOS NOS LITORAIS DOS ESTADOS DO RS E DE SC ENTRE OS DIAS 18 E 19 DE JANEIRO DE 2011**. [s.l: s.n.].

POVEDA, Germán; JARAMILLO, Liliana; VALLEJO, Luisa F. Seasonal precipitation patterns along pathways of South American low-level jets and aerial rivers. **Water Resources Research**, [s. l.], v. 50, n. 1, p. 98–118, 2014. Disponível em: <http://doi.wiley.com/10.1002/2013WR014087>

PRYOR, S. C.; BARTHELMIE, R. J. Hybrid downscaling of wind climates over the eastern USA. **Environmental Research Letters**, [s. l.], 2014.

PUGH, D. T.; VASSIE, J. M. Extreme Sea Levels From Tide and Surge Probability. **Coastal Engineering**, [s. l.], 1978.

RAMOS DA SILVA, Renato et al. Weather forecasting for eastern amazon with olam model. **Revista Brasileira de Meteorologia**, [s. l.], v. 29, p. 11–22, 2014. a.

RAMOS DA SILVA, Renato et al. Climate estimates for Eastern Amazon with OLAM model. **Revista Brasileira de Meteorologia**, [s. l.], v. 29, n. spe, p. 2–10, 2014. b. Disponível em: <http://www.scielo.br/scielo.php?script=sci_arttext&pid=S0102-77862014000500002&lng=en&tlng=en>

RAMOS DA SILVA, Renato; HAAS, Reinaldo. Ocean Global Warming Impacts on the South America Climate. **Frontiers in Earth Science**, [s. l.], v. 4, n. March, p. 1–8, 2016. Disponível em: <http://journal.frontiersin.org/Article/10.3389/feart.2016.00030/abstract>

RANDLES, C. A. et al. The MERRA-2 Aerosol Reanalysis, 1980 Onward. Part I: System Description and Data Assimilation Evaluation. **Journal of Climate**, [s. l.], 2017.

RAO, V. B.; CAVALCANTI, Iracema F. A.; HADA, Kioshi. Annual variation of rainfall over Brazil and water vapor characteristics over South America. **Journal of Geophysical Research: Atmospheres**, [s. l.], 1996.

RAO, V. B.; HADA, K. Characteristics of rainfall over Brazil: Annual variations and connections with the Southern Oscillation. **Theoretical and Applied Climatology**, [s. l.], v. 42, n. 2, p. 81–91, 1990. Disponível em: <http://link.springer.com/10.1007/BF00868215>

REBIOTA, Michelle Simões; KRUSCHE, Nisia; PICCOLI, Humberto Camargo. Climate Variability in Rio Grande, RS, Brazil: a Quantitative Analysis of Contributions Due

To Atmospheric Systems. **Revista Brasileira de Meteorologia**, [s. l.], v. 21, n. 2, p. 256–270, 2006.

REBOITA, Michelle Simões. et al. Extratropical cyclones over the southwestern South Atlantic Ocean: HadGEM2-ES and RegCM4 projections. **International Journal of Climatology**, [s. l.], v. 38, n. 6, p. 2866–2879, 2018.

REBOITA, Michelle Simões.; ROCHA, Rosmeri P. Da; AMBRIZZI, Tércio. Dynamic and Climatological Features of Cyclonic Developments Over Southwestern South Atlantic Ocean. In: **Horizons in Earth Science Research.** [s.l: s.n.]. v. 6p. 135–160.

REBOITA, Michelle Simões et al. South Atlantic Ocean cyclogenesis climatology simulated by regional climate model (RegCM3). **Climate Dynamics**, [s. l.], v. 35, n. 7–8, p. 1331–1347, 2010. Disponível em: <http://link.springer.com/10.1007/s00382-009-0668-7>

REBOITA, Michelle Simões et al. Ciclones em Superfície nas Latitudes Austrais: Parte I - Revisão Bibliográfica. **Revista Brasileira de Meteorologia**, [s. l.], v. 32, n. 2, p. 171–186, 2017. Disponível em: <http://www.scielo.br/scielo.php?script=sci_arttext&pid=S0102-77862017000200171&lng=pt&tlng=pt>

REYNOLDS, R. W.; SMITH, T. M. Improved global sea surface temperature analyses using optimum interpolation. **Journal of Climate**, [s. l.], 1994.

REYNOLDS, Richard W. et al. An improved in situ and satellite SST analysis for climate. **Journal of Climate**, [s. l.], 2002.

REYNOLDS, Richard W. et al. Daily High-Resolution-Blended Analyses for Sea Surface Temperature. **Journal of Climate**, [s. l.], v. 20, n. 22, p. 5473–5496, 2007.

Disponível em: <http://journals.ametsoc.org/doi/10.1175/2007JCLI1824.1>

RIBEIRO, Felipe Garcia et al. O impacto econômico dos desastres naturais: o caso das chuvas de 2008 em Santa Catarina. **Planejamento e Políticas Públicas**, [s. l.], v. 43, p. 299–322, 2014.

ROBERTSON, Aw; MECHOSO, Cr. Interannual and interdecadal variability of the South Atlantic Convergence Zone. **Monthly weather review**, [s. l.], 2000.

RODRIGUES, M. Laura Guimarães; YNOUE, Rita Yuri. Mesoscale and synoptic environment in three orographically enhanced rain events on the coast of Santa Catarina (Brazil). **Weather and Forecasting**, [s. l.], v. 31, n. 5, p. 1529–1546, 2016.

SAHA, Suranjana et al. The NCEP Climate Forecast System Reanalysis. **Bulletin of the American Meteorological Society**, [s. l.], v. 91, n. 8, p. 1015–1058, 2010. Disponível em: <http://journals.ametsoc.org/doi/10.1175/2010BAMS3001.1>

SAHA, Suranjana et al. The NCEP Climate Forecast System Version 2. **Journal of Climate**, [s. l.], v. 27, n. 6, p. 2185–2208, 2014. Disponível em: <http://journals.ametsoc.org/doi/10.1175/JCLI-D-12-00823.1>

SALIO, Paola. Chaco low-level jet events characterization during the austral summer season. **Journal of Geophysical Research**, [s. l.], v. 107, n. D24, p. 4816, 2002. Disponível em: <http://doi.wiley.com/10.1029/2001JD001315>

SALIO, Paola; NICOLINI, Matilde; ZIPSER, Edward J. Mesoscale Convective Systems over Southeastern South America and Their Relationship with the South American Low-Level Jet. **Monthly Weather Review**, [s. l.], v. 135, n. 4, p. 1290–1309, 2007. Disponível em: <http://journals.ametsoc.org/doi/abs/10.1175/MWR3305.1>

SATYAMURTY, Prakki; MATTOS, Luiz Fernando De. **Climatological lower**

tropospheric frontogenesis in the midlatitudes due to horizontal deformation and divergenceMonthly Weather Review, 1989.

SAUSEN, Tania Maria et al. **CICLONE EXTRATROPICAL OCORRIDO EM MAIO DE 2008 (SC E RS): GÊNESE, EVOLUÇÃO E AVALIAÇÃO DAS CONSEQUENTES INUNDAÇÕES COM O AUXÍLIO DE GEOTECNOLOGIASInstituto Nacional de Pesquisas Espaciais (INPE)**. [s.l: s.n.].

SELUCHI, Marcelo E. et al. The Northwestern Argentinean Low: A Study of Two Typical Events. **Monthly Weather Review**, [s. l.], 2003.

SELUCHI, Marcelo E.; MARENGO, José A. Tropical − Midlatitude Exchange of Air Masses During Summer and Winter in South America : Climatic Aspects. **International Journal of Climatology**, [s. l.], v. 1190, p. 1167–1190, 2000.

SHERIDAN, Scott C. The redevelopment of a weather-type classification scheme for North America. **International Journal of Climatology**, [s. l.], v. 22, n. 1, p. 51–68, 2002.

SHORT, Andrew D.; KLEIN, Antonio Henrique da F. **Brazilian Beach Systems**. Cham: Springer International Publishing, 2016. v. 17 Disponível em: <http://link.springer.com/10.1007/978-3-319-30394-9>

SILVA, Philipp Edson Dias Da. **CARACTERIZAÇÃO DO PADRÃO DE ONDAS NA COSTA DO BRASIL POR MEIO DE MODELAGEM NUMÉRICA**. 2013. Instituto Nacional de Pesquisas Espaciais, [s. l.], 2013.

SILVA DIAS, Maria Assunção F. **As chuvas de novembro de 2008 em Santa Catarina : um estudo de caso visando à melhoria do monitoramento e da previsão de eventos extremos**. [s.l: s.n.].

SINCLAIR, Mark R. A Climatology of Cyclogenesis for the Southern Hemisphere. **Monthly Weather Review**, [s. l.], v. 123, n. 6, p. 1601–1619, 1995. Disponível em: <http://journals.ametsoc.org/doi/abs/10.1175/1520-0493%281995%29123%3C1601%3AACOCFT%3E2.0.CO%3B2>

SMAGORINSKY, J. GENERAL CIRCULATION EXPERIMENTS WITH THE PRIMITIVE EQUATIONS. **Monthly Weather Review**, [s. l.], v. 91, n. 3, p. 99–164, 1963. Disponível em: <http://www.sciencemag.org/cgi/doi/10.1126/science.27.693.594>

SMALL, Christopher; NICHOLLS, Robert J. A global analysis of human settlement in coastal zones. **Journal of Coastal Research**, [s. l.], 2003.

STERL, Andreas. On the (in)homogeneity of reanalysis products. **Journal of Climate**, [s. l.], 2004.

STOCKER, Thomas F. et al. **Climate Change 2013 - The Physical Science BasisIntergovernmental Panel on Climate Change**. [s.l: s.n.].

STRAMMA, Lothar. The Brazil current transport south of 23°S. **Deep Sea Research Part A. Oceanographic Research Papers**, [s. l.], v. 36, n. 4, p. 639–646, 1989. Disponível em: <https://linkinghub.elsevier.com/retrieve/pii/0198014989900125>

STROHAECKERI, Tânia Marques. Dinâmica Populacional. In: **Macrodiagnóstico da zona costeira e marinha do brasil**. [s.l: s.n.]. p. 59–74.

SUN, Fengpeng; WALTON, Daniel B.; HALL, Alex. A hybrid dynamical-statistical downscaling technique. Part II: End-of-Century warming projections predict a new climate state in the Los Angeles region. **Journal of Climate**, [s. l.], 2015.

TAKLE, E. S. et al. Project to Intercompare Regional Climate Simulations (PIRCS): Description and initial results. **Journal of Geophysical Research Atmospheres**, [s. l.], v.

104, n. D16, 1999.

TAYLOR, Karl E.; STOUFFER, Ronald J.; MEEHL, Gerald A. An overview of CMIP5 and the experiment design. **Bulletin of the American Meteorological Society**, [s. l.], v. 93, n. 4, p. 485–498, 2012.

TEIXEIRA, Mateusda Silva; SATYAMURTY, Prakki. Dynamical and Synoptic Characteristics of Heavy Rainfall Episodes in Southern Brazil. **Monthly Weather Review**, [s. l.], v. 135, n. 2, p. 598–617, 2007. Disponível em: <http://journals.ametsoc.org/doi/abs/10.1175/MWR3302.1>

TRENBERTH, Kevin E.; HOAR, Timothy J. The 1990-1995 El Niño-Southern Oscillation Event: Longest on Record. **Geophysical Research Letters**, [s. l.], v. 23, n. 1, p. 57–60, 1996. Disponível em: <http://scholar.google.com/scholar?hl=en&btnG=Search&q=intitle:Longest+on+record#5>

TRIGO, Ricardo M. et al. Modelling wildfire activity in Iberia with different atmospheric circulation weather types. **International Journal of Climatology**, [s. l.], v. 36, n. 7, p. 2761–2778, 2016.

UNISDR. **Global assessment report on disaster risk reduction (2009)United Nations Office for Disaster Risk Reduction**. [s.l: s.n.].

UNISDR; CRED. **Economic Losses, Poverty and Disasters 1998-2017UNISDR (United Nations Office for Disaster Risk Reduction) Centre for Research on Epidemiology of Disasters (CRED)**. [s.l: s.n.].

VAN DER WIEL, Karin et al. A dynamical framework for the origin of the diagonal South Pacific and South Atlantic Convergence Zones. **Quarterly Journal of the Royal**

Meteorological Society, [s. l.], 2015.

VARIKODEN, Hamza et al. Assessment of regional downscaling simulations for long term mean, excess and deficit Indian Summer Monsoons. **Global and Planetary Change**, [s. l.], 2018.

VELASCO, I.; FRITSCH, J. M. Mesoscale convective complexes in the Americas. **Journal of Geophysical Research**, [s. l.], 1987.

VERA, Carolina S.; VIGLIAROLO, Paula K.; BERBERY, Ernesto Hugo. Cold Season Synoptic-Scale Waves over Subtropical South America. **Monthly Weather Review**, [s. l.], v. 130, n. 3, p. 684–699, 2002. Disponível em: <http://journals.ametsoc.org/doi/abs/10.1175/1520-0493%282002%29130%3C0684%3ACSSSWO%3E2.0.CO%3B2>

VIANNA, M. L. et al. Interactions between Hurricane Catarina (2004) and warm core rings in the South Atlantic Ocean. **Journal of Geophysical Research**, [s. l.], v. 115, n. C7, p. C07002, 2010. Disponível em: <http://doi.wiley.com/10.1029/2009JC005974>

VON STORCH, H. Inconsistencies at the interface of climate impact studies and global climate research. **Meteorol. Z**, [s. l.], v. 4, n. January 1995, p. 72–80, 1995.

VON STORCH, Hans. On the use of "inflation" in statistical downscaling. **Journal of Climate**, [s. l.], v. 12, n. 12, p. 3505–3506, 1999.

WALKO, Robert L. et al. New RAMS cloud microphysics parameterization Part I: the single-moment scheme. **Atmospheric Research**, [s. l.], v. 38, n. 1, p. 29–62, 1995.

WALKO, Robert L. et al. Coupled Atmosphere–Biophysics–Hydrology Models for Environmental Modeling. **Journal of Applied Meteorology**, [s. l.], 2000.

WALKO, Robert L.; AVISSAR, Roni. The Ocean–Land–Atmosphere Model

(OLAM). Part I: Shallow-Water Tests. **Monthly Weather Review**, [s. l.], v. 136, n. 11, p. 4033–4044, 2008. a. Disponível em: <http://journals.ametsoc.org/doi/abs/10.1175/2008MWR2522.1>

WALKO, Robert L.; AVISSAR, Roni. The Ocean–Land–Atmosphere Model (OLAM). Part II: Formulation and Tests of the Nonhydrostatic Dynamic Core. **Monthly Weather Review**, [s. l.], v. 136, n. 11, p. 4045–4062, 2008. b. Disponível em: <http://journals.ametsoc.org/doi/abs/10.1175/2008MWR2523.1>

WALKO, Robert L.; AVISSAR, Roni. A Direct Method for Constructing Refined Regions in Unstructured Conforming Triangular–Hexagonal Computational Grids: Application to OLAM. **Monthly Weather Review**, [s. l.], v. 139, n. 12, p. 3923–3937, 2011.

WALTON, Daniel B. et al. A hybrid dynamical-statistical downscaling technique. Part I: Development and validation of the technique. **Journal of Climate**, [s. l.], 2015.

WANG, Wanqiu et al. An assessment of the surface climate in the NCEP climate forecast system reanalysis. **Climate Dynamics**, [s. l.], 2011.

WANG, Zhaoli et al. Evaluation of the GPM IMERG satellite-based precipitation products and the hydrological utility. **Atmospheric Research**, [s. l.], 2017.

WENNEKER, I.; SEGAL, A.; WESSELING, P. A Mach-uniform unstructured staggered grid method. **International Journal for Numerical Methods in Fluids**, [s. l.], 2002.

WILBY, R. L. et al. Guidelines for Use of Climate Scenarios Developed from Statistical Downscaling Methods. In: **Supporting material of the Intergovernmental Panel on Climate Change, available from the DDC of IPCC TGCIA, 27**. [s.l: s.n.]. p. 27.

WILBY, R. L.; WIGLEY, T. M. L. **Downscaling general circulation model output: A review of methods and limitationsProgress in Physical Geography**, 1997.

WONG, Poh Poh et al. Coastal systems and low-lying areas. In: **Climate Change 2014 Impacts, Adaptation and Vulnerability: Part A: Global and Sectoral Aspects**. [s.l: s.n.].

WORLD BANK. **Report of material damages and losses due to natural disasters in Brazil - 1995-2014 : Relatório de danos materiais e prejuízos decorrentes de desastres naturais no Brasil – 1995-2014 (Portuguese)Centro Universitário de Estudos e Pesquisas sobre Desastres; World Bank**. Washingtn D.C.

ZAMBONI, Ademilson; NICOLODI, João Luiz. **Macrodiagnóstico da zona costeira e marinha do Brasil**. DF, Brasil.

ZHOU, Jiayu; LAU, K. M. Does a monsoon climate exist over South America? **Journal of Climate**, [s. l.], 1998.

ZIPSER, Edward J. et al. Where are the most: Intense thunderstorms on Earth? **Bulletin of the American Meteorological Society**, [s. l.], 2006.

APÊNDICE A – Municípios costeiros da região sul do Brasil

3. No Paraná há sete municípios costeiros: Guaraqueçaba, Antonina, Paranaguá, Pontal do Paraná, Matinhos, Guaratuba e Morretes.

4. Em Santa Catarina, 38: Itapoá, São Francisco do Sul, Joinville, Araquari, Balneário Barra do Sul, Barra Velha, Piçarras, Penha, Navegantes, Itajaí, Balneário Camboriú, Camboriú, Itapema, Bombinhas, Porto Belo, Tijucas , Governador Celso Ramos, Biguaçu, Florianópolis, São José, Palhoça, Paulo Lopes, Garopaba, Imbituba, Imaruí, Laguna, Pescaria Brava, Jaguaruna, Içara, Balneário Rincão, Araranguá, Balneário Arroio do Silva, Sombrio, Santa Rosa do Sul, Balneário Gaivota, São João do Sul e Passo de Torres.

5. No Rio Grande do Sul, 32: Dom Pedro de Alcântara, Arroio do Sal, Três Cachoeiras, Três Forquilhas, Terra de Areia, Capão da Canoa, Maquiné, Xangri-Lá, Osório, Imbé, Tramandaí, Cidreira, Balneário Pinhal, Capivari do Sul, Viamão, Palmares do Sul, Mostardas, Tavares, São José do Norte, Barra do Ribeiro, Tapes, Arambaré, Camaquã, São Lourenço do Sul,Turuçu, Pelotas, Rio Grande, Arroio Grande, Jaguarão, Santa Vitória do Palmar e Chuí.

ANEXO A – DECRETO 5.300/2004, CAPÍTULO II:

DOS LIMITES, PRINCÍPIOS, OBJETIVOS, INSTRUMENTOS E

COMPETÊNCIAS DA GESTÃO DA ZONA COSTEIRA

Seção I

Dos Limites

Art. 3º A zona costeira brasileira, considerada patrimônio nacional pela Constituição de 1988, corresponde ao espaço geográfico de interação do ar, do mar e da terra, incluindo seus recursos renováveis ou não, abrangendo uma faixa marítima e uma faixa terrestre, com os seguintes limites:

I - faixa marítima: espaço que se estende por doze milhas náuticas, medido a partir das linhas de base, compreendendo, dessa forma, a totalidade do mar territorial;

II - faixa terrestre: espaço compreendido pelos limites dos Municípios que sofrem influência direta dos fenômenos ocorrentes na zona costeira.

Art. 4º Os Municípios abrangidos pela faixa terrestre da zona costeira serão:

I - defrontantes com o mar, assim definidos em listagem estabelecida pela Fundação Instituto Brasileiro de Geografia e Estatística - IBGE;

II - não defrontantes com o mar, localizados nas regiões metropolitanas litorâneas;

III - não defrontantes com o mar, contíguos às capitais e às grandes cidades litorâneas, que apresentem conurbação;

IV - não defrontantes com o mar, distantes até cinqüenta quilômetros da linha da costa, que contemplem, em seu território, atividades ou infra-estruturas de grande impacto ambiental na zona costeira ou ecossistemas costeiros de alta relevância;

V - estuarino-lagunares, mesmo que não diretamente defrontantes com o mar;

VI - não defrontantes com o mar, mas que tenham todos os seus limites com Municípios referidos nos incisos I a V;

VII - desmembrados daqueles já inseridos na zona costeira.